

Canada

Alberta

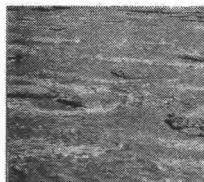


Northern River Basins Study



NORTHERN RIVER BASINS STUDY PROJECT REPORT NO. 36
**WINTER UNDER-ICE TRACER
 DYE STUDIES, TIME OF TRAVEL
 AND MIXING CHARACTERISTICS**
 PEACE RIVER, SHAFTESBURY FERRY
 TO NOTIKEWIN RIVER
 FEBRUARY AND MARCH, 1993

TC
177
.N879
1994



Prepared for the
Northern River Basins Study
under Project 120-B1

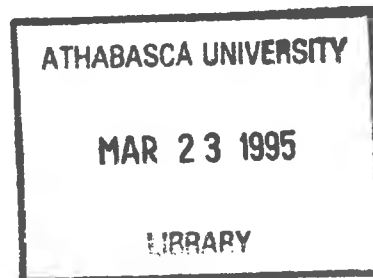
by
Northwest Hydraulic Consultants Ltd.
and Alberta Research Council

Community Contributors:

J. Bulmer, Town of Peace River
I. Granger, Daishowa-Marubeni International
O. Romaniuk, Town of Peace River
J. Smeenk, Shell Canada

NORTHERN RIVER BASINS STUDY PROJECT REPORT NO. 36
WINTER UNDER-ICE TRACER
DYE STUDIES, TIME OF TRAVEL
AND MIXING CHARACTERISTICS
PEACE RIVER, SHAFTESBURY FERRY
TO NOTIKWIN RIVER
FEBRUARY AND MARCH, 1993

Published by the
Northern River Basins Study
Edmonton, Alberta
June, 1994



CANADIAN CATALOGUING IN PUBLICATION DATA

Northwest Hydraulic Consultants Ltd.

Winter under-ice tracer dye studies, time of travel and mixing characteristics, Peace River, Shaftesbury ferry to Notikewin River, February and March, 1993

(Northern River Basins Study project report, ISSN 1192-3571 ; no. 36)

Includes bibliographical references.

ISBN 0-662-22364-0

Cat. no. R71-49/3-36E

1. Hydraulic measurements -- Peace River (B.C. and Alta.)
2. Ice on rivers, lakes, etc. -- Peace River (B.C. and Alta.)
 - I. Alberta Research Council.
 - II. Northern River Basins Study (Canada)
 - III. Series.

TC177.N67 1994 532'.051'0971231 C94-980239-5

Copyright (c) 1994 by the Northern River Basins Study.

All rights reserved. Permission is granted to reproduce all or any portion of this publication provided the reproduction includes a proper acknowledgement of the Study and a proper credit to the authors. The reproduction must be presented within its proper context and must not be used for profit. The views expressed in this publication are solely those of the authors.

PREFACE:

The Northern River basins Study was initiated through the "Canada-Alberta-Northwest Territories Agreement Respecting the Peace-Athabasca-Slave River Basin Study, Phase II - Technical Studies" which was signed September 27, 1991. The purpose of the Study is to understand and characterize the cumulative effects of development on the water and aquatic environment of the Study Area by coordinating with existing programs and undertaking appropriate new technical studies.

This publication reports the method and findings of particular work conducted as part of the Northern River Basins Study. As such, the work was governed by a specific terms of reference and is expected to contribute information about the Study Area within the context of the overall study as described by the Study Final Report. This report has been reviewed by the Study Science Advisory Committee in regards to scientific content and has been approved by the Study Board of Directors for public release.

It is explicit in the objectives of the Study to report the results of technical work regularly to the public. This objective is served by distributing project reports to an extensive network of libraries, agencies, organizations and interested individuals and by granting universal permission to reproduce the material.

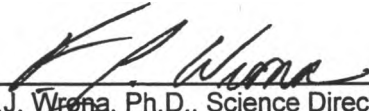
This report contains referenced data obtained from sources external to the Northern River Basins Study. Individuals interested in using external data must obtain permission to do so from the donor agency.

**NORTHERN RIVER BASINS STUDY
PROJECT REPORT RELEASE FORM**

This publication may be cited as:

Northwest Hydraulic Consultants Ltd. and Alberta Research Council. 1994. Northern River Basins Study Project Report No. 36, Winter Under-ice Tracer Dye Studies, Time of Travel and Mixing Characteristics, Peace River, Shaftesbury Ferry to Notikewin River, February and March, 1993". Northern River Basins Study, Edmonton, Alberta.

Whereas the above publication is the result of a project conducted under the Northern River Basins Study and the terms of reference for that project are deemed to be fulfilled,
IT IS THEREFORE REQUESTED BY THE STUDY OFFICE THAT;
this publication be subjected to proper and responsible review and be considered for release to the public.



(Dr. F.J. Wrona, Ph.D., Science Director)



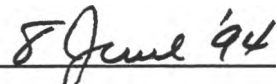
(Date)

Whereas it is an explicit term of reference of the Science Advisory Committee "to review, for scientific content, material for publication by the Board",
IT IS HERE ADVISED BY THE SCIENCE ADVISORY COMMITTEE THAT;
this publication has been reviewed for scientific content and that the scientific practices represented in the report are acceptable given the specific purposes of the project and subject to the field conditions encountered.

SUPPLEMENTAL COMMENTARY HAS BEEN ADDED TO THIS PUBLICATION: Yes No



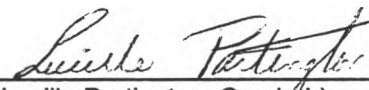
(Dr. P. A. Larkin, Ph.D., Chair)



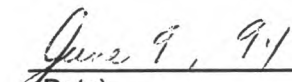
(Date)

Whereas the Study Board is satisfied that this publication has been reviewed for scientific content and for immediate health implications,

IT IS HERE APPROVED BY THE BOARD OF DIRECTORS THAT;
this publication be released to the public, and that this publication be designated for: **STANDARD AVAILABILITY** **EXPANDED AVAILABILITY**



(Lucille Partington, Co-chair)



(Date)

(Date)

**WINTER UNDER ICE TRACER DYE STUDIES,
TIME OF TRAVEL AND MIXING CHARACTERISTICS,
PEACE RIVER, SHAFTESBURY FERRY TO NOTIKEWAN RIVER,
FEBRUARY AND MARCH, 1993**

STUDY PERSPECTIVE

Understanding the hydraulic characteristics of rivers is necessary to understand how effluents and their contaminants are mixed and transported, and where they are deposited in rivers. To properly model the transport of contaminants and pollutants within freshwater systems, the mixing or dispersion characteristics must be established. The NRBS Tracer Dye study focused on the calculation of mixing coefficients and travel times using field dye tests on the Peace River between Shaftesbury Ferry and Notikewan River. The test was completed under ice covered conditions in late winter (February - March 1993), the period most critical for potential impacts on the aquatic ecosystem.

Related Study Questions

- 13 a) *What predictive tools are required to determine the cumulative effects of man made discharge on the water and aquatic environment?*

- 14) *What long term monitoring programs and predictive models are required to provide an ongoing assessment of the state of the aquatic ecosystems. These programs must ensure that all stakeholders have the opportunity for input.*

Prevailing flows during the experiment were close to the historical average for the study reach. The flows are controlled by the outflow from the Bennett Dam in British Columbia, and are much higher than natural flows for this time of year. Partly as a result of regulation, frazil slush ice deposits were extreme under the ice cover and had to be accounted for in assessing the hydraulic characteristics for the test.

It is not yet possible to accurately predict coefficients for a complete range of hydraulic and ice conditions. As the calculated transverse mixing coefficients did not compare well with other studies, the report advised that it would be premature to extend the results to the rest of the Peace River. The scatter in results from this and other studies underscores the difficulties in predicting mixing characteristics without site-specific tests.

REPORT SUMMARY

Travel time and mixing characteristics for contaminants in the Peace River downstream of the Smoky River mouth were determined by means of a dye tracer test conducted at the end of February and beginning of March 1993. A single dose of dye was injected through the ice at Shaftesbury Ferry, approximately 25 km upstream of Peace River town, and the spreading dye cloud was tracked as far as the Notikewin River, about 160 km downstream of the town. Techniques used in conducting and analyzing the dye test were generally similar to those used by Alberta Research Council in previous river tracer studies.

The average travel velocity of the dye-cloud was approximately 1.1 m/s, which is about 40% greater than the average velocity of flow as calculated from gauged river flows and surveyed cross-sections. The difference is ascribed mainly to undetected partial blockage of the channel by static accumulations of frazil ice, particularly near the banks. A method is proposed for adjusting channel hydraulic properties for purposes of determining mixing parameters.

Transverse mixing parameters were calculated from the dye test results and the channel properties. Transverse mixing in the study length is weak in comparison to other rivers previously studied in Alberta. The length required for complete transverse mixing is in the order of 100 km.

Longitudinal mixing parameters were calculated using both Beltaos' linear dispersion model and an alternative storage-and-release model. Parameter values are comparable with those found for other rivers in Alberta. The length required for the beginning of a transition from linear dispersion to Fickian mixing is found to be in the order of 200 km.

The data obtained are considered to be suitable for extrapolation to other flow and ice conditions within the study length, but not necessarily to other lengths of the Peace River without further selective tracer tests. The data improve the data base but do not resolve the difficult problem of selecting mixing coefficients for untested rivers.

CREDITS AND ACKNOWLEDGEMENTS

The following personnel of Northwest Hydraulic Consultants and Alberta Research Council participated in the study:

E.K. Yaremko (NHC):	project management;
D.D. Andres (ARC):	technical direction, reporting and review;
C.R. Neill (NHC):	hydraulic analysis and report editing;
P.G. Van Der Vinne (ARC):	field program, mixing analysis and reporting;
G. Gehmlich and B. Walsh (NHC):	field survey and mixing tests;
J. Thompson and B. Trevor (ARC):	field mixing tests and data processing;
S. Adams and S. Vetsch (NHC):	report preparation.

Grateful acknowledgement is made of valuable contributions to the study by the following persons:

T. Prowse and J. Choles of the Northern Rivers Basin Study team, for their help in establishing the final work plan;

I. Granger of Daishowa–Marubeni International, J. Bulmer and O. Romaniuk of the Town of Peace River, and J. Smeenk of Shell Canada, representing water intake operators along the Peace River, for their cooperation and understanding in dealing with passage of the dye cloud;

V. Elder of Environment Canada, for providing preliminary discharge data and assisting in the staging of the field work.

TABLE OF CONTENTS

	Page
REPORT SUMMARY	i
CREDITS & ACKNOWLEDGEMENTS	ii
TABLE OF CONTENTS	iii
LIST OF TABLES	v
LIST OF FIGURES	vi
LIST OF PHOTOGRAPHS	viii
1. INTRODUCTION	1
1.1 Objectives	1
1.2 Background	2
2. FIELD INVESTIGATIONS	3
2.1 River surveys	3
2.1.1 Site selection	3
2.1.2 Ice conditions	4
2.1.3 Cross-section surveys	6
2.2 Tracer dye test	6
2.2.1 Injection	7
2.2.2 Sampling	8
2.2.3 Data reduction	9
2.3 Frazil ice sampling	9
2.3.1 Background on frazil deposits	9
2.3.2 Nature and extent of observed frazil	10
2.3.3 Effects on dye test - initial considerations	11
2.3.4 Sampling of frazil pebbles	11
2.4 Mass balance of dye tracer	13
2.4.1 General	13
2.4.2 Results	14
3. RIVER HYDRAULICS AND TRAVEL TIMES	16
3.1 River flows	16
3.2 Channel geometry	18
3.2.1 River slopes	18
3.2.2 Cross-sections	18
3.2.3 Ice thicknesses	19
3.3 Computed channel velocities and roughnesses	20
3.4 Dye test results	21
3.5 Comparison of channel and dye-cloud velocities	22

TABLE OF CONTENTS (cont'd.)

	Page
4. TRANSVERSE MIXING	25
4.1 Theoretical summary	25
4.2 Method of evaluating coefficients from field data	27
4.3 Analysis of dye test results	28
4.4 Discussion of transverse mixing results.	30
4.5 Comparison with prediction models	31
5. LONGITUDINAL MIXING	34
5.1 Transverse mixing length	34
5.2 Theoretical summary	35
5.2.1 Turbulent mixing (linear dispersion) model	35
5.2.2 Storage and release model.	36
5.3 Method of evaluating coefficients from field data	38
5.3.1 Linear dispersion parameter.	38
5.3.2 Storage parameters	39
5.4 Analysis of dye test results	40
5.4.1 Linear dispersion parameter.	40
5.4.2 Storage parameters	41
5.5 Comparison with model predictions	42
6. CONCLUSIONS AND RECOMMENDATIONS	44
6.1 General discussion	44
6.2 Summary of principal numerical results	46
6.3 Recommendations.	47
7. REFERENCES	49
8. TABLES	
9. FIGURES	
10. PHOTOGRAPHS	
APPENDICES	
A. TERMS OF REFERENCE	
B. LIST OF SYMBOLS	
C. FIELD DATA FROM DYE TEST	

LIST OF TABLES

- 2.1 Ice cover characteristics over study length, February 1993
- 2.2 Frazil ice characteristics over study length, February 1993
- 2.3 Observed water surface elevations during surveys and dye test
- 2.4 Measured and calculated dye concentrations in the frazil zone
- 2.5 Mass recovery ratios in dye test
- 2.6 Comparison with minimum recovery ratios from other winter dye studies in Alberta
- 2.7 Reach-averaged values of parameters used to estimate dye losses to frazil
- 3.1 Hydraulic slopes along study length, February 1993
- 3.2 Measured and computed geometric and hydraulic data for study length, February 1993
- 3.3 Spatial variability of ice thickness in upper 30 km of study length, February 1983
- 3.4 Temporal variability of ice thickness at Peace River gauging section, 1983 to 1986
- 3.5 Dye-test travel times and velocities
- 3.6 Comparison by reaches of mean channel and dye-cloud velocities
- 3.7 Adopted widths and mean depths for mixing analyses
- 3.8 Comparison of composite hydraulic roughness values
- 4.1 Comparative estimates of vertical, transverse and linear mixing lengths for the Peace River
- 4.2 Dosage distribution parameters at dye-test sites
- 4.3 Computed transverse mixing parameters
- 5.1 Position parameter k_p (Equation 5.1) as function of injection location
- 5.2 Computed parameters characterizing timewise distributions of cross-sectional average concentration at each site

LIST OF TABLES (cont'd.)

- 5.3 Computed average hydraulic and linear dispersion parameters, Daishowa to Notikewin
- 5.4 Computed parameters for storage model

LIST OF FIGURES

- 1.1 Key map showing study length and sites
- 1.2 Peace River monthly flows before and after regulation
- 2.1 Ice cover characteristics along study length
- 2.2 Peace River stage records over study period
- 2.3 Laboratory correlation between dye concentrations on frazil ice pebbles and in interstitial water
- 2.4 Mass recovery ratio vs. distance from injection
- 3.1 River flows January through March at Peace River
- 3.2 Comparison of flow estimates at Peace River
- 3.3 Slope profile of study length
- 3.4a – c. Cross-sections
- 3.5a – g. Dye concentrations
- 3.6 Typical variation of travel times across the channel
- 3.7 Growth of travel times with distance from injection
- 4.1a – h. Cumulative discharge distributions across channel
- 4.2 Transverse dosage distributions for all sampling sites
- 4.3 Dosage variance versus integral of confinement function
- 4.4 Dimensionless coefficients versus hydraulic parameter
 - a. Diffusion factor
 - b. Transverse mixing coefficient
- 4.5a – d. Comparisons of measured and model-predicted dosage distributions
- 5.1 Sensitivity of storage model to storage zone number

LIST OF FIGURES (cont'd.)

- 5.2 Variation of half-duration with time-to-peak (Peace River)
- 5.3 Linear dispersion parameter versus ratio of shear velocity to mean velocity
- 5.4 Dimensionless peak concentration versus dimensionless distance from injection:
Peace and Athabasca Rivers
- 5.5a – d. Comparison of measured and model-predicted distributions of concentration
versus time
- 5.6 Sensitivity of Beltaos' model to possible range of linear dispersion parameter at
Mackenzie Cairn site
- 5.7 Sensitivity of storage model to possible range of storage coefficients at
Mackenzie Cairn site

LIST OF PHOTOGRAPHS

1. Juxtaposed ice cover in vicinity of Mackenzie Cairn: note well-defined circular ice floes
2. Close-up of juxtaposed ice cover upstream of Peace River: note surface roughness due to crushing of floe edges
3. Juxtaposed ice cover downstream of Daishowa: note large ice rafts embedded in cover
4. Juxtaposed ice cover with large embedded rafts just downstream of Cadotte River mouth
5. Consolidated ice cover in vicinity of Notikewin River
6. Close-up of consolidated cover at Notikewin River mouth: note large thick floes forming very rough surface
7. Consolidated ice cover between high shear walls just downstream of North Star
8. Ice "pebbles" formed by transport of frazil slush, as sampled at Hotchkiss site



1. INTRODUCTION

1.1 Objectives

This report describes a field and analytical study of the hydraulic, travel time and mixing characteristics under winter ice conditions of a 187-km length of the Peace River in northern Alberta. The length studied extends from Shaftesbury Ferry, approximately 25 km upstream of the Town of Peace River, to the Notikewin River, approximately 160 km downstream (Figure 1.1). Field investigations were conducted during the second half of February and the first days of March 1993. The main objectives of the study were: to conduct dye tests for determination of river velocities, times of travel and mixing coefficients; to summarize the associated geometric, hydraulic and ice characteristics of the river; and to discuss extrapolation of the results to different conditions. The results of the study are to be used in connection with water quality modelling.

Detailed terms of reference as provided by the Northern Rivers Basin Study are reproduced in Appendix A.

Literature referred to in this report is listed alphabetically by author in Section 7, References. Symbols used in equations are listed in Appendix B. Field data from the dye test are contained in Appendix C.

General technical background on the three main subjects covered in this report can be found in the following references (see Section 7):

- Open channel and river hydraulics – Henderson 1966
- River ice conditions – Ashton 1986
- River mixing – Elhadi et al 1984.

1.2 Background

From 1972 onwards, winter flows in the Peace River in Alberta have been greatly increased over natural flows by the operation of B.C. Hydro's Williston Lake reservoir and Bennett Dam in northeast British Columbia. Figure 1.2 compares typical patterns of monthly flows before and after completion of the dam. The natural range of daily winter flows was typically 200 to 500 m³/s, whereas the regulated range is typically 1000 to 2000 m³/s.

The large increases in winter flows and their fluctuations have substantially altered ice conditions in the length of interest. Freeze-up, which naturally occurred in early November, is delayed until December or January. Break-up generally occurs in April. The longer extent of open water with large flows in early winter tends to cause more dynamic freeze-up conditions and a thicker, more irregular cover. An example of a particularly severe ice accumulation occurred near Peace River town in late December and early January 1982. This was caused by a particular combination of weather patterns and fluctuating releases from Bennett Dam. This occurrence was described and analyzed by Neill and Andres (1984).

The present study was conducted under stable winter ice conditions that followed a relatively mild freeze-up. Velocities and travel times under such conditions are functions of the slope of the river, the cross-sectional dimensions of the channel, the composite roughness of the river bed and ice underside, and the river discharge. In general, the level of the ice cover adjusts to fluctuating discharges so that the energy grade line resulting from the under-ice cross-section and the composite roughness of the channel with ice cover corresponds to the overall open water slope of the river.

Similar travel time and mixing studies for the greater part of the Athabasca River were reported by Beltaos (1979), Andres et al (1989), Van Der Vinne (1992) and Van Der Vinne and Andres (1992). Relative to the Peace River, winter discharges in the Athabasca River are low because the river is not regulated by reservoirs.

2. FIELD INVESTIGATIONS

2.1 River Surveys

The entire length of river encompassed by the field investigations is referred to as the study length. Lengths between specific sampling sites are referred to as reaches.

2.1.1 Site selection

The Terms of Reference (Appendix A) stipulated that transverse dispersion characteristics were to be determined within at least three reaches upstream of the Daishowa plant outfall. Additional factors which influenced the selection of sampling sites along the 187 km long study length were as follows:

- Suitable road access was required for parking of equipment and trailers near each site.
- Sites should demarcate river reaches having distinct and relatively homogeneous characteristics with respect to ice cover and channel geometry.

During proposal preparation, six sites were suggested as sampling locations, with dye injection at Shaftesbury Ferry. Selection of these sites was based on a preliminary analysis of transverse mixing rates, as well as the use of maps, existing profiles and personal knowledge. A mixing analysis using available river cross-sections indicated that a single injection at Shaftesbury Ferry would be sufficient for determination of transverse mixing coefficients both at the mouth of the Smoky River and at Daishowa. On this basis, sampling sites in the upper part of the study length were tentatively selected immediately upstream of the Smoky River and at the Daishowa Bridge. Provision was however made to measure transverse dispersion at Daishowa using a second dye injection at Peace River town, in the event that transverse mixing was found to be much faster than anticipated.

A helicopter reconnaissance was conducted on 10 February 1993 to review the proposed set of sampling sites. Immediately prior to the reconnaissance, the Northern River Basins Study office had suggested adding another sampling site 10 km downstream of the Shaftesbury Ferry injection site. On the basis of observed ice conditions and access routes, in addition to further computational checks of transverse mixing rates, it was eventually decided to select seven sampling sites at the locations shown in Figure 1.1. It was considered that the first site at Mackenzie Cairn would provide measurements of transverse mixing upstream of the Smoky River, and that the second site could be located at Peace River town, where hydraulic and mixing characteristics were believed to be reasonably similar to those at the Smoky River mouth. It was anticipated that transverse mixing gradients would still be present downstream of the third site at the Daishowa Bridge. The remaining four sampling sites were selected largely on the basis of available access, while attempting to keep reach lengths reasonably uniform and keeping in mind any obvious changes in ice characteristics.

2.1.2 Ice conditions

The helicopter reconnaissance undertaken on 10 February 1993 enabled the study team to identify access locations and to identify the dominant ice characteristics along the study length (Figure 1.1). The intention was to infer, from the surface characteristics, the freeze-up mode and the relative differences in potential thickness and roughness of the ice cover in the various reaches. The survey also allowed sampling sites to be chosen so that ice cover characteristics were as consistent as possible within each reach.

The surface of the ice was characterized as being either smooth, which is indicative of an ice cover formed by simple juxtaposition of pans, or rough, which indicates an ice cover that has undergone substantial shoving or consolidation. Evidence of large rafts embedded in the ice cover was noted, also the existence of shear lines indicative of a consolidating ice cover. Shear lines are not necessarily related to the existing ice cover, but may be relics of a previous cover that had collapsed prior to formation of the existing cover. Nevertheless, their presence suggests

that considerable thickening and storage of frazil has occurred and that the width or the cross-sectional area of the channel may be reduced by accumulated ice in their vicinity.

Photos 1 to 7 illustrate the surficial features that were used to characterize the ice cover in the study area. Photos 1 and 2 illustrate a juxtaposed ice cover formed from single pans. Photos 3 and 4 show a juxtaposed ice cover with embedded rafts. Photos 5 and 6 illustrate the surface of a shoved ice cover. Photo 7 defines a variety of shear lines that indicate a history of unstable ice covers.

Figure 2.1 summarizes the discharge, air temperature, progression rate, and surficial characteristics of the ice cover along the study length. The cover formed between 21 December and 30 December 1992. Downstream of the Whitemud River, it developed at discharges of about 1800 to 1900 m³/s and air temperatures in the order of -25°C. This resulted in a cover that was generally rough due to shoving of the initially juxtaposed ice floes: apparently they could not be frozen in place at these temperatures before the stresses on the cover due to the high discharges and the lengthening ice cover increased to the point where the cover collapsed. Upstream of the Whitemud River, freeze-up occurred during much colder conditions (in the order of -40 °C) and at lower discharges of about 1700 m³/s. It appears that with the colder conditions and lower discharge, the cover gained sufficient strength from freezing that the juxtaposed floes were not consolidated or shoved as the head of the cover advanced upstream.

On the basis of the field observations and the above interpretation of freeze-up processes, the study length can be divided into two segments with respect to ice characteristics, as follows:

Shaftesbury Ferry to Whitemud River. The cover was generally flat, composed of either individual pans or large rafts. The roughness of the upper surface was largely due to ridges produced when individual pans collided (Photo 2). The average thickness (Table 2.1) was about 1.1 m and the variability across the channel – defined by the standard deviation of ice thickness measurements at each section – about 0.22 m.

Whitemud River to Notikewin River. The cover was generally rough, the surface roughness being due mostly to overturning and shoving of floes (Photos 5, 6, and 7). The average thickness was about 1.5 m with a standard deviation of about 0.55 m (Table 2.1). Since ice thickness measurements were not undertaken until about six weeks after freeze-up, a substantial amount of frazil redistribution may have occurred under the ice cover.

2.1.3 Cross-section surveys

Channel cross-sections at the injection and sampling sites were surveyed during the period 17–24 February 1993, prior to the dye test. The purpose of the surveys was to collect geometric and hydraulic data including ice thicknesses, water surface elevations, water depths, and flow velocities, and thereby to check calculated flow distributions across the sections.

A total of 20 holes were drilled through the ice at each site, evenly spaced across the section. Water depths and thicknesses of solid and frazil ice were measured in each hole. Velocities were measured by current meter at every other hole. The water levels were tied to Geodetic Survey of Canada (GSC) benchmarks where available nearby, otherwise to a temporary benchmark. For the latter sites, GSC tie-ins were conducted later by Northpoint Surveys Ltd. of Peace River. For reference purposes, site locations were identified on 1:50 000 scale topographic maps.

Table 2.3 summarizes elevation data as observed at the sites during the surveys and during the subsequent dye test. Other data from the surveys are presented in Section 3.

2.2 Tracer Dye Test

A single dye-tracer test was carried out between 27 February and 2 March 1993 over the 187 km length between Shaftesbury Ferry and Notikewin River. Figure 1.1 shows the location of the injection site and the seven sampling sites. Data were collected over an 80-hour period. Key features of the test were as follows:

Time of injection: 9:30 am, 27 February

Mass of 100% Rhodamine WT dye injected: 50 kg

Number of sampling sites: 7

Length from injection to last sampling: 187 km

Duration of test: 80 hours

According to the study Terms of Reference, the amount of dye injected was to be selected such that the peak concentration at the last sampling station would be approximately 1 µg/L. On the basis of previous experience and numerical modelling, a mass of 50 kg of pure dye was chosen as sufficient to meet the criterion. As will subsequently appear (Figures 3.5 f and g), the criterion was approximately met: at the last sampling site, the peak concentration was 0.5 µg/L. An important reason for the shortfall is that dye losses were greater than had been anticipated (see Section 2.4). Given the uncertainties in predicting dispersion and losses in advance, it can be said that a good estimate was made of the quantity required. A larger quantity would have increased study costs without significant improvements in the determination of mixing characteristics, whereas a smaller quantity would have increased the risk of inadequate definition.

2.2.1 Injection

A mass of 250 kg of 20% solution Rhodamine WT dye was transported to the injection sites in 20 L pails. In previous studies, an equal volume of methyl alcohol was added to the dye to make the mixture neutrally buoyant and prevent freezing. Because of the large volume of dye in the present study, this was not done because it would have slowed injection. Freezing was prevented by storing the dye indoors until injection. Neutral buoyancy was judged not to be critical because the dye was injected near the surface and would mix rapidly as it sank in the large flow depth.

The dye was injected through a 20 cm diameter hole 15 m downstream of the Shaftesbury Ferry ice bridge, at a predetermined point in the centre of the flow. An additional hole served as a water supply to flush the injection apparatus, consisting of two 1.5 m lengths of 10 cm

diameter PVC pipe. A 90° elbow was attached to the lower end to orient the dye in the direction of flow. Although certain difficulties were encountered in the dye injection, all the dye was injected into the flow virtually instantaneously, with only minor spillage. It is believed that insignificant quantities of dye were trapped under the ice. Moreover, any dye that may have been initially trapped under the ice would likely have been flushed into the flow by the water pumped into the injection hole.

2.2.2 Sampling

Two sampling crews of two persons each followed the dye downstream, each crew sampling at alternating sites. An additional crew of seven persons was employed at the first downstream sampling site (Mackenzie Cairn), because of the short transit time of the dye cloud and the need for ten sampling holes across the section. At other sites, five or six sample holes were used, located across the section so as to ensure that the discharge distribution was sampled more or less uniformly. Water levels during the sampling were referenced to temporary benchmarks established during the earlier cross-section surveys (see Section 2.1.3).

Water samples to establish dye concentrations (as indicated by the fluorescence) were taken from each hole at intervals ranging from five minutes to two hours, depending on the transit time of the dye cloud. The interval was set so that at least 20 to 30 successive samples could be taken from each hole as the dye passed by. A number of samples were also taken before the dye arrived, to establish background fluorescence. Special care was taken to define the times of first rise and of peak concentration. Sampling was continued until fluorescence (directly related to dye concentration) was reduced to less than 20% and ideally to 10% of peak values, in order to permit confident extrapolation of the tail of the concentration-time curve.

The water samples were collected in 125 mL Nalgene sample bottles, which were attached to a 4-metre pole plunged as deeply as possible into the flow. The bottles were rinsed twice before each sample was collected.

2.2.3 Data reduction

Samples were transported immediately to on-site mobile laboratories, where sample temperature was recorded and the samples were run through a fluorometer (Turner Designs Model 10). Three fluorometers were used during the study, each pre-calibrated at 20 degrees C and each dedicated to one field crew.

Three steps were necessary to convert recorded fluorescence values into dye concentrations. First, the appropriate calibration regressions were applied to the recorded fluorescence values to obtain concentration at standard temperature. Next, a temperature correction factor k_T was applied to give the true dye concentration. This factor was obtained from

$$k_T = e^{0.026(T-T_0)} \quad [2.1]$$

where T is the temperature of the samples in degrees Celsius and T_0 is the temperature of the calibration standards (Turner Designs, 1982). Finally, background concentrations were established from the initial samples at each site and then subtracted from the temperature-corrected concentrations.

2.3 Frazil Ice Sampling

2.3.1 Background on frazil deposits

The characteristics of frazil deposits under an ice cover depend on the type of cover formed during freeze-up. Frazil forms initially in open water and attaches to the underside of ice floes. As the ice cover progresses upstream, frazil is redistributed under the cover, its ultimate thickness depending on the ice discharge and the upstream progression rate of the cover. For ice covers formed by juxtaposition, frazil accumulations tend to be unobtrusive, relatively thin and porous, and variably distributed across the section. For ice covers formed by shoving,

frazil accumulations tend to be more extensive, thicker and less porous, and more evenly distributed across the main-flow part of the cross section.

Immediately after ice cover formation, accumulated frazil consists of a dense slush of frazil discs with a porosity of about 0.5. It exhibits considerable cohesion and tends to accumulate in slack water zones. In the central flow region the slush is transported and partly re-frozen. Chacho et al (1986) suggest that re-freezing involves initial freezing at grain contacts followed by freezing of interstitial water. Frazil particles are transformed during transport into rounded "ice pebbles" as seen in Photo 8.

2.3.2 Nature and extent of observed frazil

Table 2.2 summarizes observed frazil characteristics at each surveyed cross-section. Frazil was extremely variable in time and space, even from hole to hole. Accumulations were more pronounced downstream of Whitemud, which is consistent with the typically rougher ice cover noted in that length. It appears that the 1992 freeze-up was not particularly severe with respect to frazil ice production because of its rapidity and a resulting thin ice cover. For the most part, the accumulated frazil did not seem significant enough to have a large impact on channel hydraulics, dye recovery ratios, or mixing characteristics. This question is discussed further in Sections 2.4, 3.5 and 4.4.

Large quantities of frazil "pebbles", typically 0.03 m and up to 0.10 m in diameter, were observed rising in sampling holes in the main-flow channel – presumably being transported along the underside of the ice. They were the dominant form of frazil observed during the surveys and dye test. The volume of pebbles appeared to increase in the downstream direction, perhaps due to more locally contributed frazil and to reduced ice production at the head of the cover as air temperatures rose.

2.3.3 Effects on dye test – initial considerations

Frazil accumulation can result in loss of dye during a tracer test. If there is a significant amount in transport, some of the dye can attach and be stored in frazil deposit zones. It had therefore been planned to sample representative frazil deposits for dye contamination, provided there were representative frazil deposits at close proximity to the dye sampling sections. Consideration was given to a number of sampling techniques described in the literature (Brockett and Sellman 1986; Dean 1986; Chacho et al 1989). Many of these techniques require a substantial investment in time and equipment, and it was found that using these approaches it would not be feasible to complete a sampling during the passage of the dye cloud. Also, the general absence of continuous frazil deposits precluded selection of a suitable site.

A simple alternative method, involving sampling with a thin-walled tube 5 cm in diameter and 2 m long, was tested at Hotchkiss in what was considered to be a typical frazil deposit. Results were however unsatisfactory, because the frazil deposits were relatively thin and porous, making it difficult to insert the tube without disturbing the sample, and because the presence of frazil pebbles prevented the tube from capturing an undisturbed core. Given the nature of the frazil in the river, it would probably be impossible to capture a representative in-situ core with any type of non-cryogenic sampler. Even a cryogenic sampler might not be able to provide sufficient cooling for the high transport velocities.

2.3.4 Sampling of frazil pebbles

As an alternative to sampling frazil deposits, it was decided to sample the frazil pebbles that were moving along the underside of the ice and filling the sampling holes. It was reasoned that the concentration of dye attached to the frazil pebbles would indicate what was not being sampled in the water column. If the thickness of the frazil transport layer could be estimated, then at least a rough estimate could be made of the associated dye losses.

Dye concentrations attached to the frazil pebbles can be analyzed as follows. The mass of dye M_i attached to N frazil pebbles with a total volume V_i can be written as

$$M_i = N C_{po} 4 \pi r^2 t \quad [2.2]$$

where t is the thickness of the layer of attached water around each pebble, r is the radius of the pebble, and C_{po} is the dye concentration in the interstitial water within the transport layer. The volume of ice is

$$V_i = N \frac{4\pi}{3} r^3 \quad [2.3]$$

The measured dye concentration C_i of the ice volume is M_i/V_i . By combining Equations [2.2] and [2.3], the dye concentration in the water in the transport layer can be determined as a function of the measured concentration of dye attached to the ice pebbles, the thickness of the water transport layer, and the average radius of the ice pebbles, as shown in Equation [2.4]:

$$C_{po} = 3 C_i r / t \quad [2.4]$$

The thickness of the water transport layer cannot be known a priori, however laboratory measurements suggest that the ratio C_i/C_{po} is about 0.06 for C_{po} ranging from 0.08 to 6 ppb (Figure 2.3). This translates into a water film thickness of about 0.020 times the radius of the ice pebbles or about 0.6 mm. It is assumed in this analysis that the dye concentration in the interstitial water is a relic of the peak dye concentration that passed the site. The main conclusion is that the dye concentration in the interstitial water of the transport layer is about 15 times the measured dye concentration attached to the ice pebbles.

Sampling of frazil pebbles was conducted at Hotchkiss and Notikewin on 1/2 March 1993. Table 2.4 shows the measured dye concentrations in the river water at time of frazil sampling, the preceding peak concentrations in the river water during passage of the dye cloud, and the concentration attached to the frazil pebbles. Also shown are calculated values of interstitial water

concentrations, considered to be representative of dye accumulated in the transport layer during the passage of the dye cloud. The interstitial water concentrations are about 25% to 45% of the (timewise) peak dye concentrations in the main flow. Depending on the rate of exchange of dye between water and ice, this value may or may not be representative of steady-state storage of dye within the frazil transport layer.

2.4 Mass Balance of Dye Tracer

2.4.1 General

Confidence in the results of a dye test is enhanced if more or less the injected mass of dye is accounted for at all downstream sites. However, there is nearly always some apparent loss. Reliability of the travel time and mixing data does not require complete mass recovery.

Apparent change in dye mass between sites depends on both physical losses and measurement errors. Measurement errors tend to cause erratic fluctuations in calculated mass, whereas losses cause a trend of decreasing mass with distance.

Measurement errors can be classed as random, systematic and site-specific. **Random errors** affect the data on concentration, time and discharge: the combined random error in the mass estimate due to these factors is estimated to be about $\pm 6\%$. **Systematic errors** are consistently either positive or negative, and may affect temperature correction factors, estimation of concentration recessions, and stage-discharge ratings: the total systematic error could be as high as $\pm 20\%$. **Site-specific errors** may include errors in peak concentration at sampling sites 1 and 2 due to low sampling frequency, and the effects of frazil accumulations: the total site-specific error at site 7 may be as high as $\pm 25\%$.

2.4.2 Results

The recovered mass at each Peace River site was calculated by integrating the concentration profiles with respect to time and then with respect to discharge across the channel, that is:

$$M = \int_{q_0}^Q \int_{t_0}^t C dt dq_c \quad [2.5]$$

where M is the dye mass, C is the concentration, t is time and q_c is cumulative discharge across the channel. The recovered mass was divided by the injected mass to obtain the apparent recovery ratios shown in Table 2.5. The minimum value is 0.52, at the downstream end of the study length. This is low compared to most of the minimum values from previous studies in Alberta (Table 2.6); however, the Wapiti and Smoky River studies produced minimum values between 0.5 and 0.6. These rivers had considerable frazil accumulations, which may have been responsible.

In the present study, the low values of recovery ratio are believed to be due to a combination of measurement errors and dye losses. Figure 2.4 plots apparent recovery ratio versus distance using the data of Table 2.5. Possible error bars based on the discussion in Section 2.4.1 are shown, but not including general systematic errors since these do not contribute to the variability of the recovery ratio. The fitting curve attempts to discount apparent losses due to error and to represent the actual dye losses only: it can be modelled by assuming that the rate of dye loss at any section is proportional to peak concentration at that section. Values of (estimated actual) recovery ratio corresponding to the fitting curve are shown in Table 2.5 for comparison with apparent values.

A somewhat speculative effort was made to estimate the proportion of dye loss that was caused by frazil ice, using data presented previously in Section 2.3.4. The gross area occupied by frazil at any section is the mean thickness multiplied by the channel width; however, water occupies the pore space between the frazil particles, which makes up approximately 30% of the

area. On the basis of the discussion in Section 2.3.4, this pore water was assumed to have a dye concentration of roughly 35% of the peak concentration at a section. The mass recovery ratio that would result from frazil losses only can then be estimated from

$$S_f = \sum 0.105 B H_f C_p \Delta x \quad [2.6]$$

where S_f is the accumulated mass lost to the frazil, Δx is the reach length, and B , H_f and C_p are the reach-averaged values of under-ice width, frazil thickness and peak concentration. Values of those parameters as used in the calculations are given in Table 2.7. Resulting mass recovery ratios accounting for frazil losses only are given in Table 2.5 and shown as the upper curve in Figure 2.4. If the fitting curve of Figure 2.4 is accepted as an estimate of actual total dye losses (discounting errors), the estimated dye losses due to frazil account for 40% to 55% of the total losses.

3. RIVER HYDRAULICS AND TRAVEL TIMES

The terms "flow" and "discharge" are used interchangeably herein to mean rate of flow at a point in cubic metres per second (m^3/s).

Velocities calculated from discharges and cross-section areas are referred to here as mean channel velocities. Velocities calculated from dye travel times are referred to as dye-cloud velocities.

3.1 River Flows

River flows as reported at Peace River town for the period covering the surveys and dye experiment, from 17 February to 2 March 1993, varied between approximately 1600 and 1900 m^3/s . Figure 3.1, comparing daily flows for the winter of 1993 with a composite 7-year average of daily winter flows for the period 1984–90, shows that flows during the 1993 study period were fairly close to long-term averages.

In order to interpret data on flow velocities and mixing characteristics at the dye-test injection and sampling points, fluctuating discharges as gauged at Peace River town must be routed to the other sites. The following method was used to do this empirically on the basis of available river data.

Historical open-water discharge hydrographs for gauges at Peace River and Carcajou (approximately 265 km downstream of Peace River town) were compared for flows in the range of 1000 to 2000 cms. (Winter hydrographs are not available for Carcajou.) The comparison indicated that identifiable peaks and troughs had a lag time of about 2 days. The computed wave celerity is then approximately 1.5 m/s. As the open-water mean channel velocity under these flow conditions is approximately 1.0 m/s, the resulting celerity/velocity ratio is 1.5, which is within the expected range for flow in wide rivers (Henderson 1966). Use of the same ratio for winter ice conditions, when the mean channel velocity in the present study length appears to be

approximately 0.8 m/s, yields an estimated wave celerity of about 1.2 m/s. Using this value, lag times between Peace River and other points can be estimated as follows:

Shaftesbury	-6 hours
Mackenzie Cairn	-4 hours
Peace River	0
Daishowa	4 hours
Whitemud	13 hours
North Star	21 hours
Hotchkiss	29 hours
Notikewin	38 hours

Using these lag times, routed discharges were estimated at each point for the date of survey and for the date and time of dye injection and sampling. For the dye test period from 27 February to 2 March 1993, the local discharges as estimated for the various sampling points were almost constant.

Hydraulic and dye-test computations were initially conducted using a preliminary set of discharges provided by Alberta Environment, based on processing of hourly stage readings at the Peace River gauge. During report preparation, a set of preliminary daily-flow estimates was made available by Water Survey of Canada, based on a somewhat different processing of the same readings. Preliminary daily-flow estimates for the Peace Point gauge, some 740 km downstream of Peace River, were also obtained from Water Survey of Canada. Figure 3.2 compares these three data sets with respect to flows at Peace River, taking into account the lag time between Peace River and Peace Point. After consideration of this comparison, some adjustments were made to the initial computations. Overall, the surveys were conducted at discharges between 1600 and 1900 m³/s approximately, and the dye test at a discharge of about 1740 m³/s.

3.2 Channel Geometry

3.2.1 River slopes

River hydraulic slopes between study points were determined using water levels as observed in drill holes through the ice during the survey period from 17 to 24 February 1993. The observed elevations were adjusted by from 0.1 to 0.3 m to correspond to a constant discharge of approximately 1600 m³/s. The adjusted data are shown in Table 3.1 and the slope profile over the 187-km study length is shown in Figure 3.3. Reach slopes range from a maximum of approximately 0.34 m/km downstream of Peace River to a minimum of approximately 0.20 m/km upstream of Notikewin. Comparison with an approximate slope profile for the entire length of the Peace River presented by Kellerhals et al (1972) indicates that there must be a substantial flattening of slope in the downstream 80-km length between Notikewin and Carcajou.

The hydraulic slope shown between Mackenzie Cairn and Peace River checks very closely with a determination for January 1982 as reported by Neill and Andres (1984). Because of special circumstances the ice was about 4 m thick in 1982, compared to a little over 1 m in 1993.

3.2.2 Cross-sections

Cross-sections as surveyed through the ice at the 8 dye injection and sampling locations (Figure 1.1) are shown in Figures 3.4a-c. The sections are numbered from 0 (Shaftesbury Ferry, dye injection site) to 7 (Notikewin River, last sampling site). Cross-sectional properties – average ice thickness, under-ice area and top width, and hydraulic radius – are listed in Table 3.2. The hydraulic radius with ice cover is approximated as under-ice area divided by twice the under-ice surface width. (The mean depth is therefore twice the tabulated hydraulic radius.) Under-ice widths vary from 315 to 480 m, and mean depths from 4.6 to 7.5 m.

There is only a limited amount of information that can indicate how representative are the surveyed sections of the various river reaches. There is a set of 45 open-water cross-sections surveyed by Alberta Environment, mostly in 1982–84, over the upper 56 km of the study length; also a set of 8 winter cross-sections surveyed in February 1983 over the upper 30 km. Elsewhere, the only feasible comparison is with map widths. Cross-section and reach properties are therefore compared here mainly in terms of map widths.

The average under-ice width of the surveyed sections is approximately 400 m, which averages about 90% of the corresponding map widths (1:50 000 scale). Using a series of map widths reduced by 10%, an overall average under-ice width for the study length is estimated as about 450 m. This suggests that overall, the surveyed sections are a little narrower than average.

Comparison with reach-averaged map widths and with selected other cross-sections indicates that with two exceptions, the sections are reasonably representative of reaches straddling each section. The exceptions are the North Star section (no.5), which is considerably wider than the reach average and the Notikewin section (no.7), which appears to be relatively narrow.

3.2.3 Ice thicknesses

During the survey period from 17 to 24 February 1993, width-averaged total ice thicknesses at the 8 dye-test sections ranged from 1.0 to 1.9 m, with an overall average of 1.3 m (Table 3.2). At the Peace River site, the value was 1.0 m.

Some previous information on spatial variability of ice thicknesses is available from a survey by Alberta Environment of 22–24 February 1983 (Table 3.3). The data cover only the upper 30 km of the present 187-km study length. Thicknesses of solid and slush ice were quoted separately. Width-averaged solid ice thicknesses ranged from 0.6 to 0.9 m, and total thicknesses from 1.0 to 1.9 m with an overall average of 1.4 m. These total-thickness statistics are almost identical to those from the 1993 surveys.

Previous information on seasonal and year-to-year variations in ice thickness at a single point is available from annual surveys at the Water Survey of Canada winter gauging site in Peace River town. Table 3.4 shows data from a set of 13 surveys over the period 1983–86. Width-averaged solid ice thicknesses ranged from 0.4 to 1.2 m with a mean of 0.8 m, and total thicknesses from 1.0 to 1.9 m with a mean of 1.5 m. The last figure is somewhat greater than the corresponding February 1993 observation of 1.0 m.

3.3 Computed Channel Velocities and Roughnesses

Calculated mean channel velocities and composite hydraulic roughness values based on surveyed cross-sectional properties are shown in Table 3.2 for each of the 7 reaches. Tabulated mean velocities were determined by dividing the local discharge by the average under-ice cross-sectional area. Roughness coefficients were estimated by applying the Manning equation, using a reach slope based on the longitudinal profile of Figure 3.3.

Tabulated mean channel velocities range from 0.57 to 0.88 m/s with an average of 0.74 m/s. Composite roughness coefficients range from 0.039 to 0.059 with an overall average of 0.046. This average is close to the value of 0.043 reported by Neill and Andres (1984) for an 18-km reach near Peace River town in January 1982. These roughness values are composite values that include the effects of ice underside roughness, river bed roughness, expansion and contraction losses due to channel irregularity and curvature, and probably partial blockage by frazil ice. This issue is discussed further in Section 3.5.

Roughness values for individual reaches indicate that the roughness was significantly greater in the downstream half of the study length. This result is consistent with the ice cover characteristics described in Section 2.1.2 and Table 2.1, which indicate a generally rough, shoved and thicker cover downstream of Whitemud River, compared to a generally smooth, juxtaposed cover upstream of that point.

3.4 Dye Test Results

Dye concentrations as measured across each sampling cross-section are plotted as functions of time in Figures 3.5a–g. Observed travel times and associated dye-cloud velocities over the seven river reaches are shown in Table 3.5.

In dye-test time-of-travel analysis, four parameters are used to characterize a local concentration distribution with respect to time. The **leading edge** defines when the concentration first begins to rise, the **peak** defines when the maximum concentration occurs, the **centroid** defines the centre of mass of the cloud, and the **trailing edge** defines when the concentration returns to near background levels. Travel times of all these parameters vary across the channel, typically being shorter in the centre and longer near the banks, as shown for example for the Notikewin section in Figure 3.6.

For each cross-section, the centroid travel times of the several concentration distributions across the channel were converted into a width-averaged value by numerically integrating their cross-channel distribution with respect to cumulative mass distribution of dye. The other three time-of-travel values (leading edge, peak and trailing edge) were width-averaged by integrating their cross-channel distributions with respect to cumulative discharge. It should be noted that the end points in Figure 3.6 and similar plots are extrapolated, not sampled.

In most cases, the travel time of the peak is slightly shorter than that of the centroid. However, in the final reach between Hotchkiss and Notikewin, the peak travel time appears to be longer (Table 3.5): minor variations in peak and centroid travel times produce this effect. As shown in Figure 3.7, where the cumulative travel times are compared as functions of distances from the injection point, the centroid never actually overtakes the peak. The travel time of the centroid is typically about 5% longer than that of the peak.

It can be argued that in a natural stream with zones of stagnant or slow-moving water, dye-cloud peak velocities should be more representative than centroid velocities of the stream's

hydraulic characteristics. In this case, however, those differences (Table 3.5) are small compared to differences between dye-cloud velocities as a whole and mean channel velocities as calculated from river discharges and cross-sectional areas (Table 3.2). These larger differences are examined in Section 3.5 below.

It can be inferred from Figures 3.5 a-c that in the upper part of the study length, more frequent sampling and a greater number of sampling holes per cross-section would have permitted more reliable determination of dosage and of concentrations at the sides of the channel. These points should receive consideration in planning future field programs of a similar nature; however, the optimal sampling program cannot be always identified "a priori".

3.5 Comparison of Channel and Dye-cloud Velocities

Table 3.6 compares reach-averaged values of mean channel velocity calculated from the cross-sectional data (Table 3.2) with dye-cloud velocities determined from travel times (Table 3.5). Over the whole study length (for discharges in the vicinity of 1700 m³/s) the dye-cloud velocity appears to exceed the mean channel velocities by 40%, and in individual reaches the exceedance is up to 60%. The extent of these differences is somewhat surprising. Three possible reasons are discussed below.

1. Incomplete transverse mixing. In the first four reaches extending from Shaftesbury Ferry to the Whitemud River, transverse mixing was not fully established (see Table 4.1 and Section 5.1). This means that the dye cloud moved predominantly in a central zone of the flow at a velocity exceeding the cross-sectional mean (described here as the mean channel velocity). In a previous study on the North Saskatchewan River (Van Der Vinne 1991) it was found that in the initial reach downstream of a central injection site the dye-cloud velocity could exceed the cross-sectional mean by about 10%. In the present case, however, the exceedance is

considerably larger and persists downstream into reaches where transverse mixing was fully developed. This explanation therefore cannot fully account for the differences.

2. Unrepresentative surveyed cross-sections. The surveyed cross-sections on which the Table 3.2 velocities are based may be larger in cross-sectional area than the average channel sections for each reach. A comparison with average map widths, however, indicated that if anything the surveyed sections were narrower than average (see Section 3.2.2). Although information on average depths between sections is generally lacking, it seems unlikely that this hypothesis can explain much of the difference.

3. Frazil blockage. It is known that frazil or slush ice was present under the ice cover. Initial interpretation of observations at the surveyed sections suggested that accumulated frazil was not significant enough to have a large impact on channel hydraulics (see Section 2.3.2). However, the surveyed sections were far apart and little is known of under-ice conditions between them. It is therefore possible that channel blockage by frazil accumulations was generally more significant than it appeared. All things considered, this appears to be the most likely explanation for the greater part of the differences.

The transverse discharge distributions shown in Figures 4.1a-d show that the "theoretical" curves based on the Manning formula (see Section 4.3) over-estimate the actual partial discharges in the shallow zones near the banks. To carry the argument a little farther, if it is assumed that a certain portion of the cross-section near the banks does not effectively contribute to conveyance because of very low velocities due to frazil blockage or very shallow depths, then there is a central "effective" area associated with a greater mean velocity and mean depth than computed from the full under-ice cross-section. If the effective area is defined as that accounting for 90% of the theoretical discharge distribution as plotted in Figures 4.1a-h (discounting 5% at each side), then the effective under-ice width is reduced to approximately

70% of the surveyed width. Table 3.7 shows channel widths and mean depths as re-computed using this concept.

Traditional practice in analyzing open channel hydraulics utilizes a mean velocity equal to the discharge divided by the cross-sectional area. This may not be the best approach for analyzing certain river channels, especially under ice cover, where there are zones of very low velocity near the banks and the velocities in the central zone are considerably higher than the cross-sectional mean. Using the alternative approach suggested above, effective roughness values computed for the central zone are considerably lower than those computed for the whole section, as shown in Table 3.8. Such a result raises difficulties regarding comparability with other studies and in deciding "a priori" (in future cases) what are the fundamental channel characteristics on the basis of only a few surveyed cross-sections.

4. TRANSVERSE MIXING

4.1 Theoretical Summary

The theory of transverse mixing has been presented fully in a previous report (Van Der Vinne 1992) and is given here in condensed form.

River mixing from a point source begins as a three-dimensional process, but concentrations become uniform over the depth in a relatively short distance. Using equations by Elhadi et al (1984), the vertical mixing length for the present study can be estimated as only 0.9 km, whereas the length of the first reach is 8.3 km. The mixing process can therefore be treated as effectively two-dimensional in the horizontal plane. Table 4.1 compares the vertical mixing length with estimates of the transverse mixing length (see Section 5.1) and the linear mixing length (see Section 5.2.1).

The basic partial differential equation for mass transport in 2-D steady-state mixing can be transformed (Yotsukura and Sayre 1976) to

$$\frac{\partial C}{\partial x} = \frac{\partial}{\partial q_c} \left(u h^2 e_z \frac{\partial C}{\partial q_c} \right) \quad [4.1]$$

where C is local depth-averaged concentration, x denotes distance along the river, q_c is cumulative discharge across the channel (normally measured from the left bank), u is local depth-averaged velocity, h is local depth, and e_z is the transverse mixing coefficient. This equation can be simplified further by introducing a diffusion factor D_z , which in terms of average flow parameters is defined (Beltaos 1978a) by

$$D_z = \psi UH^2 m_x e_z \quad [4.2]$$

where U , H , m_x , and e_z are cross-section average values and ψ is a shape-velocity factor defined as

$$\psi = \int_0^1 \left(\frac{h}{H}\right)^3 \left(\frac{u}{U}\right)^2 d\left(\frac{z}{B}\right) \quad [4.3]$$

where B is the river width and z is the transverse distance from the left bank. The value of ψ is generally between 1.0 and 3.2 for natural channels (Beltaos, 1978a). Values of ψ calculated from the Peace River cross-sections range between 1.7 and 3.2 (Table 4.2).

Transverse mixing coefficients can be evaluated using time-varying concentration data by introducing the concept of dosage θ , defined as the area under the time-concentration curve

$$\theta = \int_0^{\infty} C dt \quad [4.4]$$

where C is the concentration and t is the time from injection. Beltaos (1975) showed that the dosage for an instantaneous injection behaves exactly the same as the steady-state concentration for a continuous injection. Equation [4.1] thus becomes

$$\frac{\partial \theta}{\partial x} = D_z \frac{\partial^2 \theta}{\partial z^2} \quad [4.5]$$

A number of dimensionless mixing parameters have been proposed to facilitate the estimation of mixing coefficients from known hydraulic characteristics. Gowda (1984) proposed a dimensionless diffusion factor, β_z , defined as

$$\beta_z = \frac{D_z B}{Q^2} = \frac{\psi m_x e_z}{UB} \quad [4.6]$$

This form of the dimensionless diffusion factor can be obtained by restating Equation [4.5] using the dimensionless cumulative discharge, $\eta = q_d/Q$, a dimensionless distance, $\chi = x/B$, and a dimensionless dosage $\phi = \theta Q/M_0$. The resulting equation is

$$\frac{\partial \phi}{\partial \chi} = \beta_z \frac{\partial^2 \phi}{\partial \eta^2} \quad [4.7]$$

where the dimensionless diffusion factor is defined in Equation [4.6]. Alternatively, Fischer et al. (1979) recommended the following dimensionless transverse mixing coefficient:

$$k_t = \frac{e_z}{U_* H} = \frac{D_z}{\psi m_x U_* U H^3} \quad [4.8]$$

4.2 Method of Evaluating Coefficients from Field Data

The diffusion factor, D_z can be evaluated using the following relationship (Beltaos 1978a)

$$D_z = \frac{Q^2 \sigma_\eta^2}{2 \int_0^x f(x) dx} \quad [4.9]$$

where σ_η^2 is the variance of the dosage distribution with respect to the dimensionless cumulative discharge, $\eta = q_d/Q$ and $f(x)$ is a function of x which accounts for the confining effect of the river banks on the dosage distribution. The confinement function is defined as

$$f(x) = 1 - (1 - \eta_0) \frac{Q}{M} \theta_{RB} - \eta_0 \frac{Q}{M} \theta_{LB} \quad [4.10]$$

where η_0 is the transverse proportional location of the centroid of the dosage distribution, M is the total mass of pollutant, and θ_{RB} and θ_{LB} are the dosages at the right and left banks respectively.

The transverse mixing coefficient, e_z can be evaluated from the diffusion factor using Equation [4.2]. This requires that appropriate mean velocities U and mean depths H be evaluated for the transverse mixing zone. (In the present study, the river curvature coefficient m_c can be neglected as it is very close to unity.) The mean velocities can be obtained directly from the travel time measurements. The mean depths are more difficult to evaluate because insufficient data are available to define reach-average depths independently. However, as discussed in Section 3.5, an effective flow area can be calculated by dividing the discharge by the mean dye-cloud velocity. Reach-average depths can then be estimated by dividing effective flow areas by effective widths as defined in Section 3.5.

4.3 Analysis of Dye Test Results

Cumulative discharge distributions across the channel at the sample sites are plotted in Figures 4.1a – h. To calculate those, local velocities were estimated from local depths using the following relationship based on the Manning equation:

$$\frac{u}{U} = \left(\frac{h}{H} \right)^{\frac{2}{3}} \quad [4.11]$$

Local velocities were calculated rather than measured at most sites because the discharges and depths during the tests were different from those during the surveys and there was lack of

confidence in the velocity measurements at some sites. However, measured velocities at Peace River town should be reasonably accurate as they were provided by the Water Survey of Canada. Figure 4.1c compares the measured discharge distribution at Peace River with those estimated by Equation [4.11]; the discrepancies amount to less than 4% of the total discharge. It is considered that errors in calculated velocities may be as great as 10% at some other sites, especially if slack water or an eddy was present as suggested by velocity measurements at Daishowa (Figure 4.1d) and Notikewin (Figure 4.1h). Local depths were adjusted from survey depths to account for changes in water levels between the surveys and the dye test.

Transverse dosage distributions for all the sampling sites are shown in Figure 4.2, and dosage distribution parameters are summarized in Table 4.2. Right and left bank dosages were estimated by linear extrapolation from calculated values at the nearest two sample holes. The sites nearest the injection point exhibit high dosages in the centre of the channel and low values near the banks. The sites from Whitemud River downstream exhibit very uniform distributions, indicating that transverse mixing was more or less complete somewhere between Daishowa and Whitemud River.

Dosage distribution parameters summarized in Table 4.2 are those required to evaluate the diffusion factor using Equation [4.9]. The theoretical upper limit of the variance is 0.083 for an uniform distribution. Once the variance approaches this value, transverse mixing is complete and values farther downstream do not contribute to the solution. The diffusion factor for the transverse mixing length was evaluated using a plot (Figure 4.3) of dosage variance against the distance integral of the confinement function as defined in Equation [4.10]. The slope of the linear regression line was used in Equation 4.9 to calculate an average value of D_z . This value of D_z for the transverse mixing length is shown in Table 4.3, along with calculated values for individual reaches. Some of the reach-to-reach variation is probably due to minor errors in dosage distributions, which are compounded in the calculations.

Values of the transverse mixing coefficient e_z were calculated from D_z using Equation 4.2. The hydraulic characteristics used in the calculations were obtained from the travel times as explained in Section 4.2. Table 4.3 shows calculated values of e_z for each of the first four reaches, also the average for the transverse mixing length.

Two sets of dimensionless diffusion factors and transverse mixing coefficients were calculated and are listed in Table 4.3. The first set was calculated from the hydraulic characteristics obtained using the adjusted river widths presented in Section 3.5, and the second set was calculated from the hydraulic characteristics obtained using the full river widths. This second set of values is included so that the results of this study can be compared with those of previous studies. Figures 4.4a and 4.4b plot the results for the Peace River and other rivers against a composite hydraulic parameter composed of the ratio of mean to shear velocity and the channel aspect ratio (Elhadi et al. 1984). The values obtained using the full widths are similar to those of previous studies; however, the reduced width analysis produced values below this range. The parameters from previous studies might also be reduced if they were to be calculated using a reduced width; however, the triangular shape of the Peace River cross-sections tends to make the reductions in the present study more significant. That is, the more trapezoidal cross-sections of the rivers in most previous studies makes the difference in mean flow depth between the two types of analysis much smaller than in the present study. Open water data from previous studies are included in Figure 4.4 for comparison: it is difficult to discern any systematic distinction between ice-covered and open-water data.

4.4 Discussion of Transverse Mixing Results

Some of the scatter in the dimensional parameter values shown in Figure 4.4 may be due to errors in estimating hydraulic characteristics. For example, mean velocities determined from peak dye travel times are likely to be over-estimates, because at first only the central portion of the channel is occupied by dye. Also, under-ice widths used in many of the studies are likely

to be too large: closer correspondence with present study results would be obtained if effective widths were used. Some of the scatter in the data has also been attributed to river sinuosity (Lau and Krishnappan, 1981).

There is likely to be less error in the determination of the dimensionless diffusion factor, β_z , than in the dimensionless transverse mixing coefficient, k_t , because β_z is calculated directly from the measured parameters of top width and discharge rather than depending on the cube of the estimated mean depth. According to Equation [4.6], the dimensionless diffusion factor should be independent of hydraulic characteristics; however, the data in Figure 4.4a do appear to exhibit a slight dependence on channel aspect ratio and the ratio of mean to shear velocity. Figure 4.4b, on the other hand, suggests that k_t may be independent of these factors.

The overall scatter and uncertainty in the data make it difficult to predict the transverse mixing characteristics of a given river without actual field measurements. The fact that coefficients determined from the present study fall below the previous range does not improve confidence in transfer of the data. Also, the data do not conclusively indicate which dimensionless parameter is more appropriate or how the parameters vary with hydraulic characteristics.

4.5 Comparison with Prediction Models

Two different techniques are available to model transverse mixing: (1) analytical solutions which assume reach-average values for the hydraulic and mixing characteristics, and (2) numerical solutions which use a series of local hydraulic and mixing values. Analytical models are relatively quick and easy to use for preliminary assessments, and are also sufficient if few field data are available. For example, transverse mixing coefficients were evaluated in the present study using an analytical model because there were insufficient winter cross-sections to

warrant use of a numerical model: the numerical model would provide similar results but require greater effort.

An analytical solution of the two-dimensional steady-state mixing equation for a point source located at η_i is

$$\frac{C}{C_\infty} = \frac{\theta}{\theta_\infty} = \frac{1}{\sqrt{2\pi\xi}} \sum_{n=-\infty}^{\infty} \left[\exp\left(-\frac{(\eta-2n+\eta_i)^2}{2\xi}\right) + \exp\left(-\frac{(\eta-2n-\eta_i)^2}{2\xi}\right) \right] \quad [4.12]$$

where C_∞ is defined as the injected mass per unit time, $\partial M/\partial t$, divided by the total discharge Q ; θ_∞ is the injected mass divided by the total discharge; $\eta = q_i/Q$ is the cumulative fraction of discharge; $\xi = 2xD_i/Q^2$ is a dimensionless distance, and n is an integer which accounts for the reflections from the opposite bank (Fischer et al., 1979). Equation 4.12 is a more concise form of the original equation proposed by Yotsukura and Cobb (1972).

Figures 4.5a–g compare measured dosage distributions at the seven Peace River sampling sites with predictions obtained from this equation for a centreline injection ($\eta_i = 0.5$). The predicted values consistently exceed the measured values because they do not allow for dye losses. Even after taking this into account, the predicted dosages near the banks are consistently higher than those estimated from the linear extrapolation technique discussed in Section 4.3.

Numerical models such as TRANSMIX (Putz, 1984) or RIVMIX (Lau and Krishnappan, 1982) are more accurate than the above analytical model when there are sufficient cross-sections available to characterize the variations in width and depth in each subreach. Numerical models, however, require more time and effort because of the increased data requirements.

All the models discussed above deal with steady-state conditions, but in some cases it is desirable to model two-dimensional unsteady mixing using models such as MIX2DARC (Beltaos and Arora, 1988). If the present dye-test were to be modelled numerically, such a procedure might be advisable.

5. LONGITUDINAL MIXING

5.1 Transverse Mixing Length

Longitudinal mixing becomes the dominant mixing process once transverse mixing is completed. For unsteady injections, as from the present field test or from a pollutant spill, mixing continues due to longitudinal dispersion, which spreads the dye or pollutant in the direction of flow. For steady state injections, on the other hand, no further mixing occurs once transverse mixing is completed.

Transverse mixing is considered complete when concentrations or dosages become essentially uniform over the channel width. This is usually defined as where the variations in dosage across the channel are less than 5% of the mean. The distance from the source at which this occurs is called the transverse mixing length, L_t , which can be estimated from

$$L_t = \frac{1}{\psi k_t k_p} \frac{UB^2}{U_* H} \quad [5.1]$$

where k_p is a position parameter (Yotsukura and Cobb 1972) which varies with the position of the source in the cross-section, as shown in Table 5.1. A shape factor ψ , as defined in Eq. 4.3, is included in Equation 5.1 because average hydraulic characteristics are used. (Other symbols are defined in Appendix B.)

For the Peace River study length, the calculated transverse mixing length is 107 km (Table 4.1) which places the point of complete mixing between the Whitemud River and North Star sampling sites. This length was calculated using a weighted average value of 2.9 for the shape factor ψ between Shaftesbury Ferry and Whitemud River, the weighting being done according to the reach lengths. The calculated length is slightly greater than indicated by dosage

distribution data (Figure 4.2), which suggest a virtually uniform transverse distribution upstream of Whitemud River, 83 km from the injection point.

5.2 Theoretical Summary

Longitudinal dispersion data can be interpreted by two different techniques: (1) as an extension of turbulent mixing (Fickian dispersion), or (2) as a storage and release phenomenon. Both processes occur physically, but the governing equation has been solved only for cases where one of the processes is assumed to be dominant.

5.2.1 Turbulent mixing (linear dispersion) model

In computing longitudinal mixing characteristics, cross-sectional average values of concentration are used in order to eliminate the transverse variations. The theory of Fickian longitudinal dispersion results in a longitudinal dispersion coefficient D_x defined by

$$D_x = \frac{U^3}{2} \frac{d\sigma_t^2}{dx} \quad [5.2]$$

where U is the cross-sectional mean velocity and σ_t^2 is the variance of the concentration distribution with respect to time.

Fickian dispersion does not occur immediately after transverse mixing is complete. At first, differential advection and variations in channel geometry cause faster longitudinal mixing. Field measurements suggest that in this intermediate region the standard deviation σ_t of the time-concentration distribution grows linearly with distance; this type of mixing is therefore called linear dispersion.

Beltaos (1978b) proposed the following empirical solution for linear dispersion based on the available data:

$$\bar{C} = \frac{MU}{Qx\sqrt{2\pi\beta_x}} \left[\frac{Ut}{x} \exp\left(1 - \frac{Ut}{x}\right) \right]^{1/\beta_x} \quad [5.3]$$

where β_x is a dimensionless parameter defined by

$$\beta_x = \left(\frac{U\sigma_t}{x} \right)^2 \quad [5.4]$$

The location of the transition from linear dispersion to Fickian dispersion can be estimated using

$$L_L = \alpha_L \frac{UB^2}{U_*H} \quad [5.5]$$

where L_L is called the linear mixing length and α_L is a factor varying between 0.48 and 1.8 depending on the degree of channel irregularity (Beltaos, 1978b). The transition to Fickian dispersion occurs gradually between L_L and $3L_L$; however, in most cases it is sufficient to define the transition at $2L_L$. The linear mixing length L_L estimated by assuming $\alpha_L = 1.0$ is given in Table 4.1. The value of 186 km indicates that Fickian dispersion does not occur within the Peace River study length. The Fickian dispersion coefficient therefore cannot be evaluated from the test data.

5.2.2 Storage and release model

Some researchers such as Beer and Young (1983) and Sabol and Nordin (1978) have proposed that the non-Fickian behaviour observed in the linear dispersion region is the result of the storage and subsequent release of pollutant in 'dead zones'. These dead zones are areas of the river such as eddies in which little or no net flow occurs. Beer and Young (1983) proposed

that a storage component be substituted for the dispersive component in the usual one-dimensional mixing equation. The resulting modified equation is

$$\frac{\partial \bar{C}}{\partial t} + U \frac{\partial \bar{C}}{\partial x} = \frac{1}{T_e} (C_s - \bar{C}) \quad [5.6]$$

which represents an aggregated storage model in which each reach of the river has two components: a length of pure translational flow with a concentration C_s , following by a mixing tank with an exit concentration \bar{C} . The reach length is defined so that the aggregated effects of the dead zones within the reach are represented by a single mixing tank with an effective time constant T_e (Beer and Young, 1983). It is assumed that this time constant is proportional to the peak travel time through the reach, t_p , since the mixing tank represents the aggregate effects of storage in the dead zones. That is

$$\alpha_x = \frac{t_p}{T_e} \quad [5.7]$$

where α_x is a dimensionless parameter inversely proportional to the dead-zone (or mixing-tank) volume.

A solution can be obtained for equation [5.6] if the output from one reach is used as the input for the next reach. It takes the form

$$\bar{C} = \frac{M \alpha_x}{t_p Q m!} \left(\alpha_x \frac{t_s}{t_p} \right)^m \exp \left(-\alpha_x \frac{t_s}{t_p} \right) \quad [5.8]$$

where m is an integer representing the number of reaches, each having a length corresponding to the transverse mixing length L_t . This solution assumes that the pollutant is completely mixed across the channel in one reach before entering the next. The distance required to completely mix the pollutant across the channel is the transverse mixing length, therefore this length can be used to define the reach length.

The local time t_s is defined as

$$t_s = t - \frac{x}{U} + \frac{m}{\alpha_x} \frac{x}{U} \quad [5.9]$$

where t is the total time from injection, x/U represents the peak travel time t_p , and the last term accounts for the increasing lag of the peak concentration behind the leading edge as the pollutant spreads longitudinally.

5.3 Method of Evaluating Coefficients from Field Data

The linear dispersion parameter and the storage parameters of the above-described models can be evaluated directly from dye-test data using the following techniques.

5.3.1 Linear dispersion parameter

Evaluation of the linear dispersion parameter β_x from measured concentrations can be simplified by defining the pollutant spread in terms of the half-duration ΔT rather than the standard deviation. The half-duration is defined as the period of time during which the concentration is greater than one-half of the peak concentration. The half-duration of the empirical curve described by Equation [5.3] is equal to $2.36 \sigma_x$; therefore β_x can be defined in terms of ΔT as follows

$$\beta_x = 0.18 \left(\frac{\Delta T}{t_p} \right)^2 \quad [5.10]$$

5.3.2 Storage parameters

The storage zone number, m for a given site can be obtained from

$$m = \left(1 + \frac{x}{L_t} \right) \quad [5.11]$$

where m is truncated to a whole number because the length of each storage zone was defined previously as the transverse mixing length, L_t . The behaviour of the model is such that as m increases with distance, the shape of the concentration distributions becomes less skewed. When m becomes greater than about 10, the storage model predicts symmetrical distributions typical of Fickian dispersion (Figure 5.1). The curves in Figure 5.1 indicate that a significant change in shape occurs with changes in m . Nevertheless, L_t can usually be estimated within a factor of 2 using Equation 5.1, therefore the error in the predicted peak concentration will be only a fraction of the range shown in Figure 5.1.

An expression for evaluating the storage coefficient α_x can be obtained by differentiating Equation [5.8] to find the time of the peak concentration relative to the leading edge. This time is substituted back into Equation [5.8] to obtain an equation for the peak concentration, C_p . This equation can then be rearranged to define the storage coefficient

$$\alpha_x = \frac{C_p t_p Q}{M} \left(\frac{m!}{m^m e^{(-m)}} \right) \quad [5.12]$$

in terms of directly measurable parameters as well as the zone number m .

5.4 Analysis of Dye Test Results

5.4.1 Linear dispersion parameter

The values of half-duration and time-to-peak for each reach are given in Table 5.2, along with other variables which describe the cross-sectionally averaged concentration distributions with respect to time. (Times-to-peak in Table 5.2 are slightly different from those used to calculate travel times, because a different method of averaging was used.)

Average values of the linear dispersion parameter β_x for the whole Peace River study length can be obtained from the slope of the best fit line through the half-duration versus time-to-peak data shown in Figure 5.2. However, the data indicate that incomplete transverse mixing may have reduced the apparent value of β_x in the reaches between Shaftesbury Ferry and Daishowa. Therefore, the most appropriate value is obtained from the data between Daishowa and Notikewin. This value is presented in Table 5.3 along with two sets of hydraulic characteristics: one calculated using the full river width and the other calculated using a reduced river width. The full river width basis is more appropriate for comparing the linear dispersion parameter with those other rivers, whereas the reduced width basis is considered better for describing the hydraulic characteristics of the Peace River, as discussed in Section 3.5.

The calculated value of β_x , 0.014, is quite high compared to previously studied rivers, especially relative to the correlation of β_x with U^*/U shown in Figure 5.3. The use of different river widths to evaluate the hydraulic characteristics does not significantly affect the comparison. The high value of β_x for the Peace River can be explained on the basis of the generally triangular shape of the cross-sections. This type of cross-section tends to have a greater cross-sectional variation in velocity than a trapezoidal section. The action of differential advection, a major cause of linear dispersion, is therefore enhanced.

5.4.2 Storage parameters

The dimensionless peak concentration $C_p t_p Q/M$ was found to decrease with distance in the first storage zone and then become essentially constant in the second zone, as shown in Figure 5.4. The fall in dimensionless peak concentration through the first storage zone signifies an increase in measured storage, which might be due to an actual increase in storage or to more effective measurement as the dye cloud spreads across the channel. (This question could only be resolved by an additional dye test with injection farther upstream.)

Figure 5.4 includes data for three previous dye tests in the Athabasca River between Athabasca and Bitumont (Van Der Vinne 1992b). The ranges in dimensionless peak concentration are similar for both rivers, but only one of the Athabasca River lengths exhibits such a marked drop between the first and second storage zones. The high initial values in those two lengths may be due to incomplete transverse mixing where the storage effects of the near-bank areas were not accounted for. The data indicate a trend to values of around 4 to 6 at some distance from the injection points.

Calculated values of $C_p t_p Q/M$, m and α_x for each reach between sampling points are given in Table 5.4. Because of the limited data, no relationship between the α_x and hydraulic characteristics can be established at this time, which limits the present usefulness of the storage model. However, the storage model more accurately reproduces the shape of the concentration distributions at any location. Additional efforts to quantify the storage parameters may therefore be useful. The reaches with the lowest values of α_x (high storage volume) are the same reaches with the greatest variability in ice thickness, and possibly also in width and depth. The rate of longitudinal mixing may depend on the variability of geometric and hydraulic parameters along the channel rather than on mean values, because it is the variability of these parameters which produces the storage zones. Defining the variability of these parameters, however, is more difficult than establishing mean values.

5.5 Comparison with Model Predictions

The applicability to the present study of both the linear dispersion model and the storage model can be improved if t_p is calculated as the sum of reach travel times rather than from a mean velocity over the whole study length. This was done in generating the model predictions that are compared with field data in Figures 5.5a–d.

Peak concentrations predicted by the storage model might be expected to be more compatible with the data than those of the linear dispersion model, because the storage coefficient was evaluated from measured peaks whereas the linear dispersion parameter was evaluated using the spread of the concentration distributions. Figures 5.5a–d also indicate that the storage model curves provide the better fit to the shape of the data sets. Both models predict peak concentrations higher than the measured values: this is because the model predictions were generated assuming conservation of the injected mass, whereas measurements indicate losses of as great as 40% (see Section 2.4).

The wide scatter in the plot of linear dispersion parameter β_x versus U^*/U presented in Figure 5.3 shows that it is difficult to select an appropriate value using only hydraulic data for an untested river length. The sensitivity of Beltraos' linear dispersion model to a similar range of scatter is illustrated in Figure 5.6. A similar difficulty arises in selecting a storage parameter. The sensitivity of the storage model to the range of α_x shown in Table 5.4 is illustrated in Figure 5.7. For both models, the predicted peak concentrations produced by the assumed ranges in α_x vary by a factor of four. Local tracer measurements, such as those obtained from the present study, therefore appear to be necessary if reliable estimation of peak concentrations is required.

The storage parameter α_x might be expected to increase with increasing discharge, because the storage area in a typical cross-section would be reduced relative to the effective flow area.

For winter flows, where discharge variations are relatively small, α_r can probably be assumed constant. Further work is evidently needed to determine the sensitivity of α_r to hydraulic characteristics.

6. CONCLUSIONS AND RECOMMENDATIONS

6.1 General Discussion

Before summarizing the quantitative results of the study, a number of points of a general or qualitative nature will be discussed.

1. Overall result of study. The field investigations and office analyses described herein have enabled quantification by reaches of the average hydraulic characteristics of a 187-km ice-covered length of the Peace River, and thereby have allowed determination of under-ice travel times and mixing parameters.

2. Effects of frazil ice. The winter season of 1992-93, during which the field dye test was performed, was not particularly severe with respect to ice conditions including accumulations of frazil. Even so, practical difficulties were encountered in measuring dye concentrations where there were considerable frazil accumulations, and in defining reach-averaged hydraulic characteristics that took proper account of frazil effects. Apparent dye losses in the order of 40% were found at sampling sites which exhibited frazil accumulations. Fortunately, reliable determination of the mixing parameters does not require conservation of the dye mass. However, comparison of the calculated mixing characteristics with those of previous studies is complicated by the way the hydraulic characteristics are defined, as discussed further below.

3. Definition of reach hydraulics. Efforts were made to resolve differences between mean velocities (1) as calculated from channel geometry at surveyed cross-sections, and (2) as indicated by the travel times of the dye cloud. On the average, the dye-cloud velocities were approximately 40% higher than those calculated from the surveyed cross-sections, suggesting that effective flow areas were substantially smaller than indicated by the cross-sections. Another aspect of the same problem is that if an under-ice top width consistent with the surveyed cross-

sections and topographic maps is used in conjunction with measured dye–cloud velocities to calculate flow depths and hydraulic radii – as has been done in some previous studies – those calculated parameters are substantially smaller than indicated by the cross–section surveys. To resolve those discrepancies, the hypothesis was adopted that frazil accumulations created dead zones such that 5% of the theoretical discharge was discounted at each bank. The effective top widths were thereby reduced to represent the middle 70% or so of the channel width only. Using these reduced widths, effective flow depths and hydraulic radii calculated from dye–cloud velocities correspond more closely to those determined from the surveyed cross–sections.

This deviation from previous local practice in analyzing dye tests analysis produces some inconsistencies in calculating representative roughness coefficients and mixing parameters, which introduce difficulties when comparing results with previous studies in which there was no basis for reducing the width or obtaining an independent measure of velocity. Despite those difficulties, however, it is considered that the effects of frazil accumulations on the hydraulic characteristics were significant enough in the present study to warrant a modified method of data treatment. Mixing characteristics were evaluated on the basis of both full–width and reduced–width hydraulic parameters.

4. Mixing characteristics. Transverse mixing was found to be weak in the Peace River, but within the range of values for other ice covered rivers when transverse mixing parameters were evaluated using the full top width. However, when the dimensionless transverse mixing coefficient was evaluated using reduced top widths which were more consistent with the hydraulic characteristics, the values were found to be lower than in previous river studies and lower even than in laboratory flume studies (see Elhadi et al 1984). The linear dispersion parameter, on the other hand, was at the top end of the range of values determined from other studies. These findings are consistent with the relatively straight alignment and generally triangular shape of the channel compared to the rivers in other studies.

Some hypotheses can be advanced to explain these differences between the findings on transverse and longitudinal mixing. The presence of easily-transportable frazil may allow the flow to generate a particularly efficient channel shape that reduces bed and bank resistance and the effects of depth variability on velocity profiles. This would tend to reduce the size and intensity of turbulent eddies and hence produce higher velocities and less intense transverse mixing than would be the case for an immobile channel boundary. Longitudinal mixing, on the other hand, might be unaffected because it is controlled mostly by storage (dead zones) within the channel.

5. Extrapolability of results within Peace River. The results of the present study should be capable of extrapolation to other winter discharges and ice conditions within the present study reach. With respect to transfer to other lengths, however, the study length represents only about 20% of the total length of concern between the mouth of the Smoky River and the head of the Slave River. Since the calculated transverse mixing characteristics do not compare well with other studies, it would be premature to assume that the results of the present study can be extended with confidence to the entire Peace River.

6. General predictability of river mixing. The very wide scatter in published correlations of mixing parameters – which is not improved by the present results – remains a major problem in predicting river mixing. As a result, predictions for previously untested rivers or reaches cannot in general be made with a satisfactory degree of confidence using theory and existing data, and reach-specific field investigations continue to be recommended despite the growing number of previous investigations.

6.2 Summary of Principal Numerical Results

1. Travel times and velocities. Travel times and associated dye-cloud velocities from the dye test are shown in Table 3.5. Channel mean velocities as calculated from discharge and

cross-sectional data are shown in Table 3.2. The two sets of velocities are compared in Table 3.6. The differences are discussed in Section 3.5.

For the entire study length, calculated mean channel velocity averaged 0.76 m/s whereas measured dye-cloud velocity averaged 1.07 m/s, a ratio of 1.40. Corresponding ratios for individual reaches ranged from 1.60 (Cairn to Peace River) to 1.14 (Hotchkiss to Notikewin).

2. Transverse mixing. The length required for complete transverse mixing is in the order of 100 km (Table 4.1 and Section 5.1). Transverse mixing parameters as calculated from the data are shown in Table 4.3 and are compared with those from previous studies in Figure 4.4. The transverse mixing coefficient e_z (Equation 4.2) is given as 0.048 m²/s and the dimensionless equivalent k_t (Equation 4.8) as 0.21.

3. Longitudinal mixing. The concept of the linear mixing length, beyond which a transition from linear to Fickian dispersion begins, is explained in Section 5.2.1. This length is given in Table 4.1 and is in the order of 200 km.

The calculated value of the dimensionless linear dispersion parameter β_x is 0.014 (Table 5.3). Calculated parameters for the alternative storage model of longitudinal mixing are shown in Table 5.4. These results are compared with those from previous studies in Figures 5.3 and 5.4.

6.3 Recommendations

The following recommendations are made on the basis of the preceding analyses and conclusions:

1. Application of study results. The results provided herein can be used for water quality modelling for the study length over the normal range of winter flows and ice conditions.

2. Additional field studies. Further similar studies should be undertaken in selected reaches farther downstream, to characterize the lower portions of the Peace River between Carcajou and the head of the Slave River. These studies should include surveys of channel cross-sections, freeze-up processes and ice conditions downstream of Fort Vermilion.

3. Peace River flow gauging. The program for gauging river discharges at Peace River town at intervals during the winter period (which was discontinued some years ago) should be re-established, in order to provide more reliable information for analysis of water-quality related investigations.

4. Re-examination of previous mixing analyses. Previous studies on the mixing characteristics of ice-covered rivers in Alberta should be re-examined, with a view to resolving differences caused by alternative ways of evaluating the reach-averaged hydraulic characteristics.

5. Research on hydraulics of ice-covered channels. Additional research should be undertaken towards improving understanding of the impact of ice covers on velocity distributions, and the consequent effects on practical aspects of the usual one-dimensional flow approximations used for hydraulic calculations.

6. Research on mixing theory. It appears reasonable to question whether the conventional theoretical framework for analyzing mixing data is the most appropriate from a practical viewpoint, given the continuing difficulties in predicting without extensive field testing. Consideration could be given as to whether a more empirical approach, for example one based on dimensional analysis rather than turbulence theory, might provide better results.

7. REFERENCES

- Andres, D., Van der Vinne, G. and Trevor, B. 1989. Low flow winter travel time characteristics of the Athabasca River, Hinton to Athabasca. Report SWE-89/06, Resource Technologies Department, Alberta Research Council.
- Ashton, G.D. (editor) 1986. River and lake ice engineering. Water Resources Publications, Littleton, Colorado.
- Beer, T. and Young, P.C. 1983. Longitudinal dispersion in natural streams. *Journal of Environmental Engineering* Vol. 109 No. 5 pp. 1049-1067.
- Beltaos, S. 1975. Evaluation of transverse mixing coefficients from slug tests. *Journal of Hydraulic Research (IAHR)* Vol. 13 No. 4.
- Beltaos, S. 1978 a. Transverse mixing in natural streams. Report SWE-78/01, Transportation and Surface Water Engineering Division, Alberta Research Council.
- Beltaos, S. 1978 b. An interpretation of longitudinal dispersion data in rivers. Report SWE-78/03, Transportation and Surface Water Engineering Division, Alberta Research Council.
- Beltaos, S. 1979. Mixing characteristics of the Athabasca River below Fort McMurray - winter conditions. Report 40, Alberta Oil Sands Environmental Research Program. (Also, Contribution Series 943, Alberta Research Council.)
- Beltaos, S. and Arora, V.K. 1988. An explicit algorithm to simulate transient transverse mixing in rivers. *Canadian Journal of Civil Engineering* Vol. 15 pp. 964-976.
- Brockett, B.E. and P. Sellman 1986. Development of a frazil ice sampler. USA Cold Regions Research and Engineering Laboratory, Special Report 86-37.
- Chacho, E.F., D.E. Lawson, and B.E. Brockett 1986. Frazil pebbles: frazil ice aggregates in the Tanana River near Fairbanks, Alaska. *Proceedings of 8th IAHR Ice Symposium, August 1986, Iowa City, vol.I* pp. 475-484.
- Chacho, E.F., B.E. Brockett, and D.E. Lawson 1989. Cryogenic sampling of frazil ice deposits. USA Cold Regions Research and Engineering Laboratory, Special Report 89-28.

- Dean, A.M. Jr. 1986. Field techniques for obtaining engineering characteristics of frazil ice accumulations. Proceedings of 8th IAHR Ice Symposium, August 1986, Iowa City, vol.III pp. 265–278.
- Elhadi, N., A. Harrington, I. Hill, Y.L. Lau and B.G. Krishnappan 1984. River mixing – a state-of-the-art report. Canadian Journal of Civil Engineering Vol. 11 No. 3 pp. 585–609.
- Engmann, E.O. 1974. Transverse mixing characteristics of open and ice-covered channel flows. Ph.D thesis, Dept. of Civil Engineering, University of Alberta, Edmonton.
- Fischer, H.B., E.J. List, R.C. Koh, G.N. Berger and N.H. Brooks 1979. Mixing in inland and coastal waters. Academic Press, New York.
- Gowda, T.P.H. 1984. Water quality prediction in mixing zones of rivers. ASCE Journal of Environmental Engineering Vol. 110 No. 4 pp. 751–769.
- Henderson, F.M. 1966. Open channel flow. Macmillan, New York.
- Holley, E.R., J. Siemons and G. Abraham 1972. Some aspects of analyzing transverse diffusion in rivers. Journal of Hydraulic Research Vol. 10 pp. 27–57.
- Kellerhals, R., C.R. Neill and D.I. Bray 1972. Hydraulic and geomorphic characteristics of rivers in Alberta. River Engineering and Surface Hydrology Report 72–1, Alberta Research Council.
- Lau, Y.L. and B.G. Krishnappan 1981. Modelling transverse mixing in natural streams. Journal of Hydraulics Division ASCE Vol. 107 No. HY2 pp. 209–226.
- Lau, Y.L. and B.G. Krishnappan 1982. User's manual, prediction of transverse mixing in natural streams model – RIVMIX MK1. Environmental Hydraulics Section, National Water Research Institute, Burlington, Ontario.
- Neill, C.R. and D.D. Andres 1984. Freeze-up flood stages associated with fluctuating reservoir releases. Proc. ASCE/CSCE Cold Regions Engineering Conference, Edmonton.
- Putz, G. 1984. TRANSMIX (transverse mixing computer model) users manual. Environmental Engineering Technical Report 84–2, Dept. of Civil Engineering, University of Alberta.
- Sabol, G.V. and C.F. Nordin 1978. Dispersion in rivers as related to storage zones. Journal of Hydraulics Division ASCE Vol. 104 No. HY5 pp. 695–708.

Sayre, W.W. and F.M. Chang 1968. A laboratory investigation of open channel dispersion processes for dissolved, suspended, and floating dispersants. U.S Geological Survey Professional Paper 433-E.

Turner Designs 1982. Fluorometric facts: flow measurements. Turner Designs, Mountainview, California.

Van Der Vinne, G. 1991. Winter tracer dye studies on the North Saskatchewan River, Edmonton to Saskatchewan border. Report SWE-91/04, Environmental Research and Engineering Department, Alberta Research Council.

Van Der Vinne, G. 1992. Winter low flow tracer dye studies, Athabasca River: Athabasca to Bitumount, Part II: mixing characteristics. Report SWE-92/04, Environmental Research and Engineering Department, Alberta Research Council.

Van Der Vinne, G. and Andres, D.D. 1992. Winter low flow tracer dye studies, Athabasca River: Athabasca to Bitumount, Part I: time of travel. Report SWE-92/03, Environmental Research and Engineering Department, Alberta Research Council.

Yotsukura, N. and W.W. Sayre 1976. Transverse mixing in natural channels. Water Resources Research Vol. 12 pp. 695-704.

Yotsukura, N. and E.D. Cobb 1972. Transverse diffusion of solutes in natural channels. U.S. Geological Survey Professional Paper 582-C.

SECTION 8

TABLES

Table 2.1 Ice cover characteristics over study length, February 1993

Location	Cumulative distance (km)	Average thickness (m)	Standard deviation (m)	Adopted reach-averaged thickness (m)	Nature of cover
0. Shaftesbury	0	0.99	0.15		smooth, juxtaposed
1. Mackenzie Caim	8.3	1.26	0.38	1.1	smooth, juxtaposed
2. Peace River	24.8	1.03	0.16	1.1	smooth, juxtaposed
3. Daishowa	42.4	1.05	0.21	1.0	smooth, juxtaposed
4. Whitemud River	82.6	1.22	0.28	1.1	smooth, juxtaposed
5. North Star	117.6	1.86	0.70	1.5	rough, shoved
6. Hotchkiss	149.2	1.06	0.28	1.5	rough, shoved
6A. Crummy Lake ¹	172.0	1.35	0.89	1.4	smooth, juxtaposed
7. Notikewin River	187.0	1.77	0.59		rough, shoved

¹ This site was used for ice observations only

Table 2.2 Frazil ice characteristics over study length, February 1993

Location	Extent of frazil ¹	Frazil thickness (m)	Thickness of transport layer (m)	Comments
Shaftesbury Ferry	0/20	--	--	No frazil observed.
Mackenzie Cairn	4/20	< 0.10	not measurable	Small amounts of fine-grained frazil collecting in holes.
Peace River ²	--	--	--	Very little frazil at section.
Daishowa	16/20	< 0.10	not measured	Small amounts of fine-grained frazil collecting in holes.
Whitemud	9/20	0.07 - 0.67	not measured	Variable thicknesses of fine-grained frazil across channel, considerable sediment in the frazil.
North Star	18/20	0.2 - 2.0	not measured	Variable thickness and density of predominantly fine-grained frazil.
Hotchkiss	13/20	0.2 - 0.6	not measured	Variable thickness and density; frazil pebbles evident within the fine-grained accumulation.
Crummy Lake	4/12	< 0.4	not measured	Most holes clear of frazil, some frazil pebbles collecting in holes.
Notikewin	17/20	0.15 - 1.3	0.15 - 0.30	Frazil slush accumulated to the bed along both banks; frazil pebbles up to 0.10 m in diameter.

¹ Number of holes at which frazil ice was observed relative to number of holes sampled.

² WSC gauging section: ice conditions noted only in a qualitative way.

Table 2.3 Observed water surface elevations during surveys and dye test

Site	Benchmark no.	Benchmark elevation (m)	Date of observation¹	Water surface elevation (m)
0. Shaftesbury	83-D-59 ARC 1- 1993	323.69 324.27	17 Feb.	321.25
1. Mack. Cairn	ARC 2 - 1993	322.04	18 Feb. 27 Feb.	319.05 319.18
2. Peace River	Gauge datum	305.00	18 Feb. 27 Feb.	313.77 313.86
3. Daishowa	Alta. Trans. 5611779	316.29	19 Feb. 27 Feb.	307.98 307.67
4. Whitemud	87D-31	302.80	21 Feb. 28 Feb.	296.86 296.56
5. North Star	ARC 3 - 1993	293.69	22 Feb. 1 Mar.	288.42 288.34
6. Hotchkiss	Spike tied to 87-D-27	284.05	23 Feb. 28 Feb. 1 Mar.	279.66 279.62 279.65
7. Notikewin	87-D-26	275.43	24 Feb. 1 Mar. 2 Mar.	271.77 271.88 271.98

¹ Dates 17 - 24 Feb. represent surveys; later dates represent dye test.

Table 2.4 Measured and calculated dye concentrations in the frazil zone

	Hotchkiss	Notikewin
Time 1/2 March 1993	15.00 – 18.00 hrs	22.00 – 06.00 hrs
Number of samples	16	12
Dye concentrations ($\mu\text{g/L}$)		
In river water at time of frazil sampling	0.08	0.07
Dye-cloud peak, C_p	0.85	0.50
Attached to frazil ice pebbles, C_i	0.023	0.008
In interstitial water, C_{po}	0.38 ¹	0.13 ¹
Ratio C_{po}/C_p	0.45	0.26

¹ Calculated using relationship derived from laboratory study: $C_{po}/C_i = 16.7$ approx.

Table 2.5 Mass recovery ratios in dye test

Location	Distance from Injection (km)	Mass recovery ratios			Deviation of measurements from fitting curve (%)
		Measured ¹	Fitting curve ²	Frazil losses only ³	
Shaftesbury	0.0	1.00	1.00	1.00	0
Mackenzie Caim	8.3	0.87	0.89	0.95	-2
Peace River	24.8	0.75	0.81	0.92	-8
Daishowa	42.4	0.72	0.78	0.90	-7
Whitemud River	82.6	0.78	0.75	0.89	4
North Star	117.6	0.58	0.75	0.87	-22
Hotchkiss	149.2	0.77	0.74	0.86	3
Notikewin River	187.0	0.52	0.74	0.85	-30

¹ As calculated by integrating concentration profiles (Equation 2.5)

² As drawn in Figure 2.4 (full line)

³ As drawn in Figure 2.4 (broken line)

Table 2.6 Comparison with minimum recovery ratios from other winter dye studies in Alberta

River	Injection location	Study length (km)	Minimum recovery ratio
Athabasca	Hinton	102.2	0.80
Athabasca	Berland River	104.8	0.91
Athabasca	Whitecourt	139.9	0.77
Athabasca	Vega Ferry	98.5	0.81
Athabasca	Hondo	119.0	0.93
Athabasca	Athabasca	170.2	0.91
Athabasca	Upper Wells	221.5	1.00
Athabasca	McMurray	72.1	0.83
N. Saskatchewan	Edmonton	198.1	0.75
N. Saskatchewan	Shandro	189.6	0.78
Peace	Shaftesbury Ferry	187.0	0.52
Smoky	Bezanson	121.0	0.62
Smoky	Watino	70.8	0.60
Wapiti	Grande Prairie	64.2	0.50
Mean			0.77

Table 2.7 Reach-averaged values of parameters used to estimate dye losses to frazil

Reach	Length	Width	Peak Concentration	Frazil Thickness	Dye Loss due to Frazil
	Δx (km)	B (m)	C_p ($\mu\text{g/L}$)	H_r (m)	S_r (kg)
Shaftesbury-Cairn	8.3	430	61.4	0.10	2.3
Cairn-Peace	24.8	430	24.7	0.10	1.8
Peace-Daishowa	42.4	470	9.9	0.10	0.9
Daishowa-Whitemud	82.6	410	3.2	0.14	0.7
Whitemud-Northstar	117.6	370	1.1	0.58	0.8
Northstar-Hotchkiss	149.2	430	0.6	0.63	0.5
Hotchkiss-Notikewin	187.0	520	0.4	0.44	0.3

Table 3.1 Hydraulic slopes along study length, February 1993

Location	Adjusted water surface elevation* (m)	Cumulative distance (km)	Elevation difference (m)	Reach length (km)	Reach slope (m/km)
0. Shaftesbury	321.3	0	2.3	8.3	0.277
1. Mackenzie Cairn	319.0	8.3	5.4	16.5	0.327
2. Peace River	313.6	24.8	6.0	17.6	0.341
3. Daishowa	307.6	42.4	11.1	40.2	0.276
4. Whitemud	296.5	82.6	8.3	35.0	0.237
5. North Star	288.2	117.6	8.7	31.6	0.275
6. Hotchkiss	279.5	149.2	7.7	37.8	0.204
7. Notikewin	271.8	187.0			

* Locally observed elevation adjusted to correspond to constant discharge of 1600 m³/s; maximum adjustment = 0.3 m.

Table 3.2 Measured and computed geometric and hydraulic data for study length, February 1993

Site	Date of Survey	Av. total ice thickness (m)	Under-ice surface width B (m)	Under-ice area A (m ²)	Est'd. local discharge Q (m ³ /s)	Mean velocity U = Q/A (m/s)	Hydr. radius R = A/2B (m)	Reach-averaged values U (m/s)	R (m)	Slope S	Roughness n = R ^{2/3} S ^{1/2} /U
0. Shaftesbury	17 Feb.	1.0	385	2010	1600	0.80	2.61	0.835	2.76	.00028	0.039
1. Mackenzie Cairn	18 Feb.	1.3	315	1840	1600	0.87	2.92	0.875	2.60	.00033	0.039
2. Peace River	18 Feb.	1.0	400	1820	1600	0.88	2.28	0.845	2.52	.00034	0.040
3. Daishowa	19 Feb.	1.1	400	2210	1800	0.81	2.76	0.765	3.26	.00028	0.048
4. Whitemud River	21 Feb.	1.2	350	2640	1900	0.72	3.77	0.645	3.26	.00024	0.053
5. North Star	22 Feb.	1.9	580	3180	1800	0.57	2.74	0.595	3.01	.00028	0.059
6. Hotchkiss	23 Feb.	1.0	430	2830	1750	0.62	3.29	0.735	3.43	.00020	0.044
7. Notkewin River	24 Feb.	1.8	280	2000	1700	0.85	3.57				
Averages		1.3	390	2320	1720	(0.74)	(2.97)			(.00026)	(0.046)

Note: calculated values of n include effects of ice underside roughness, river bed roughness, expansion and contraction losses, and possibly frazil blockage.

**Table 3.3 Spatial variability of ice thickness in upper
30 km of study length, February 1983**

Location	Cumulative Distance (km)	Average ice thickness		Water surface elevation	
		solid (m)	total (m)	(m)	
				1983	(1993)
Shaftesbury	0	0.6	1.1	321.2	(321.3)
Jail	11	0.7	1.8	318.0	
McLeod Caim	16.2	0.8	1.3	316.3	
Gravel Pit		0.7	1.2	315.3	
Heart River	24.6	0.6	1.7	313.4	
WSC Gauge	26.2	0.7	1.0	313.2	(313.6)
Bewley Island	27.2	0.7	1.0	313.1	
Dick's Diving	30.5	0.9	2.2	311.3	
	average	0.71	1.41		

Based on data from River Engineering Branch, Alberta Environment

Table 3.4 Temporal variability of ice thickness at Peace River gauging section, 1983 to 1986

Date	Width averaged ice thickness		Average elevation of ice underside	Discharge
	solid (m)	total (m)	(m)	(m ³ /s)
21 Jan. 83	0.4	1.1	313.2	720
22 Feb. 83	0.7	1.0	312.2	640
17 Mar. 83	0.8	1.1	311.7	540
6 Jan. 84	0.6	1.4	312.9	1620
31 Jan. 84	0.9	1.5	311.9	1010
20 Feb. 84	1.0	1.5	311.5	970
16 Mar. 84	1.0	1.5	310.8	650
10 Jan. 85	0.7	1.9	313.1	1350
6 Feb. 85	1.0	1.2	313.1	1610
12 Mar. 85	1.2	1.9	312.8	1670
8 Jan. 86	0.7	1.8	312.8	1820
4 Feb. 86	0.8	1.7	311.1	790
4 Mar. 86	1.0	1.8	311.2	1160
Average	0.8	1.5		

Based on data from Water Survey of Canada

Table 3.5 Dye-test travel times and velocities

Reach	Reach Length (km)	Travel Times (hrs)				Associated Dye-cloud velocities (m/s)	
		Leading Edge	Peak	Centroid	Trailing Edge	Peak	Centroid
Shaftesbury – Cairn	8.3	1.8	2.1	2.1	3.0	1.10	1.08
Cairn – Peace River	16.5	3.1	3.2	3.3	4.0	1.43	1.39
Peace River – Daishowa	17.6	3.3	3.8	4.0	6.3	1.29	1.22
Daishowa – Whitemud	40.2	8.3	9.2	9.8	16.7	1.21	1.14
Whitemud – North Star	35.0	9.9	11.5	11.7	14.4	0.85	0.83
North Star – Hotchkiss	31.6	8.6	8.9	11.1	19.3	0.99	0.79
Hotchkiss – Notikewin	37.8	11.1	12.9	12.0	15.9	0.81	0.88

Table 3.6 Comparison by reaches of mean channel velocities and dye–cloud velocities

Reach	Mean channel velocity (Table 3.2) (m/s)	Dye–cloud velocity¹ (Table 3.5) (m/s)	Ratio
Shaftesbury – Cairn	0.84	1.10	1.31
Cairn – Peace River	0.88	1.41	1.60
Peace River – Daishowa	0.85	1.25	1.47
Daishowa – Whitemud	0.77	1.17	1.52
Whitemud – North Star	0.65	0.84	1.29
North Star – Hotchkiss	0.60	0.89	1.48
Notchkiss – Notikewin	0.74	0.84	1.14
averages	0.76	1.07	1.40

¹ Average of peak and centroid values

Table 3.7 Adopted widths and mean depths for mixing analyses

Reach	Full surveyed width¹ (m)	Reduced effective width² (m)	Dye-cloud velocity³ (m/s)	Effective mean depth⁴ (m)
Shaftesbury – Cairn	350	220	1.10	7.2
Cairn – Peace River	360	225	1.43	5.4
Peace River – Daishowa	400	260	1.29	5.2
Daishowa – Whitemud	375	250	1.21	5.8
Whitemud – North Star	465	330	0.85	6.2
North Star – Hotchkiss	505	375	0.99	4.7
Hotchkiss – Notikewin	255	265	0.81	8.1

¹ Average of 2 ends of reach

² Reduced to exclude 5% of theoretical discharge distribution at each bank

³ From Table 3.5 column 6

⁴ Calculated as $Q = 1740 / (\text{effective width} \times \text{dye-cloud velocity})$

Table. 3.8 Comparison of composite hydraulic roughness values

Reach	Composite ¹ Manning roughness n	
	Using surveyed cross-sections ² (Table 3.2)	Using data of Table 3.7 ³
Shaftesbury Cairn	0.039	0.036
Cairn – Peace River	0.039	0.025
Peace River – Daishowa	0.040	0.027
Daishowa – Whitemud	0.048	0.028
Whitemud – North Star	0.053	0.038
North Star – Hotchkiss	0.059	0.030
Hotchkiss – Notikewin	0.044	0.027
Averages	0.046	0.030

¹ Including effects of channel bed plus ice underside

² Global values including effects of frazil blockage

³ Reduced values based on concept of effective section – see Section 3.5 of text

Table 4.1 Comparative estimates of vertical, transverse and linear mixing lengths for the Peace River

Type of mixing	Estimated length (km)	Relevant section of report text
Vertical	0.86	4.1
Transverse	107	5.1
Linear	186	5.2.1

Table 4.2 Dosage distribution parameters at dye-test sites

Location	Distance from injection (km)	Left bank dosage ($\mu\text{g}\cdot\text{h}/\text{L}$)	Right bank dosage ($\mu\text{g}\cdot\text{h}/\text{L}$)	Proportional discharge at dosage centroid (η_b)	Confining function $f(x)$	Integral of confining function with distance $\int f(x)dx$ (km)	Dosage variance with η σ_η^2	Channel shape factor ψ
Shaftesbury	0.0	0.00	0.00	0.50	1.00	0.0	0.000	2.1
Cairn	8.3	0.05	0.00	0.56	1.00	8.3	0.014	2.7
Peace River	24.8	0.00	0.00	0.52	1.00	24.8	0.034	3.2
Daishowa	42.4	0.74	0.00	0.52	0.95	41.9	0.048	2.9
Whitemud	82.6	6.44	5.24	0.49	0.27	66.5	0.079	2.8
Northstar	117.6	5.41	5.83	0.51	0.30	76.4	0.089	1.7
Hotchkiss	149.2	5.98	5.59	0.50	0.28	85.4	0.078	2.2
Notikewin	187.0	3.54	2.83	0.48	0.23	95.0	0.075	2.1

Table 4.3 Computed transverse mixing parameters

Reach	Diffusion Factor D_z (m^2/s^2)	Transverse mixing coefficient e_z (m^2/s)		Dimensionless diffusion factor β_z		Dimensionless transverse mixing coefficient k_t	
		reduced width	full width	reduced width	full width	reduced width	full width
Shaftesbury – Cairn	2.49	0.028	0.069	0.00022	0.00035	0.051	0.25
Cairn – Peace River	1.84	0.021	0.053	0.00016	0.00026	0.053	0.27
Peace River – Daishowa	1.25	0.016	0.039	0.00012	0.00019	0.044	0.21
Daishowa – Whitemud	1.91	0.020	0.045	0.00017	0.00026	0.047	0.19
Average Shaftesbury to Whitemud	1.81	0.020	0.048	0.00017	0.00026	0.047	0.21

Table 5.1 Position parameter k_p (Equation 5.1) as function of injection location

Fraction of cumulative discharge from nearest bank	Position parameter k_p
0.0	3.8
0.1	3.9
0.2	4.5
0.3	5.8
0.4	7.2
0.5	15.7

Table 5.2 Computed parameters characterizing timewise distributions of cross-sectional average concentration at each site

Location	Distance (km)	Time to Peak (hrs)	Distribution parameters			
			Half-duration ΔT (hrs)	Variance σ_t^2 (hrs ²)	Peak Concentration ($\mu\text{g/L}$)	Mass Recovery Ratio
Shaftesbury	0.0	0.0	0.00	0.00	--	1.00
Caim	8.3	2.0	0.18	0.01	35.18	0.87
Peace	24.8	5.1	0.26	0.08	17.38	0.75
Daishowa	42.4	8.9	0.80	0.64	5.65	0.72
Whitemud	82.6	18.8	2.66	7.49	1.78	0.78
North Star	117.6	29.4	6.382	2.43	0.63	0.58
Hotchkiss	149.2	38.4	8.144	2.41	0.60	0.77
Notikewin	187.0	49.21	2.107	3.88	0.30	0.52

Table 5.3 Computed average hydraulic and linear dispersion parameters, Daishowa to Notikewin

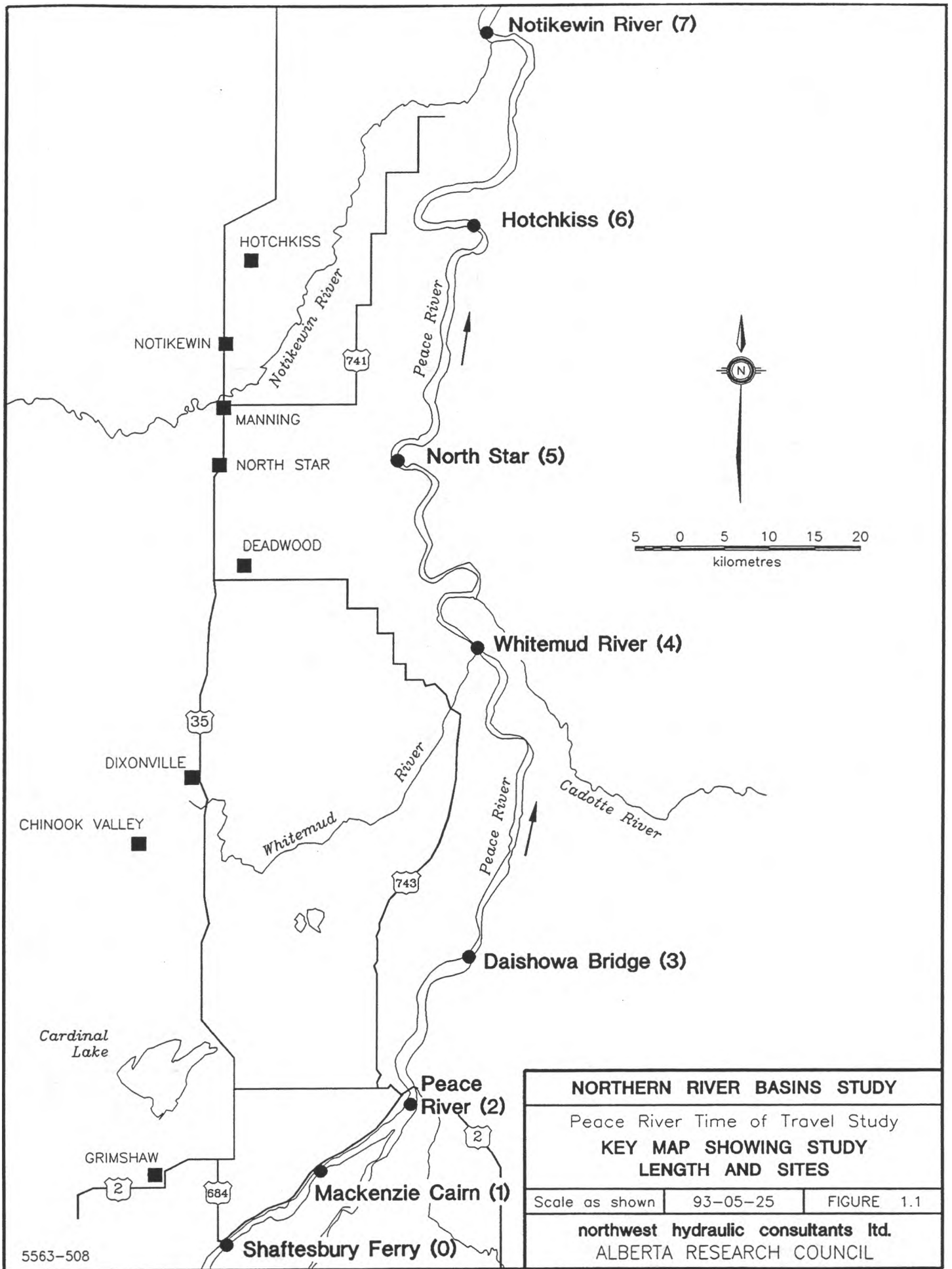
Method of Analysis	Width (m)	Depth (m)	Velocity (m/s)	Shear Velocity (m/s)	Linear Dispersion Parameter (β_s)
Full width basis	437	4.10	0.97	0.070	0.014
Reduced width basis	310	5.77	0.97	0.084	0.014

Table 5.4 Computed parameters for storage model

Location	Dimensionless Peak Concentration $C_p t_p Q/M$	Zone Number = m	Storage Parameter α_s
Cairn	10.3	1	28
Peace	14.9	1	40
Daishowa	8.7	1	24
Whitemud	5.3	1	14
North Star	4.0	2	15
Hotchkiss	3.8	2	14
Notikewin	3.6	2	13
Mean	7.2		21

SECTION 9

FIGURES



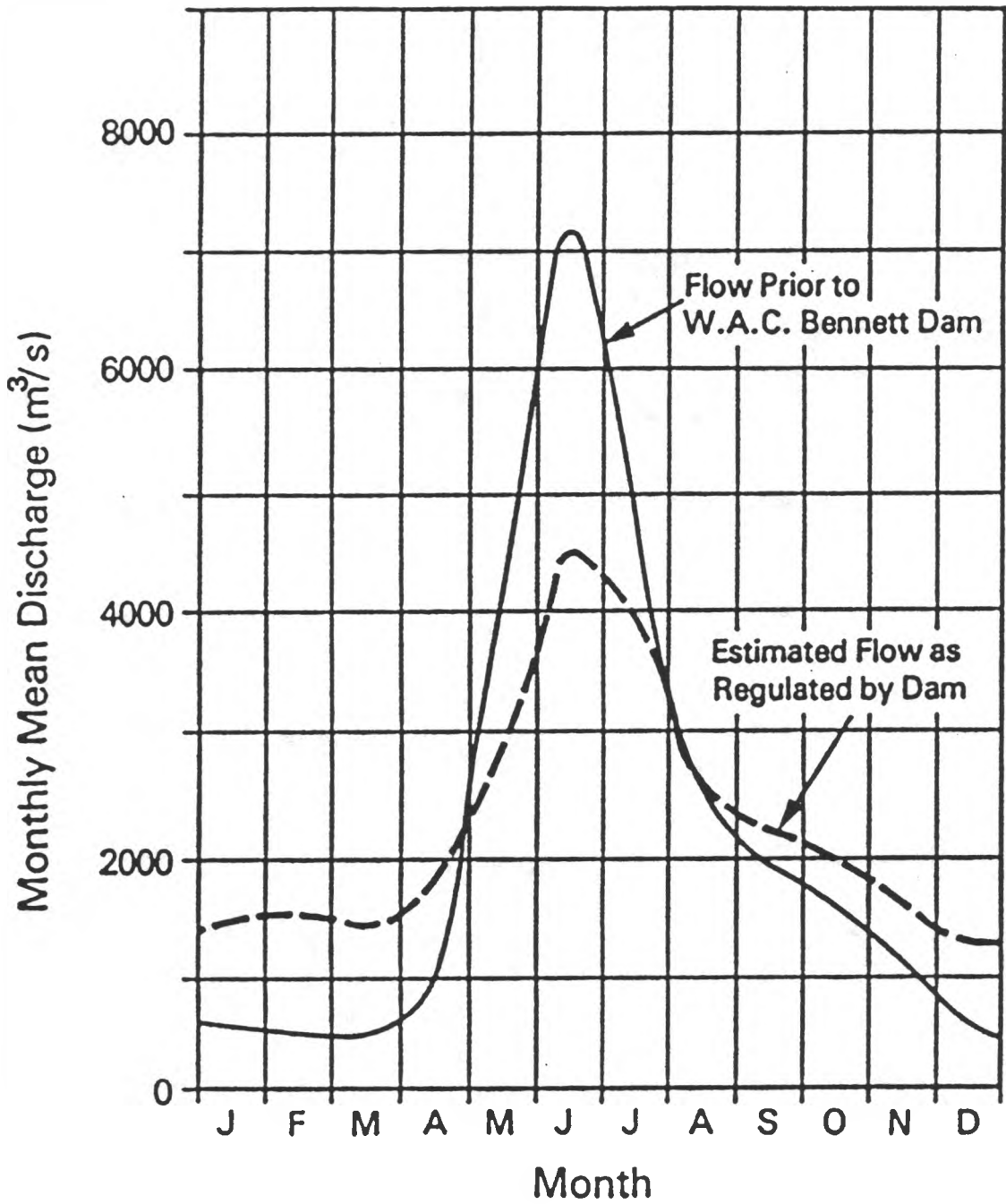
NORTHERN RIVER BASINS STUDY

Peace River Time of Travel Study

KEY MAP SHOWING STUDY LENGTH AND SITES

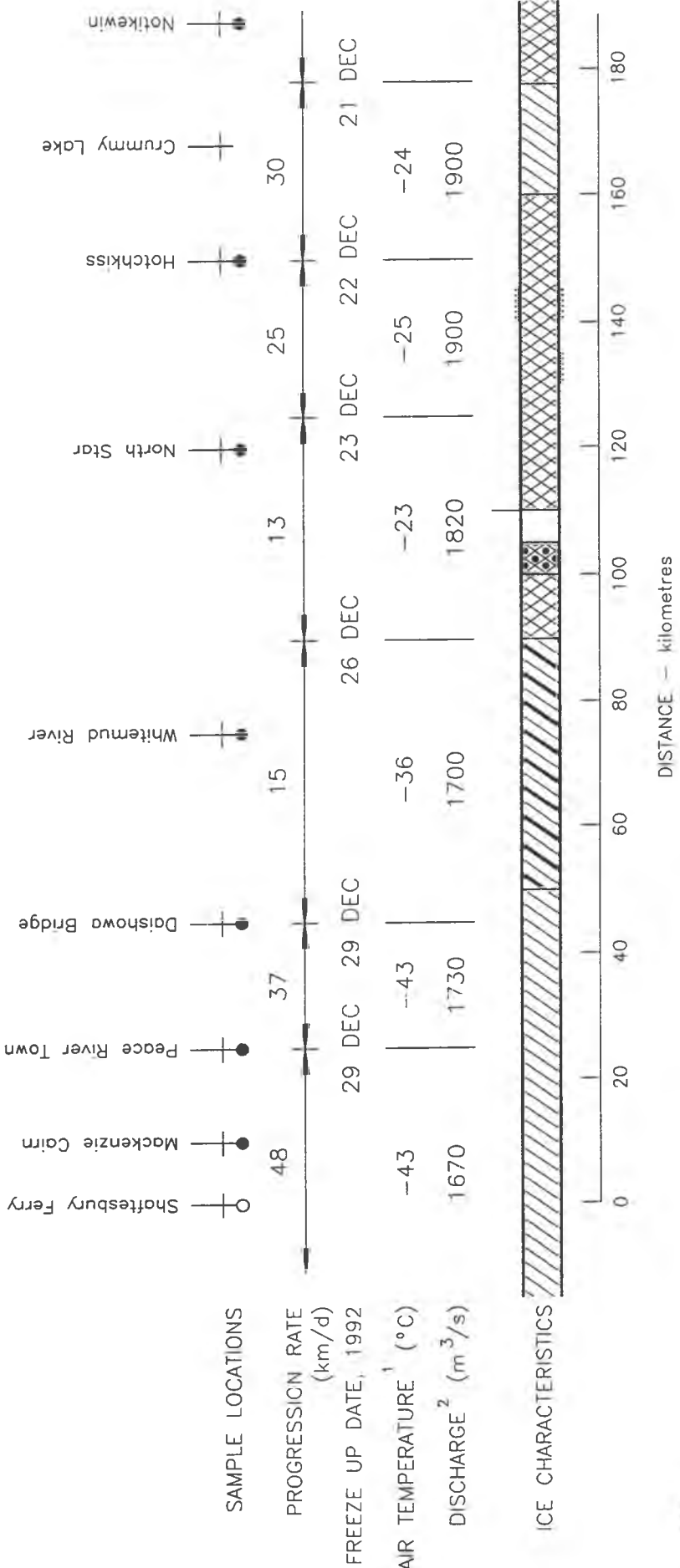
Scale as shown	93-05-25	FIGURE 1.1
----------------	----------	------------

northwest hydraulic consultants ltd.
ALBERTA RESEARCH COUNCIL



From: Neill and Andres 1984.

NORTHERN RIVER BASINS STUDY		
Peace River Time of Travel Study		
TYPICAL MONTHLY FLOWS IN PEACE RIVER BEFORE AND AFTER REGULATION BY B.C. HYDRO		
Scale as shown	93-05-25	FIGURE 1.2
northwest hydraulic consultants ltd. ALBERTA RESEARCH COUNCIL		



NOTES:

1. Mean daily air temperature averaged over observation interval.
2. Mean daily discharge on date of freeze-up averaged over observation interval and lagged by 4 days from Bennett Dam.

LEGEND:

- INJECTION LOCATION
- SAMPLING LOCATION
- + CROSS SECTION LOCATION
- ▨ SMOOTH JUXTAPOSED ICE COVER
- ▧ SMOOTH JUXTAPOSED ICE COVER WITH LARGE RAFTS IMBEDDED
- ▩ ROUGH ICE COVER DUE TO SHOWING OF JUXTAPOSED ICE
- ROUGH ICE COVER WITH LARGE RAFTS IMBEDDED
- SHEAR WALLS
- OPEN WATER

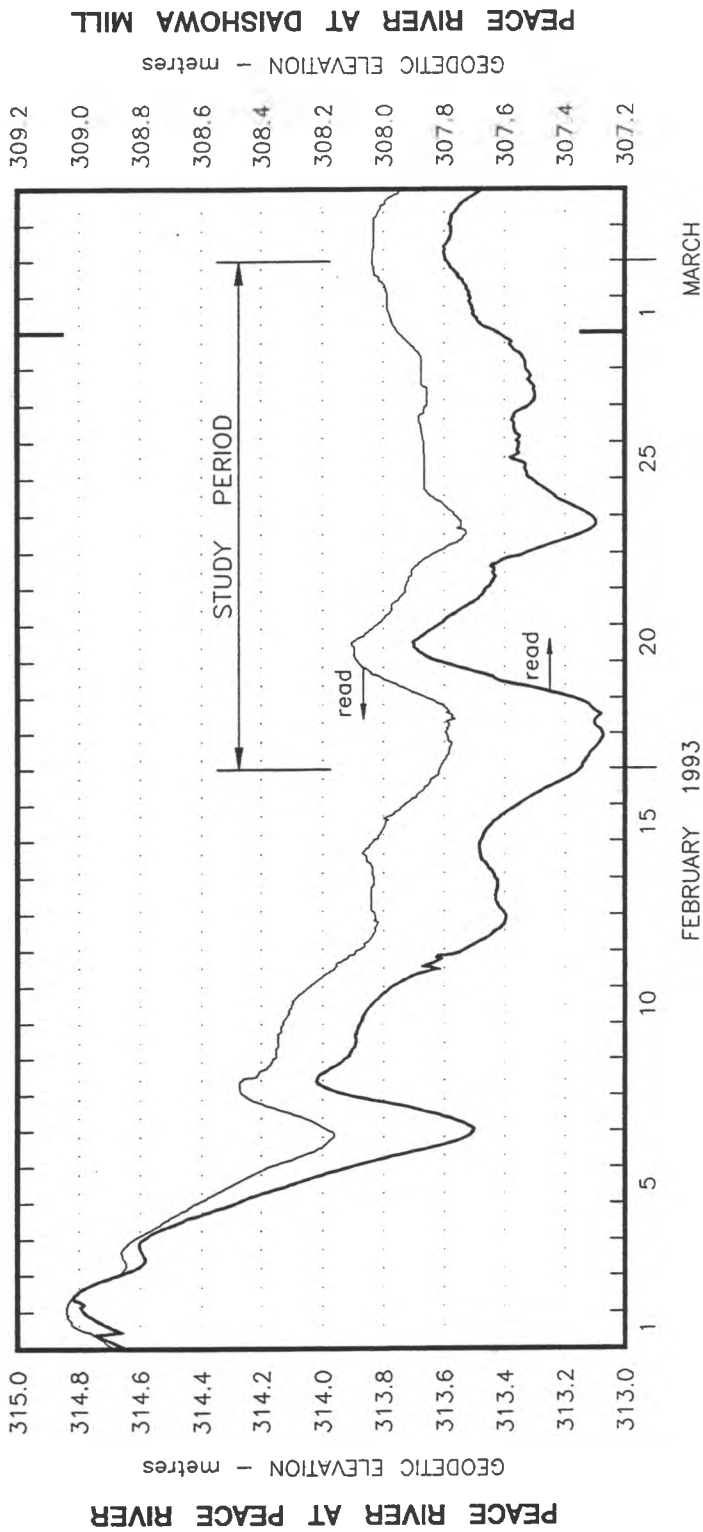
NORTHERN RIVER BASINS STUDY

Peace River Time of Travel Study

**ICE COVER CHARACTERISTICS
ALONG STUDY LENGTH**

Scale as shown 93-06-14 FIGURE 2.1

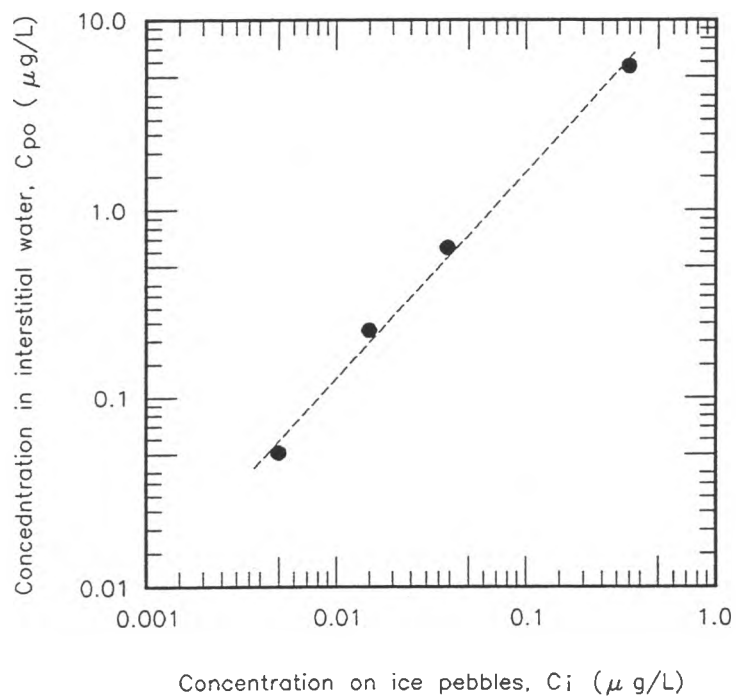
northwest hydraulic consultants ltd.
ALBERTA RESEARCH COUNCIL



LEGEND:

- PEACE RIVER AT PEACE RIVER
- PEACE RIVER AT DAISHOWA MILL

NORTHERN RIVER BASINS STUDY
 Peace River Time of Travel Study
**PEACE RIVER STAGE RECORDS
 OVER STUDY PERIOD**
 Scale as shown 93-04-13 FIGURE 2.2
northwest hydraulic consultants ltd.
 ALBERTA RESEARCH COUNCIL

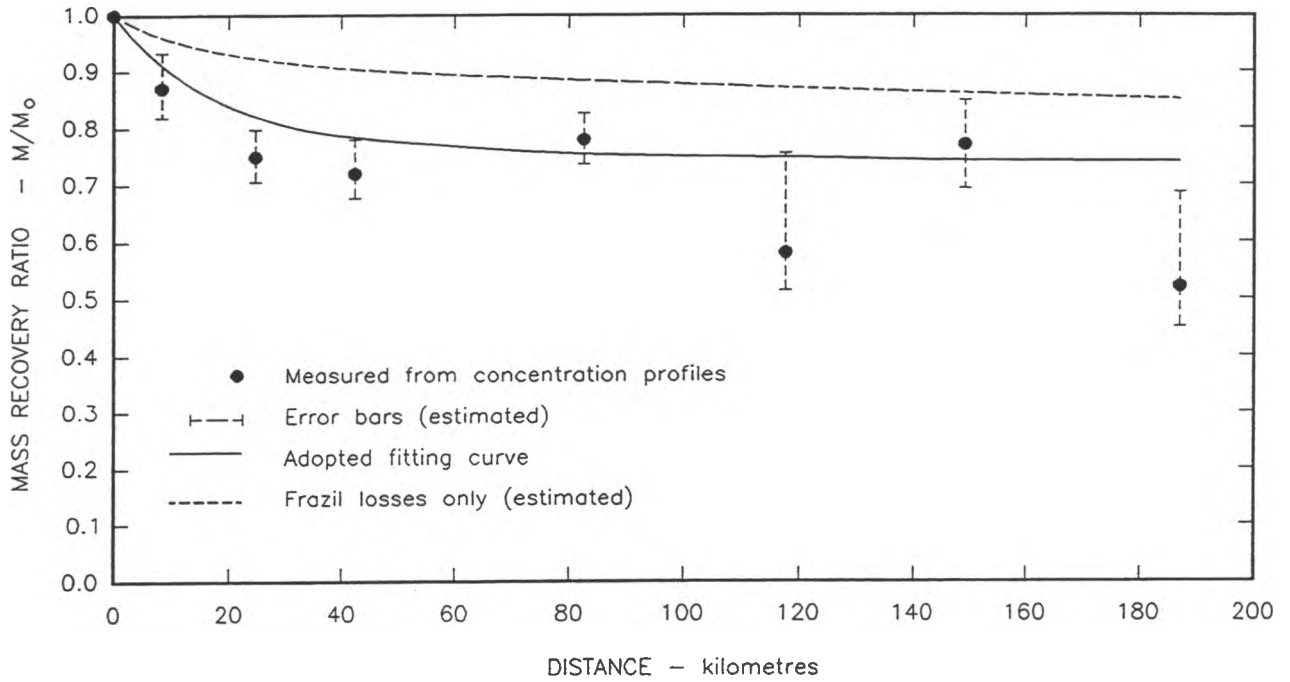


NORTHERN RIVER BASINS STUDY

Peace River Time of Travel Study
**LABORATORY CORRELATION BETWEEN DYE
 CONCENTRATIONS ON FRAZIL ICE PEBBLES
 AND IN INTERSTITIAL WATER**

Scale as shown | 93-06-17 | FIGURE 2.3

northwest hydraulic consultants ltd.
 ALBERTA RESEARCH COUNCIL



NORTHERN RIVER BASINS STUDY

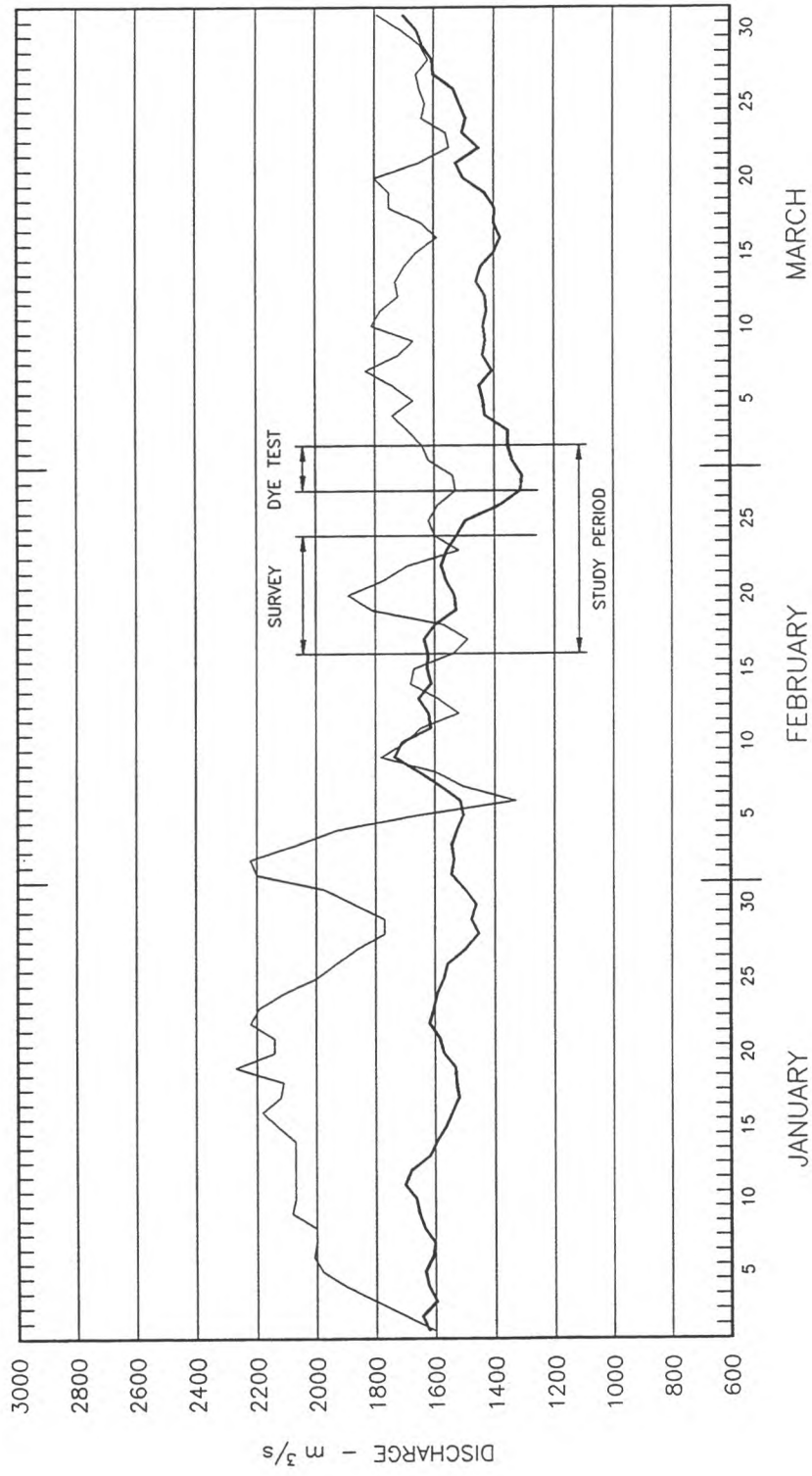
Peace River Time of Travel Study
**MASS RECOVERY RATIO vs.
 DISTANCE FROM INJECTION**

Scale as shown

93-07-06

FIGURE 2.4

northwest hydraulic consultants ltd.
 ALBERTA RESEARCH COUNCIL



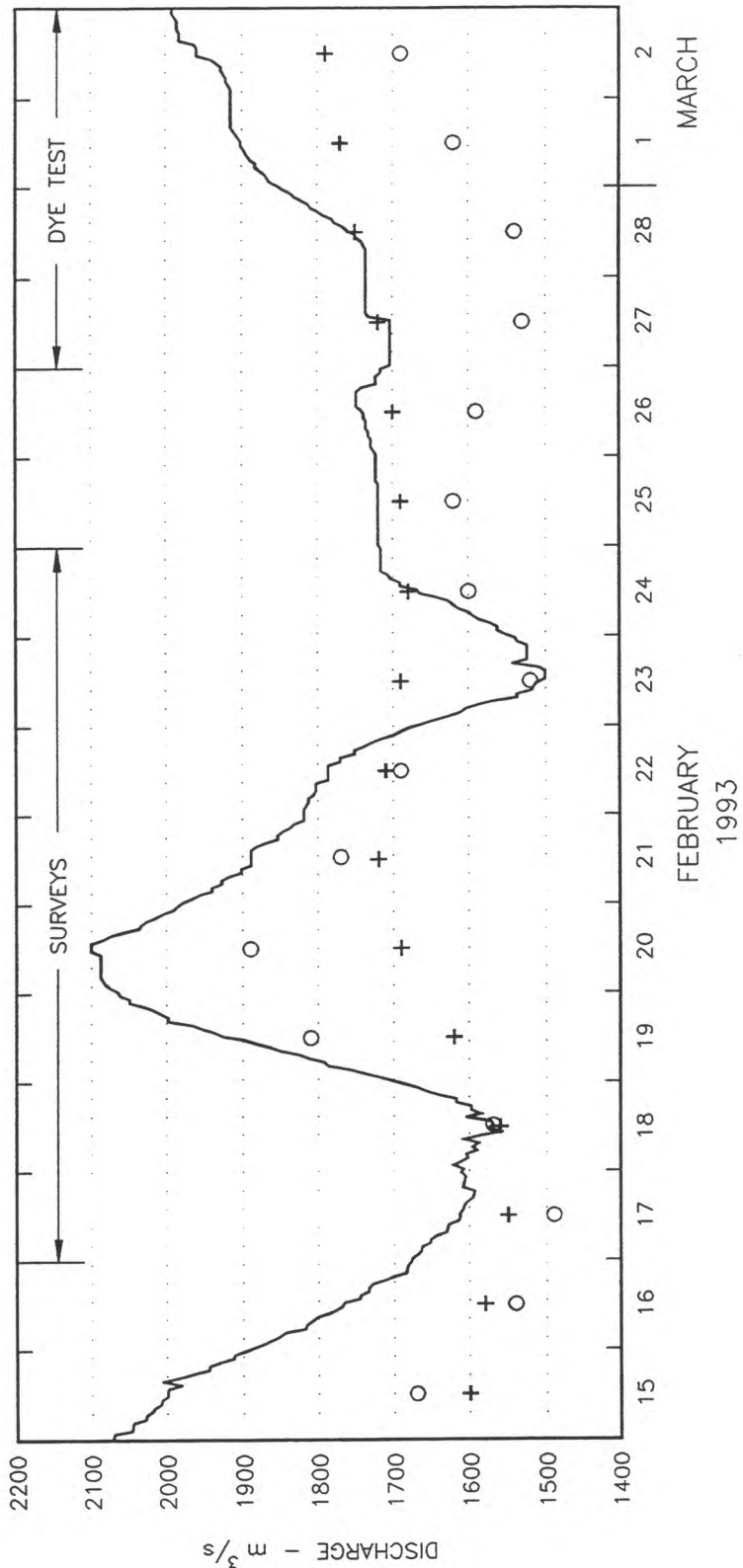
LEGEND:

- 1993
- 7-YEAR AVERAGE (1984 - 90)

NOTE:

1993 GRAPH BASED ON PRELIMINARY WSC DATA.

NORTHERN RIVER BASINS STUDY	
Peace River Time of Travel Study	
RIVER FLOWS JANUARY THROUGH MARCH AT PEACE RIVER	
Scale as shown	93-05-27
FIGURE 3.1	
northwest hydraulic consultants ltd.	
ALBERTA RESEARCH COUNCIL	

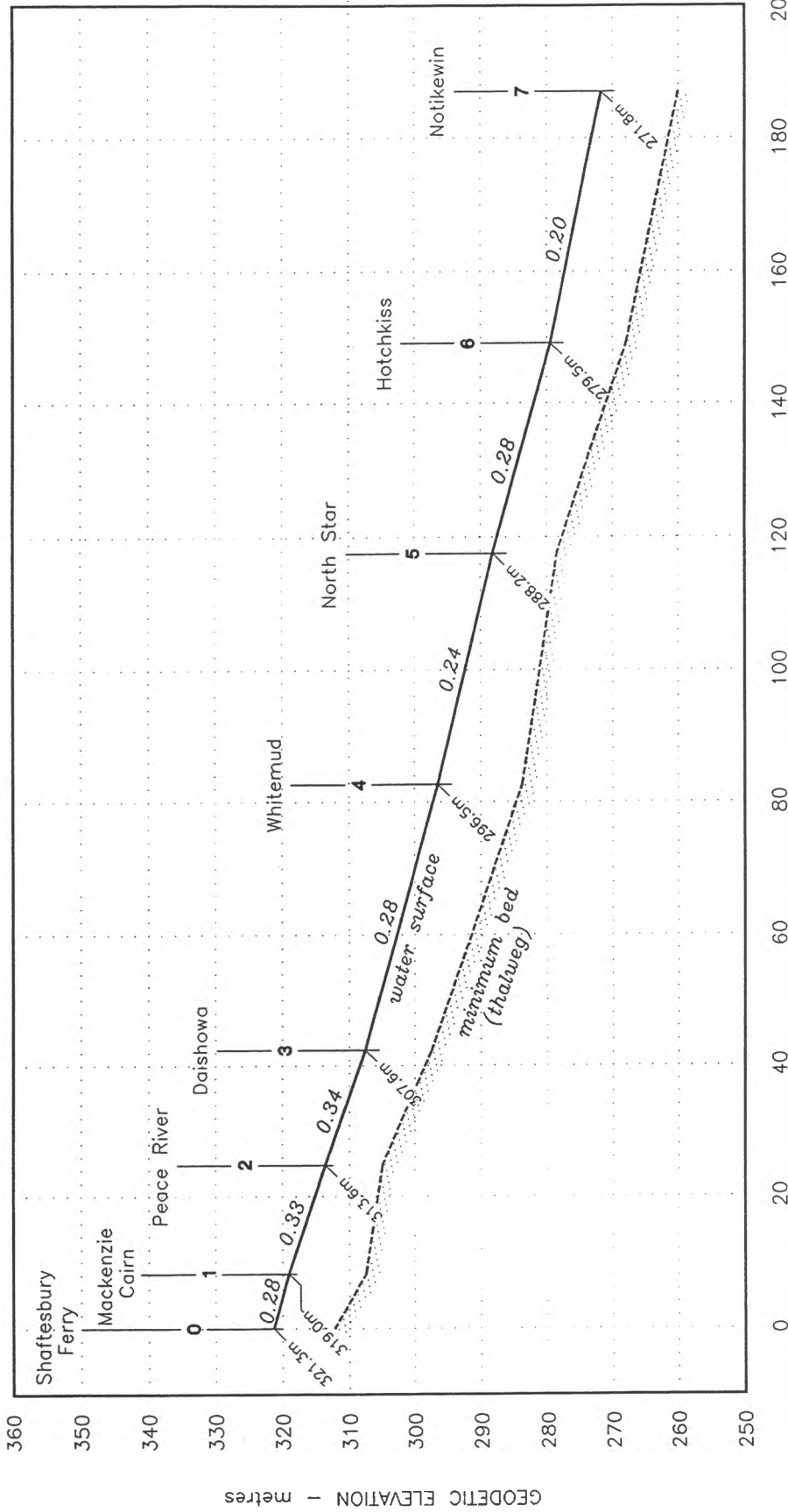


LEGEND:

-  Preliminary hourly discharges from Alberta Environment.
-  Preliminary daily discharges from Water Survey of Canada for Peace River.
-  Preliminary daily discharges from Water Survey of Canada for Peace Point (lagged 7 days).

NORTHERN RIVER BASINS STUDY	
Peace River Time of Travel Study	
COMPARISON OF FLOW ESTIMATES AT PEACE RIVER	
Scale as shown	93-05-25
	FIGURE 3.2
northwest hydraulic consultants ltd. ALBERTA RESEARCH COUNCIL	

0 8.3 24.8 42.4 82.6 117.6 149.2 187.0 km



DISTANCE - kilometres

NORTHERN RIVER BASINS STUDY

Peace River Time of Travel Study

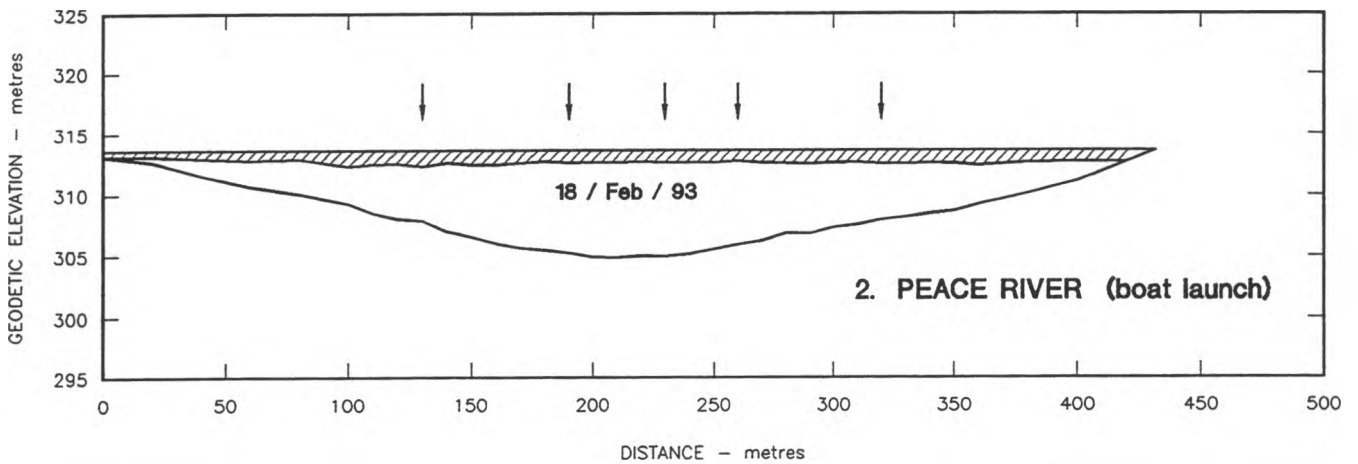
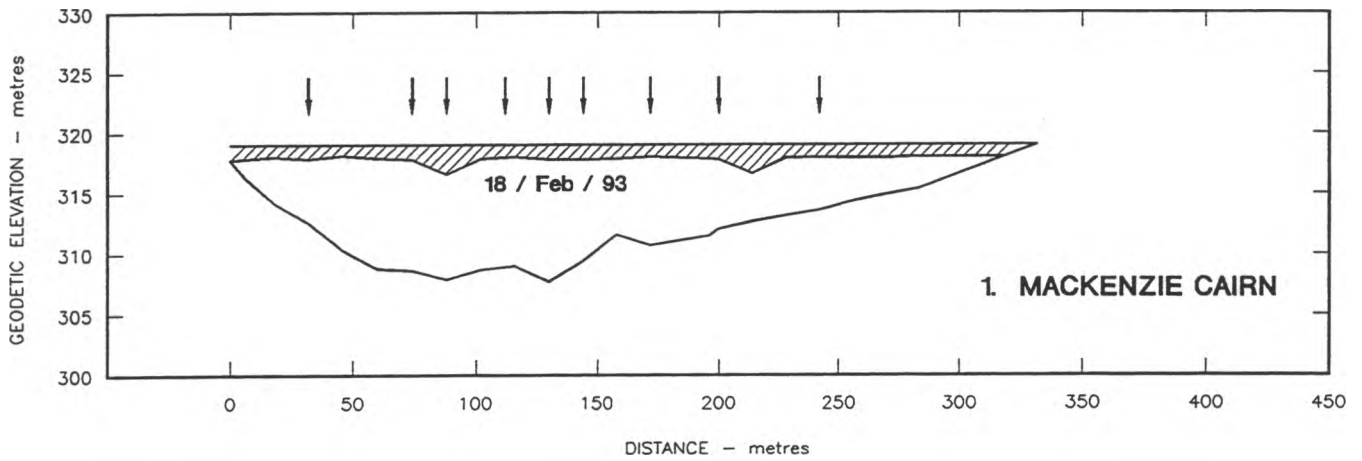
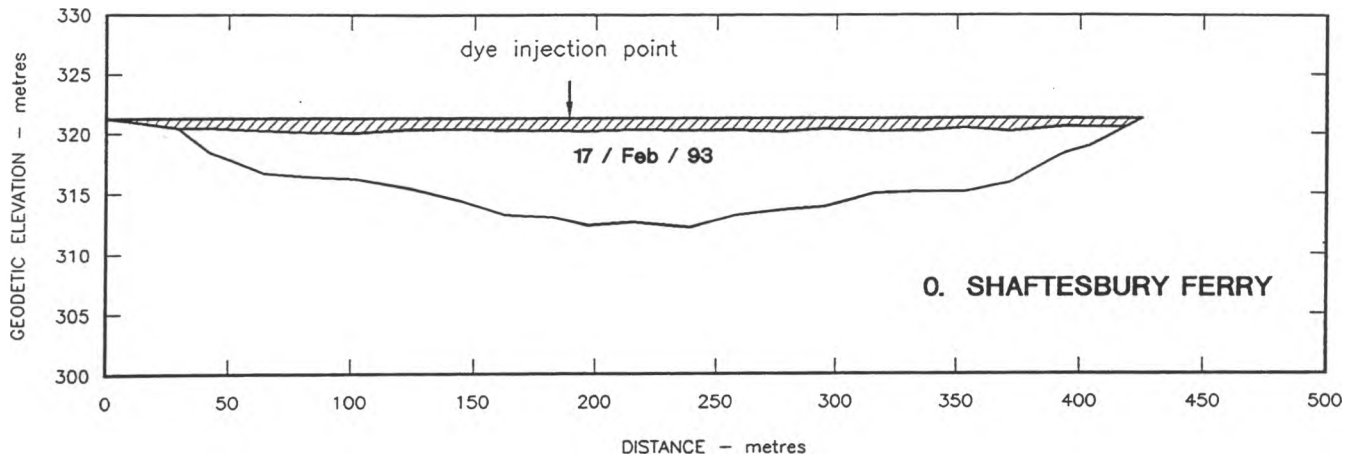
SLOPE PROFILE OF STUDY LENGTH

Scale as shown 93-06-01 FIGURE 3.3

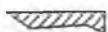
northwest hydraulic consultants ltd.
ALBERTA RESEARCH COUNCIL

NOTES:

1. SLOPES SHOWN IN m/km.
2. ELEVATIONS ADJUSTED TO CONSTANT DISCHARGE OF 1600 m³/s UNDER ICE



LEGEND:

-  ICE LAYER (TOTAL)
-  SAMPLE LOCATION

NOTES:

1. SECTIONS SHOWN VIEWING DOWNSTREAM.
2. SEE FIGURE 1.1 FOR SECTION LOCATIONS.

NORTHERN RIVER BASINS STUDY

Peace River Time of Travel Study

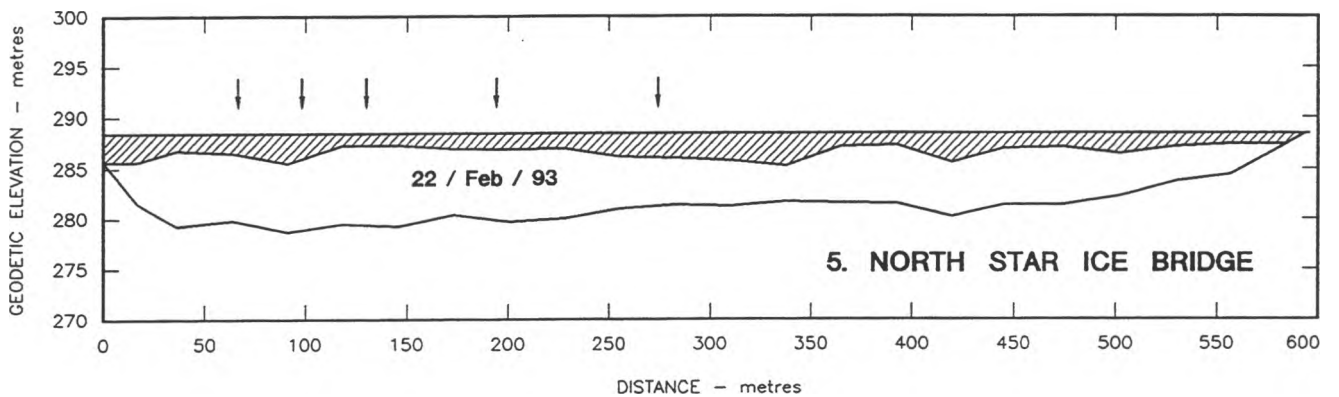
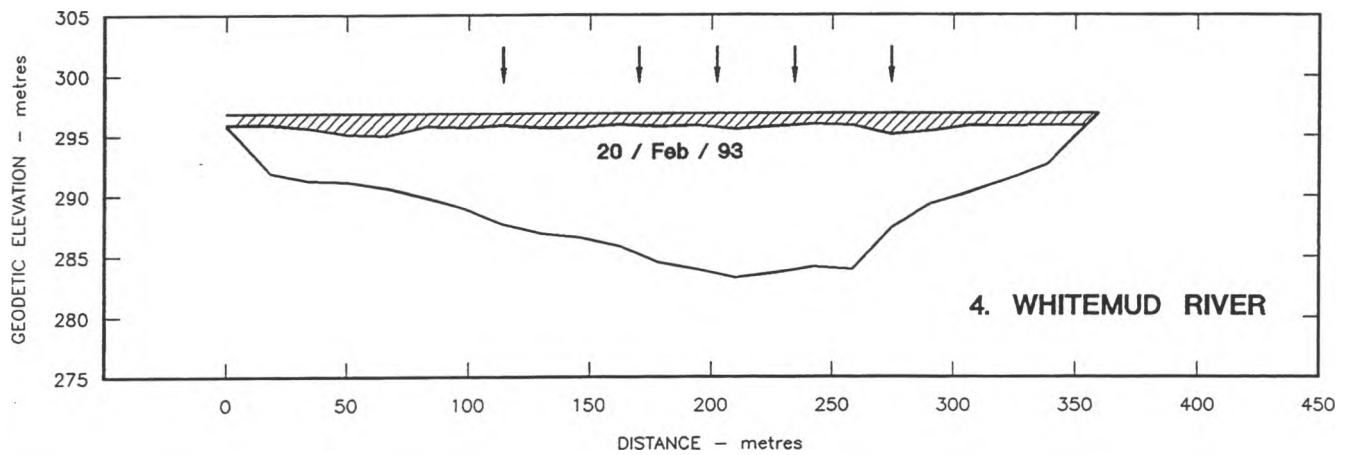
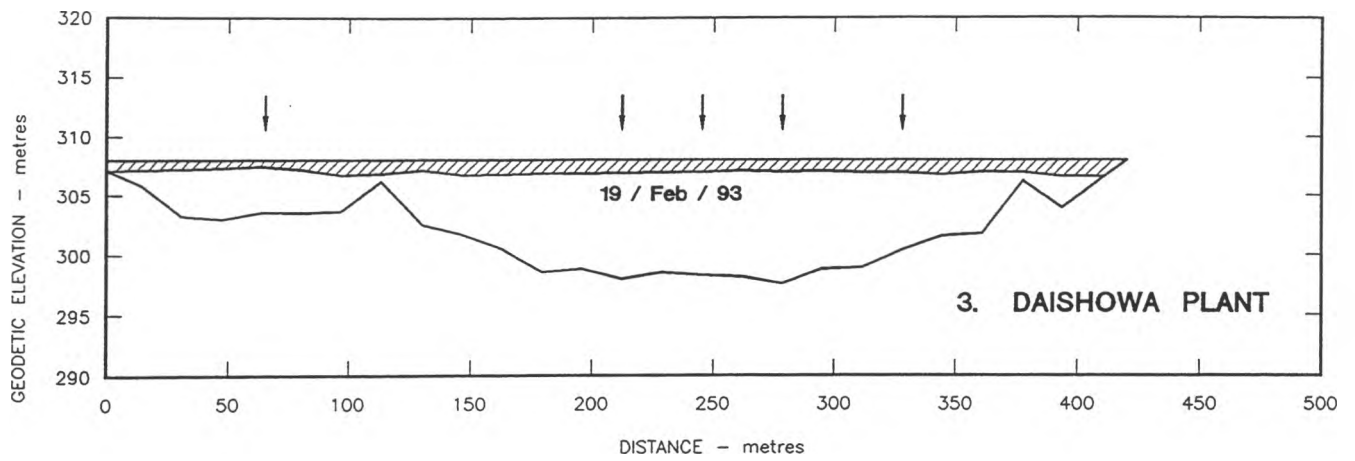
CROSS SECTIONS NOS. 0, 1, 2

Scale as shown

93-05-28

FIGURE 3.4a

northwest hydraulic consultants ltd.
ALBERTA RESEARCH COUNCIL



LEGEND:

-  ICE LAYER (TOTAL)
-  SAMPLE LOCATION

NOTES:

1. SECTIONS SHOWN VIEWING DOWNSTREAM.
2. SEE FIGURE 1.1 FOR SECTION LOCATIONS.

NORTHERN RIVER BASINS STUDY

Peace River Time of Travel Study

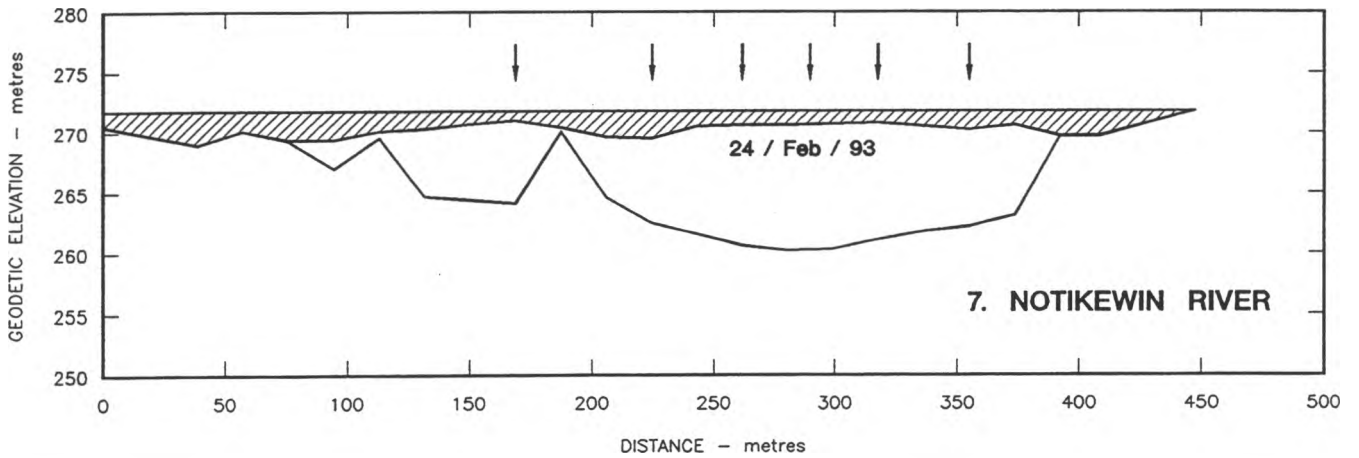
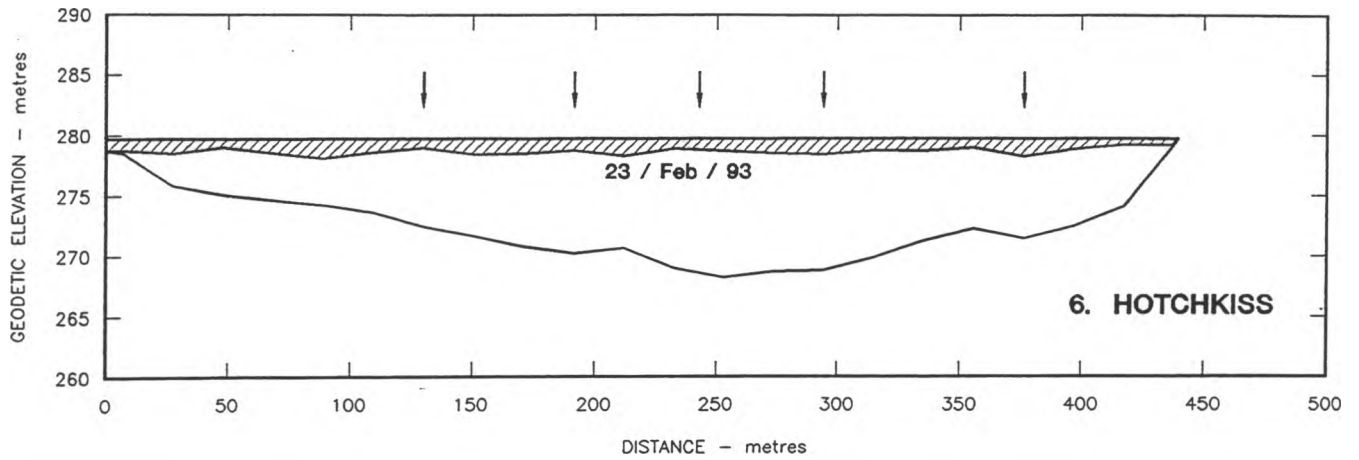
CROSS SECTIONS NOS. 3, 4, 5

Scale as shown

93-05-28

FIGURE 3.4b

northwest hydraulic consultants ltd.
ALBERTA RESEARCH COUNCIL



LEGEND:

-  ICE LAYER (TOTAL)
-  SAMPLE LOCATION

NOTES:

1. SECTIONS SHOWN VIEWING DOWNSTREAM.
2. SEE FIGURE 1.1 FOR SECTION LOCATIONS.

NORTHERN RIVER BASINS STUDY

Peace River Time of Travel Study

CROSS SECTIONS NOS. 6 & 7

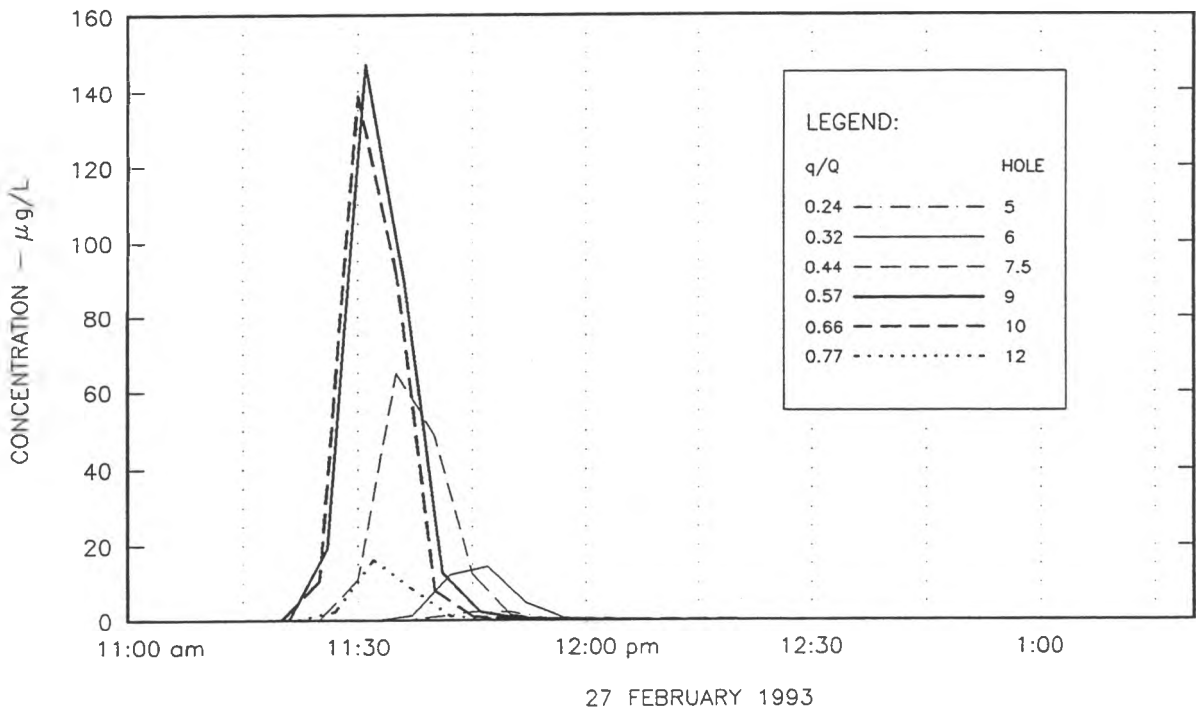
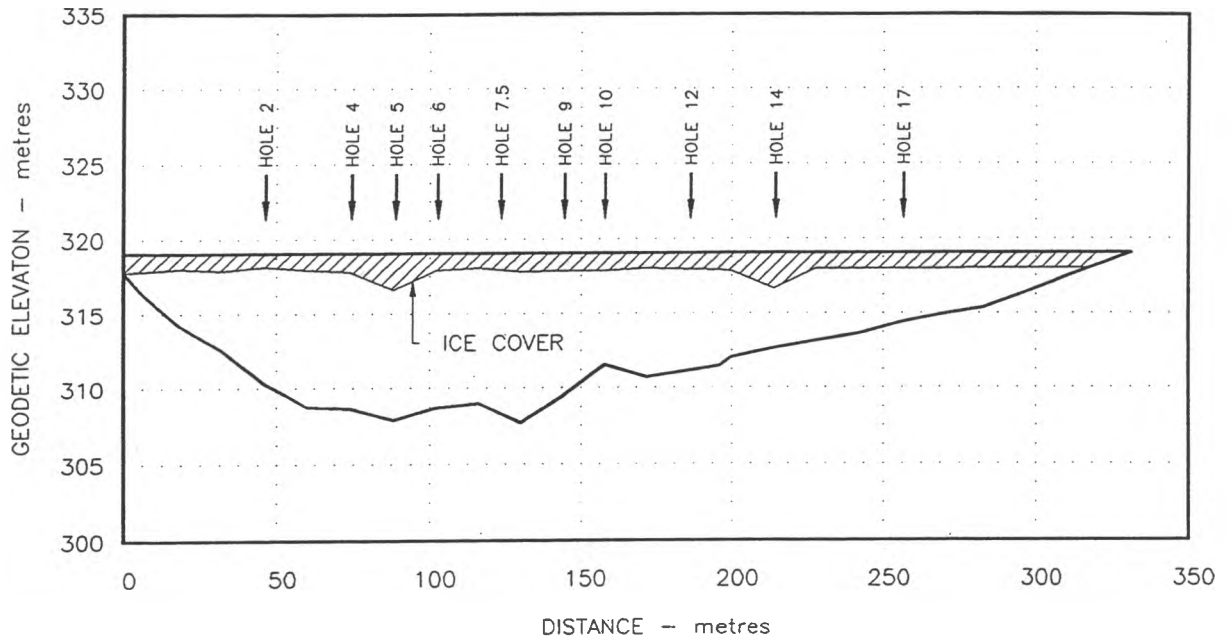
Scale as shown

93-05-29

FIGURE 3.4c

northwest hydraulic consultants ltd.
ALBERTA RESEARCH COUNCIL

MACKENZIE CAIRN



NOTES:

1. Section shown viewing downstream.
2. Concentration of Rhodamine WT dye ($\mu\text{g/L}$ or parts per billion)
3. Approximate Peace River discharge: $1740 \text{ m}^3/\text{s}$.

NORTHERN RIVER BASINS STUDY

Peace River Time of Travel Study

DYE CONCENTRATIONS: SITE 1

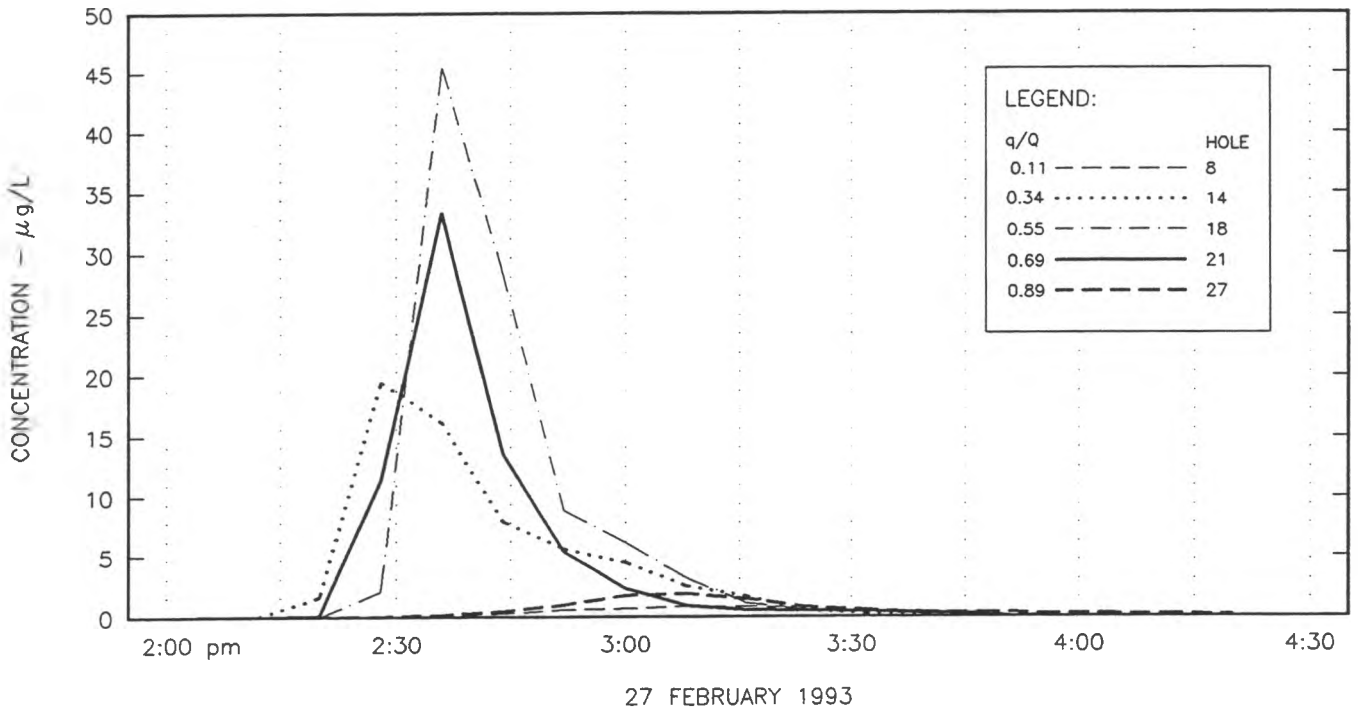
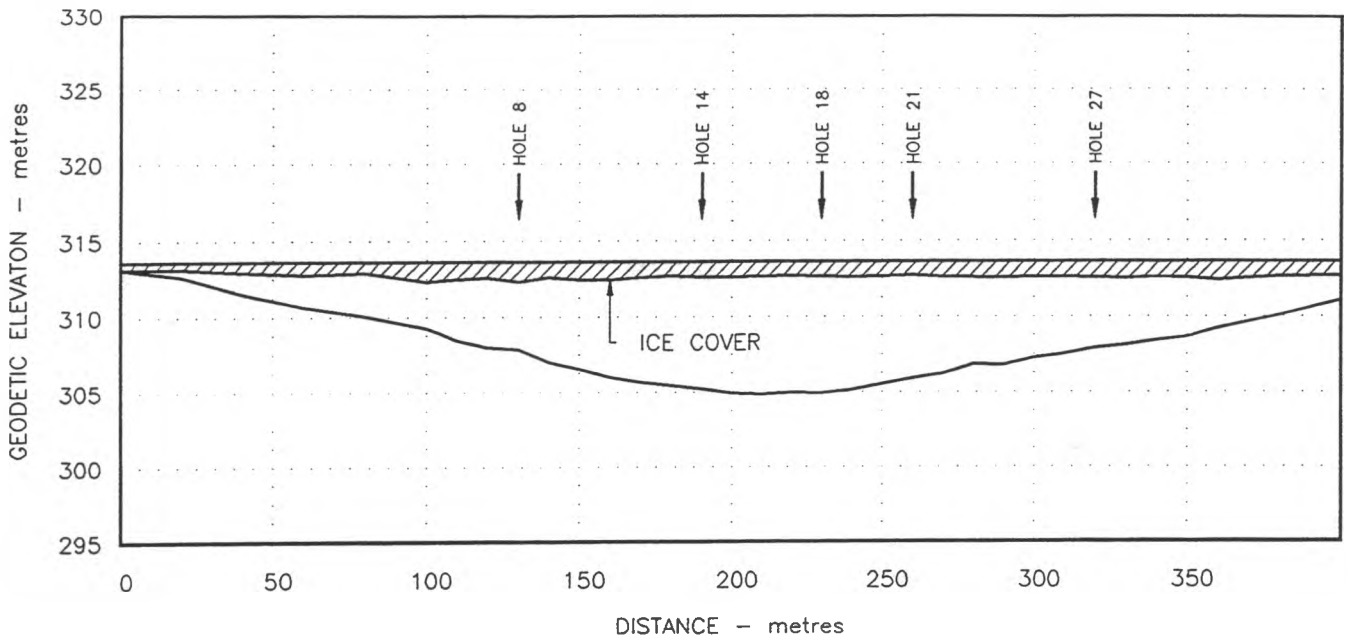
Scale as shown

93-04-06

FIGURE 3.5a

northwest hydraulic consultants ltd.
ALBERTA RESEARCH COUNCIL

TOWN OF PEACE RIVER



NOTES:

1. Section shown viewing downstream.
2. Concentration of Rhodamine WT dye ($\mu\text{g/L}$ or parts per billion)
3. Approximate Peace River discharge: $1740 \text{ m}^3/\text{s}$.

NORTHERN RIVER BASINS STUDY

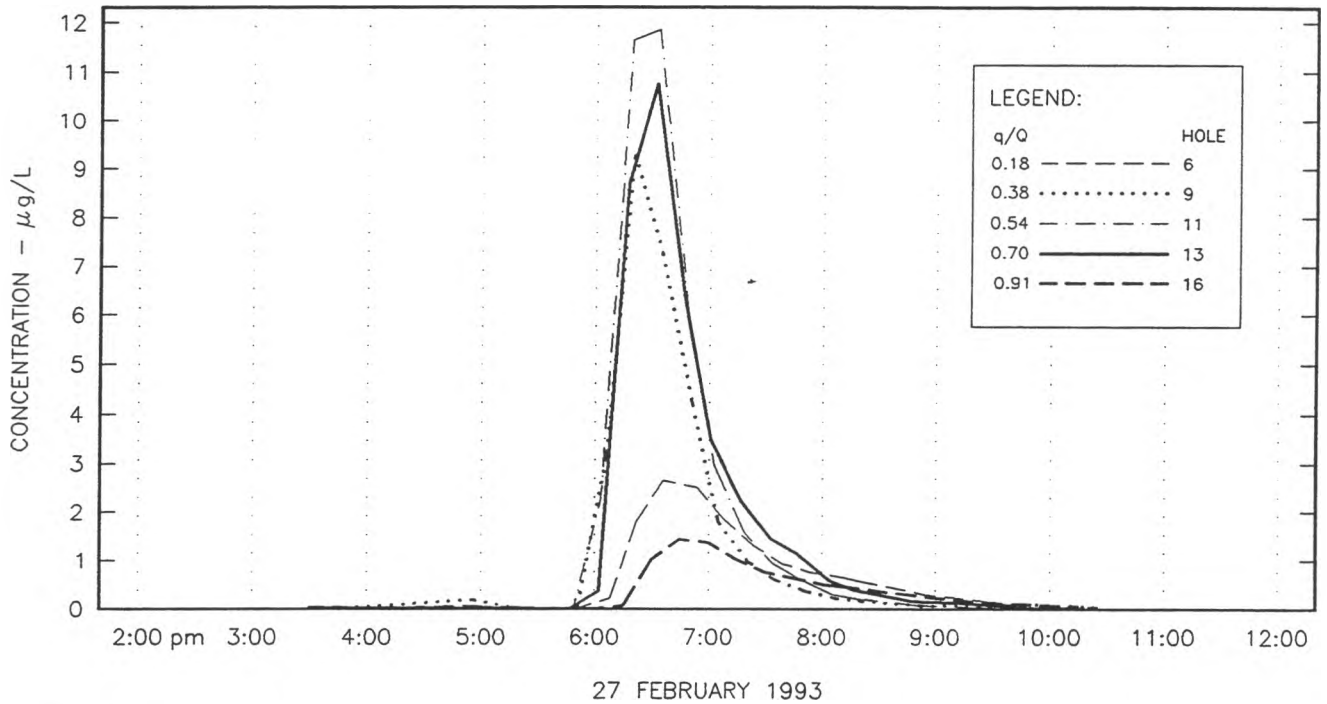
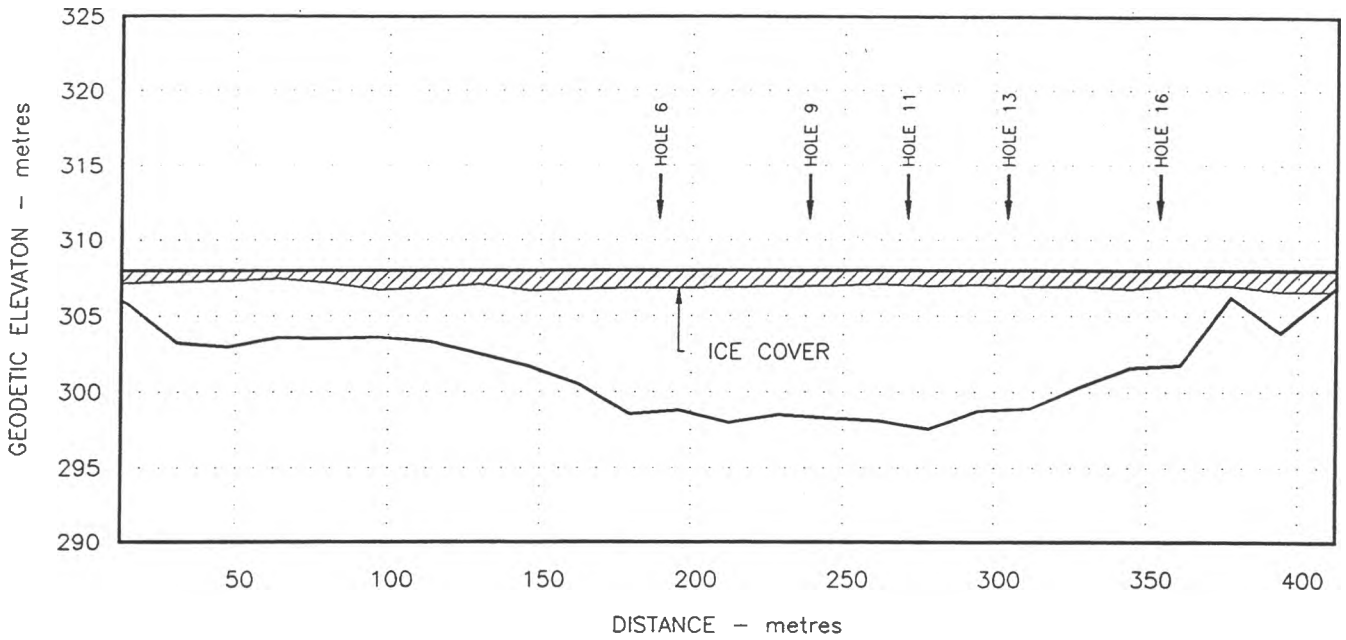
Peace River Time of Travel Study

DYE CONCENTRATIONS: SITE 2

Scale as shown	93-04-14	FIGURE 3.5b
----------------	----------	-------------

northwest hydraulic consultants ltd.
ALBERTA RESEARCH COUNCIL

DAISHOWA BRIDGE



NOTES:

1. Section shown viewing downstream.
2. Concentration of Rhodamine WT dye ($\mu\text{g/L}$ or parts per billion)
3. Approximate Peace River discharge: $1740 \text{ m}^3/\text{s}$.

NORTHERN RIVER BASINS STUDY

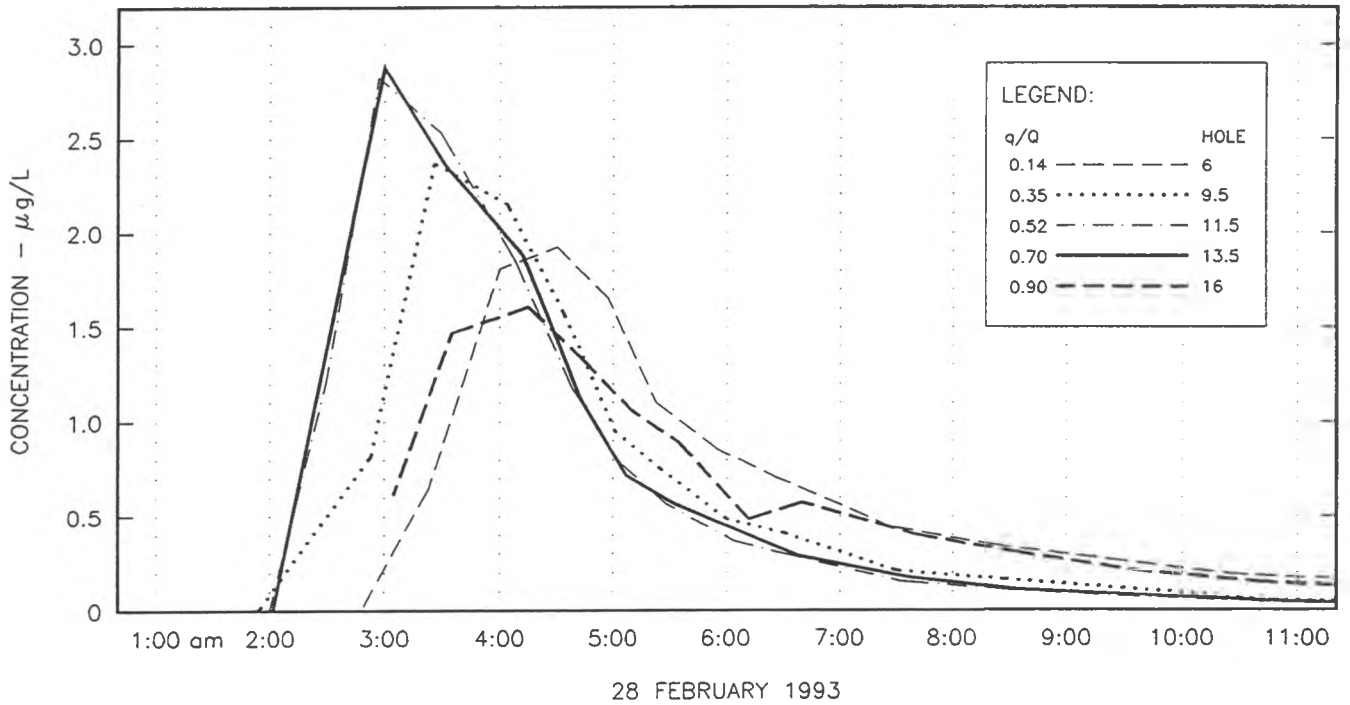
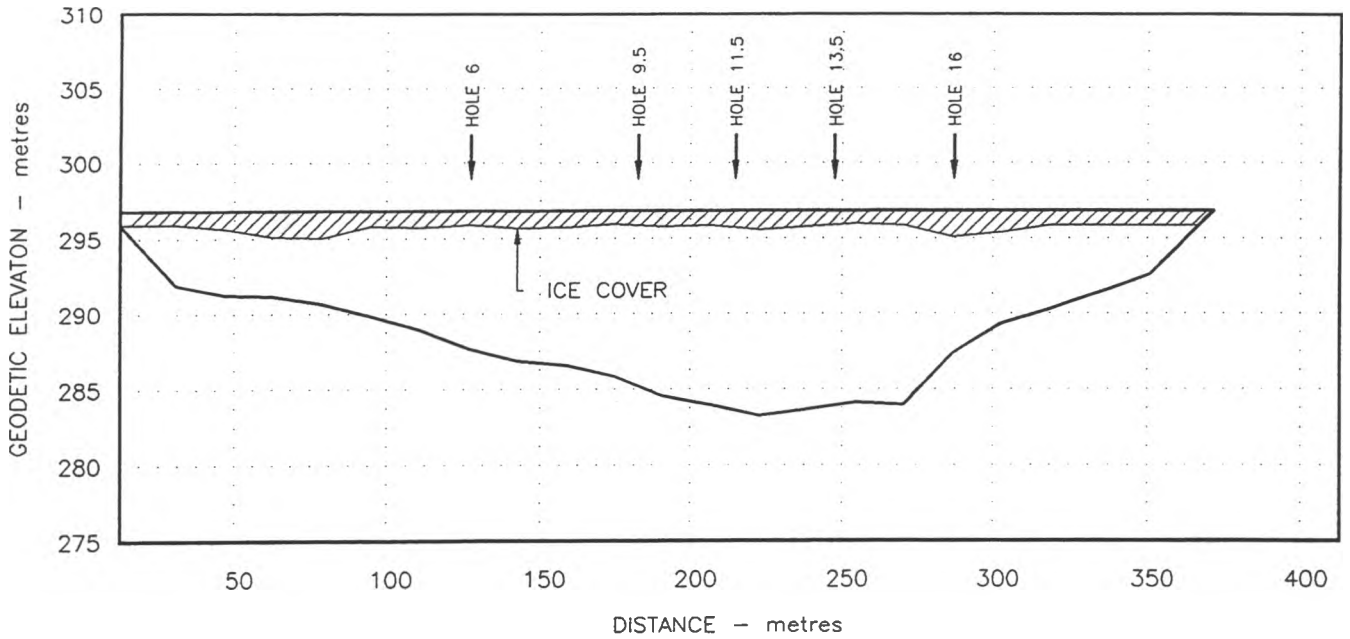
Peace River Time of Travel Study

DYE CONCENTRATIONS: SITE 3

Scale as shown	93-04-15	FIGURE 3.5c
----------------	----------	-------------

northwest hydraulic consultants ltd.
ALBERTA RESEARCH COUNCIL

WHITEMUD RIVER

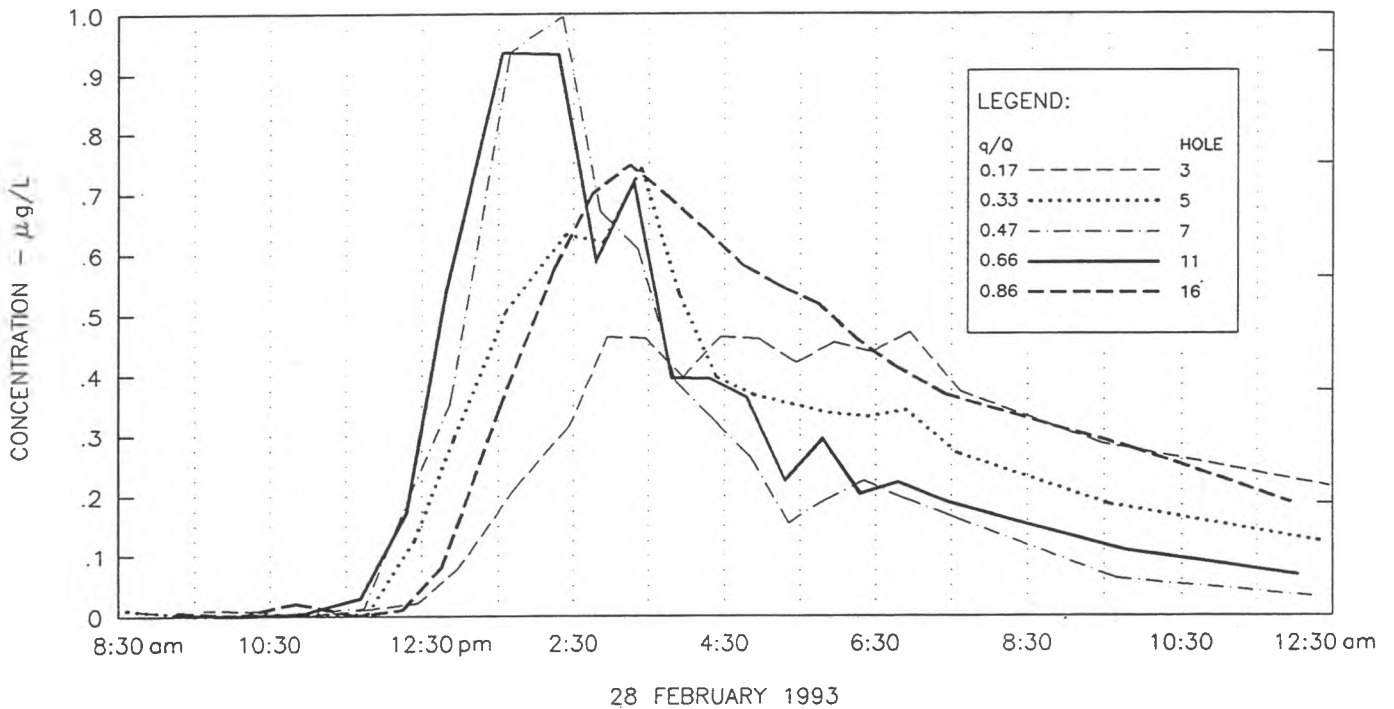
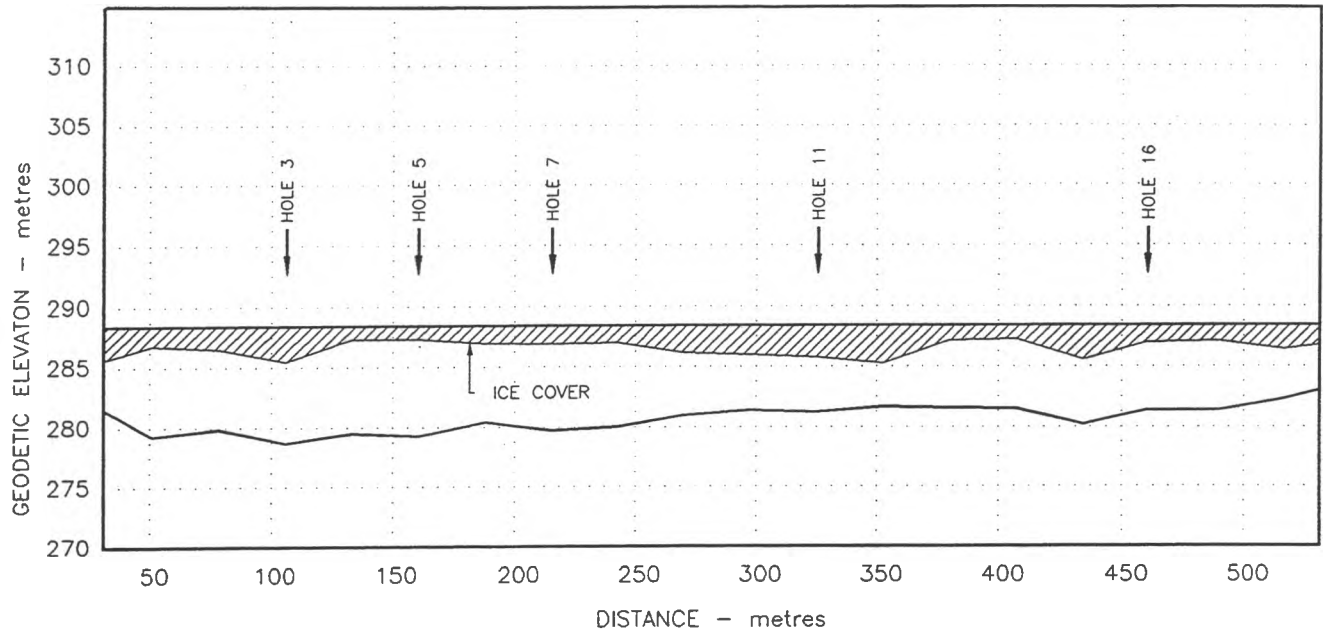


NOTES:

1. Section shown viewing downstream.
2. Concentration of Rhodamine WT dye ($\mu\text{g/L}$ or parts per billion)
3. Approximate Peace River discharge: $1740 \text{ m}^3/\text{s}$.

NORTHERN RIVER BASINS STUDY		
Peace River Time of Travel Study		
DYE CONCENTRATIONS: SITE 4		
Scale as shown	93-04-15	FIGURE 3.5d
northwest hydraulic consultants ltd. ALBERTA RESEARCH COUNCIL		

NORTH STAR



NOTES:

1. Section shown viewing downstream.
2. Concentration of Rhodamine WT dye ($\mu\text{g/L}$ or parts per billion)
3. Approximate Peace River discharge: $1740 \text{ m}^3/\text{s}$.

NORTHERN RIVER BASINS STUDY

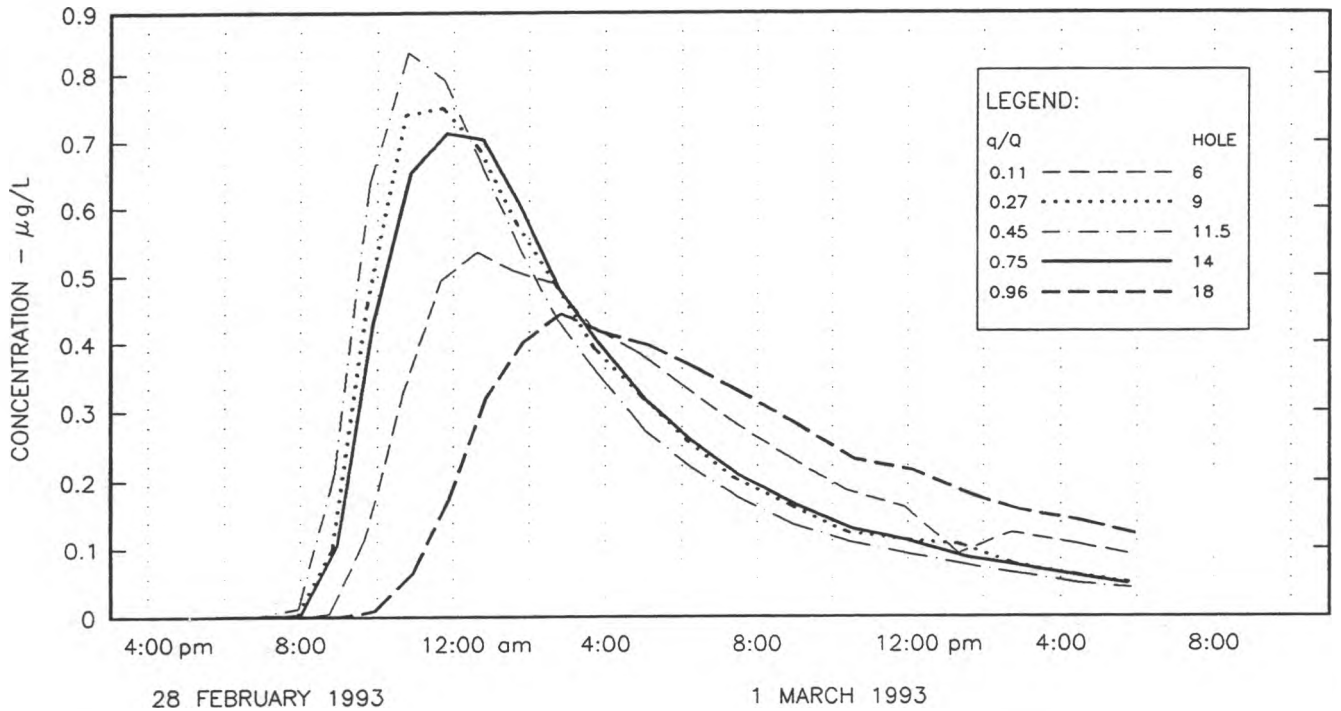
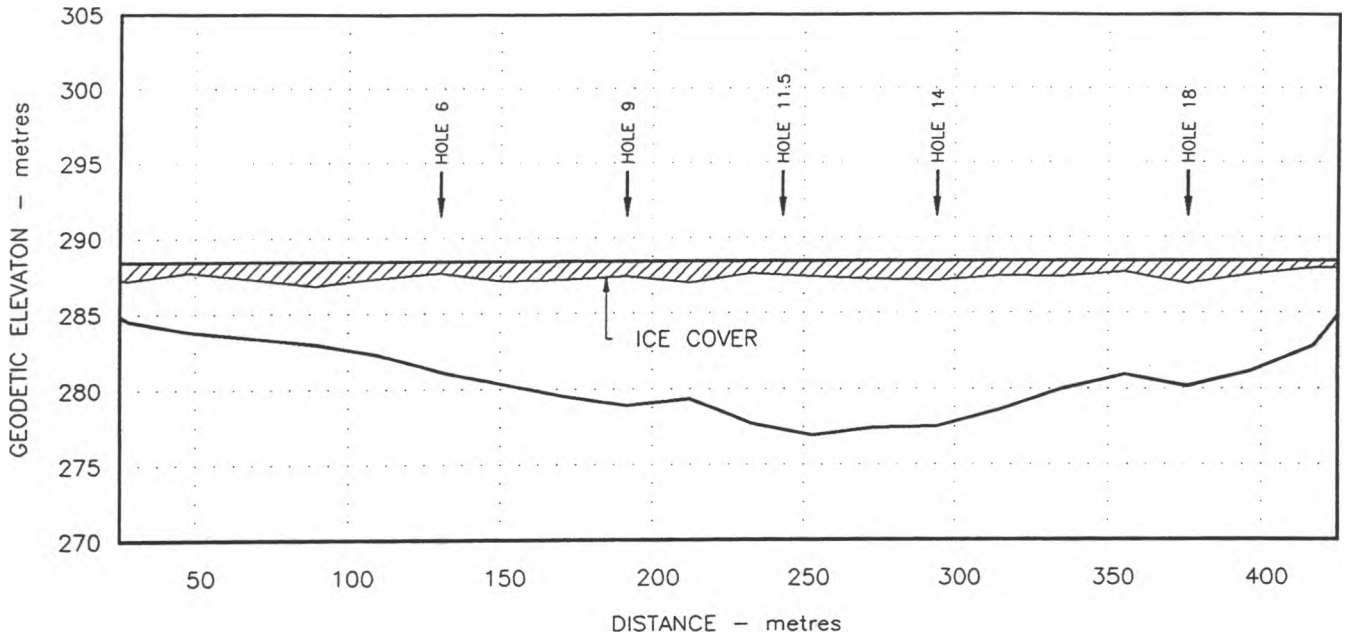
Peace River Time of Travel Study

DYE CONCENTRATIONS: SITE 5

Scale as shown	93-04-15	FIGURE 3.5e
----------------	----------	-------------

northwest hydraulic consultants ltd.
ALBERTA RESEARCH COUNCIL

HOTCHKISS

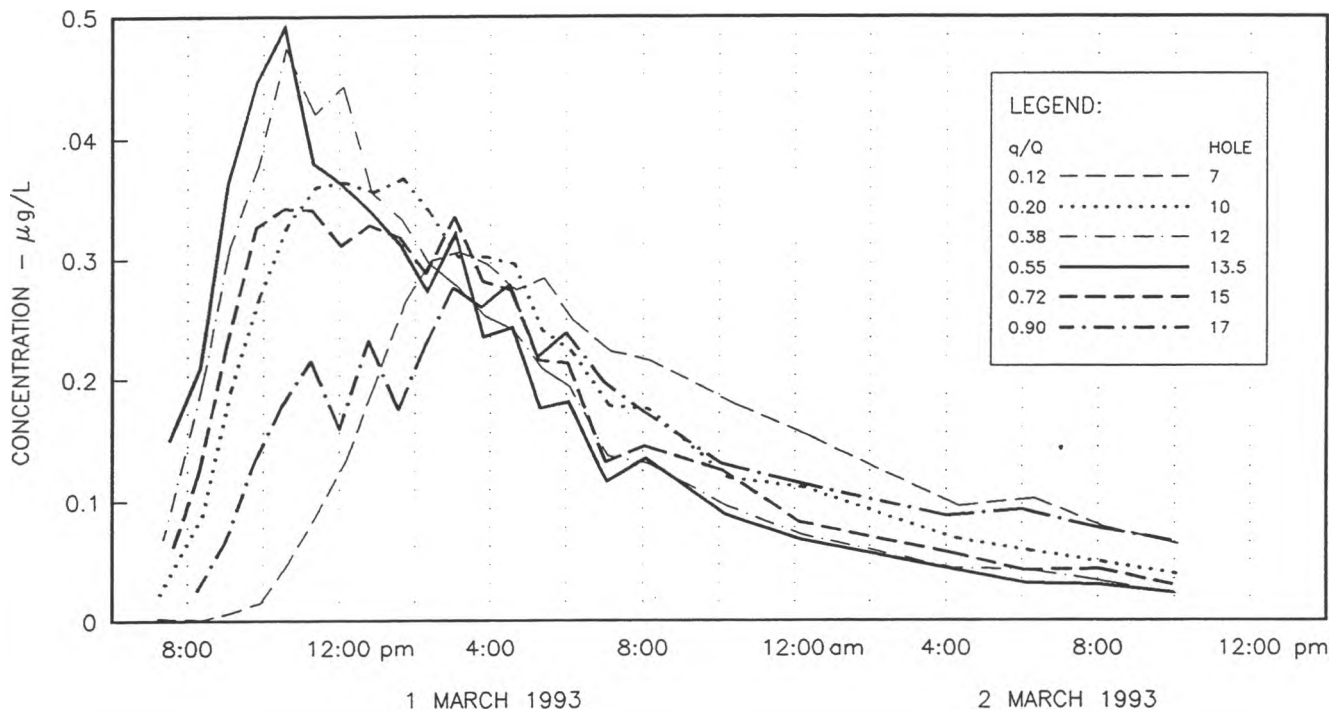
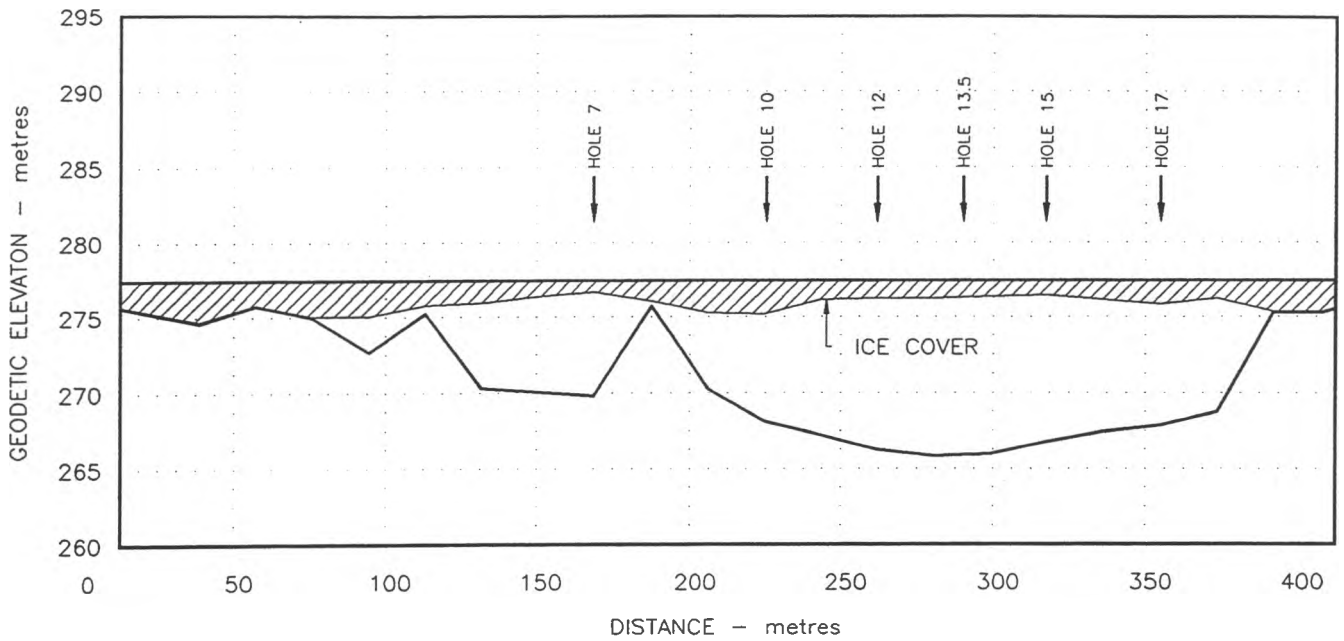


NOTES:

1. Section shown viewing downstream.
2. Concentration of Rhodamine WT dye ($\mu\text{g/L}$ or parts per billion)
3. Approximate Peace River discharge: $1740 \text{ m}^3/\text{s}$.

NORTHERN RIVER BASINS STUDY		
Peace River Time of Travel Study		
DYE CONCENTRATIONS: SITE 6		
Scale as shown	93-04-06	FIGURE 3.5f
northwest hydraulic consultants ltd. ALBERTA RESEARCH COUNCIL		

NOTIKEWIN RIVER



NOTES:

1. Section shown viewing downstream.
2. Concentration of Rhodamine WT dye ($\mu\text{g/L}$ or parts per billion)
3. Approximate Peace River discharge: $1740 \text{ m}^3/\text{s}$.

NORTHERN RIVER BASINS STUDY

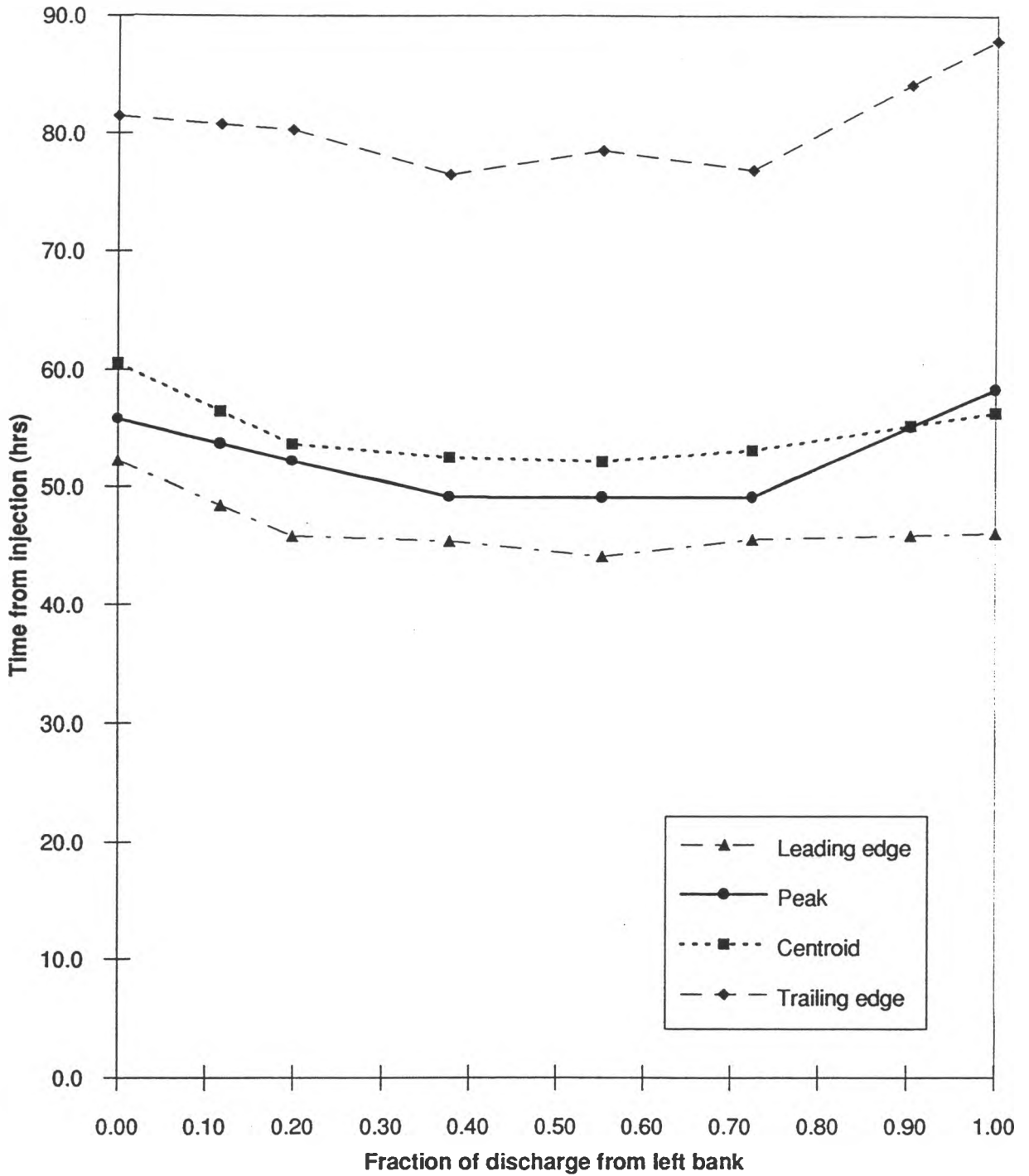
Peace River Time of Travel Study

DYE CONCENTRATIONS: SITE 7

Scale as shown 93-04-06 FIGURE 3.5g

northwest hydraulic consultants ltd.
ALBERTA RESEARCH COUNCIL

Notikewin River



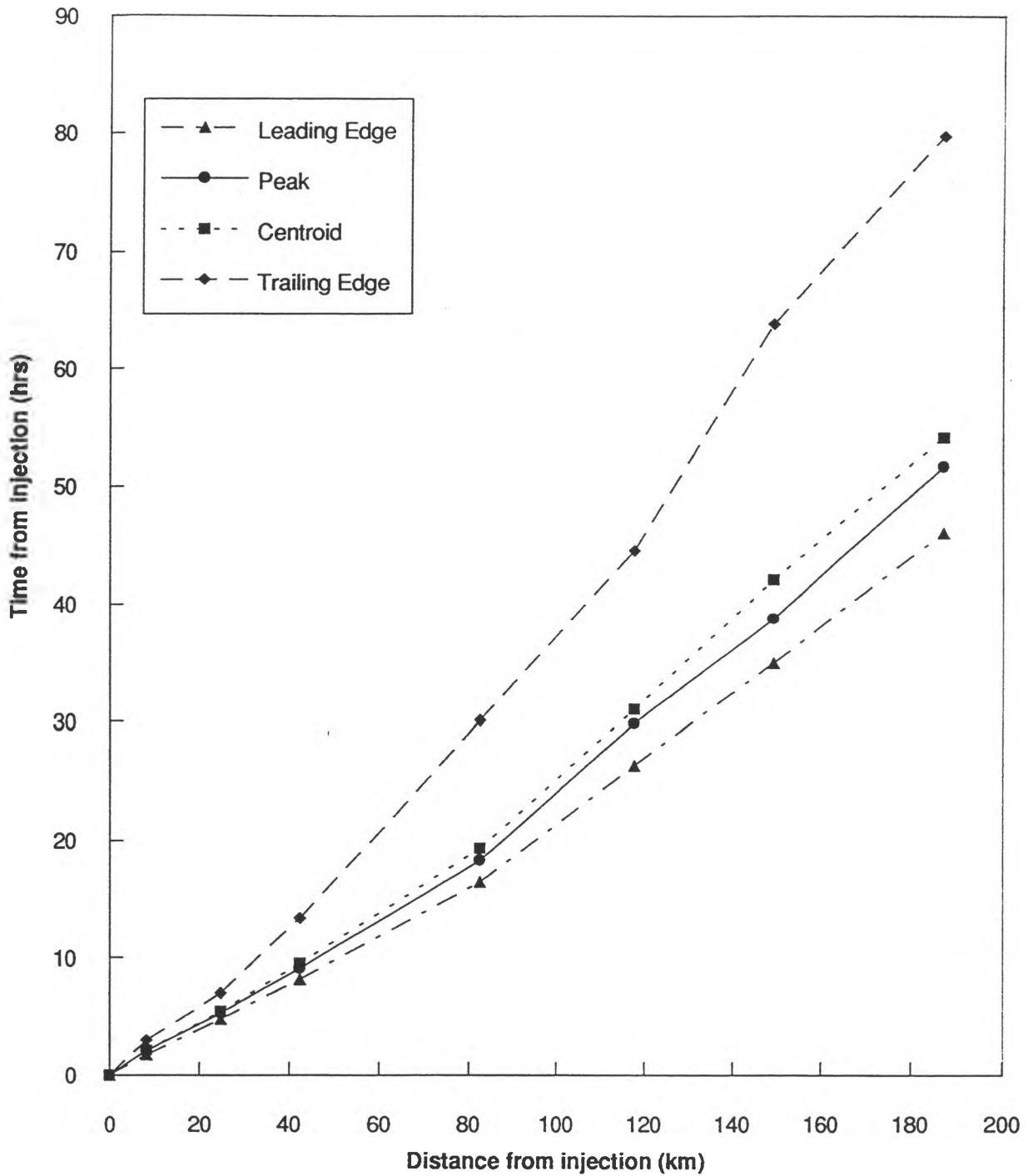
NORTHERN RIVER BASINS STUDY

Peace River Time of Travel Study

TYPICAL VARIATION OF TRAVEL TIMES ACROSS THE CHANNEL

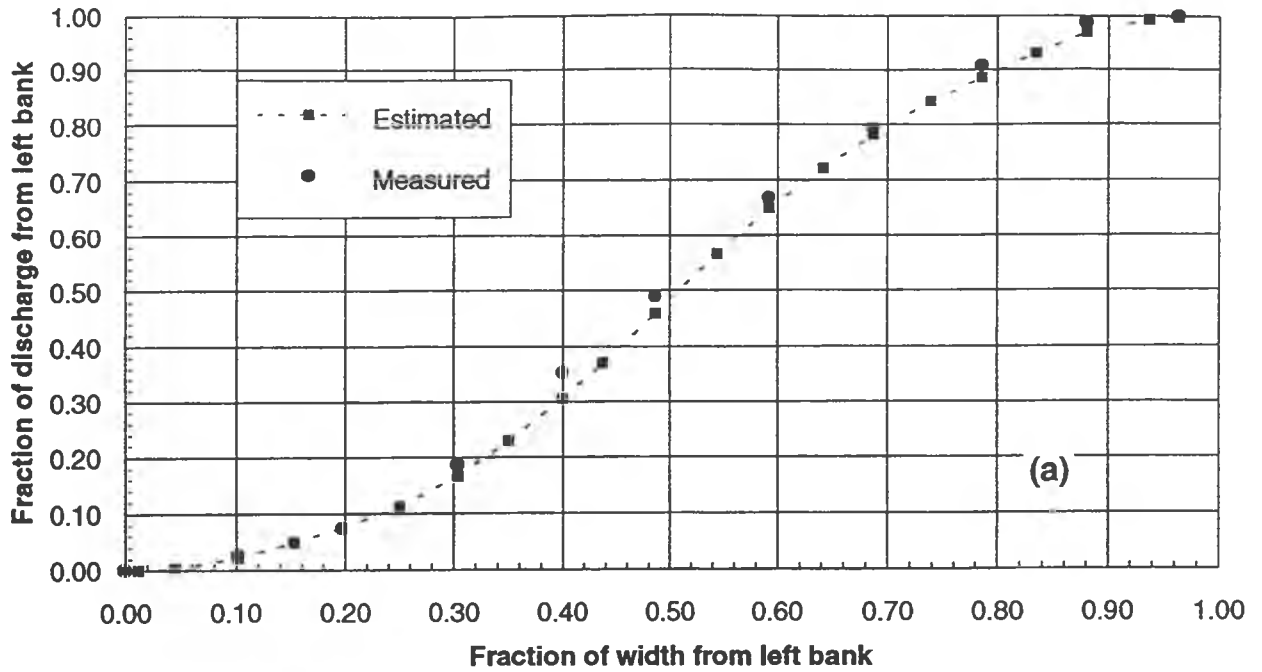
Scale as shown	93-06-15	FIGURE 3.6
----------------	----------	------------

northwest hydraulic consultants ltd.
ALBERTA RESEARCH COUNCIL

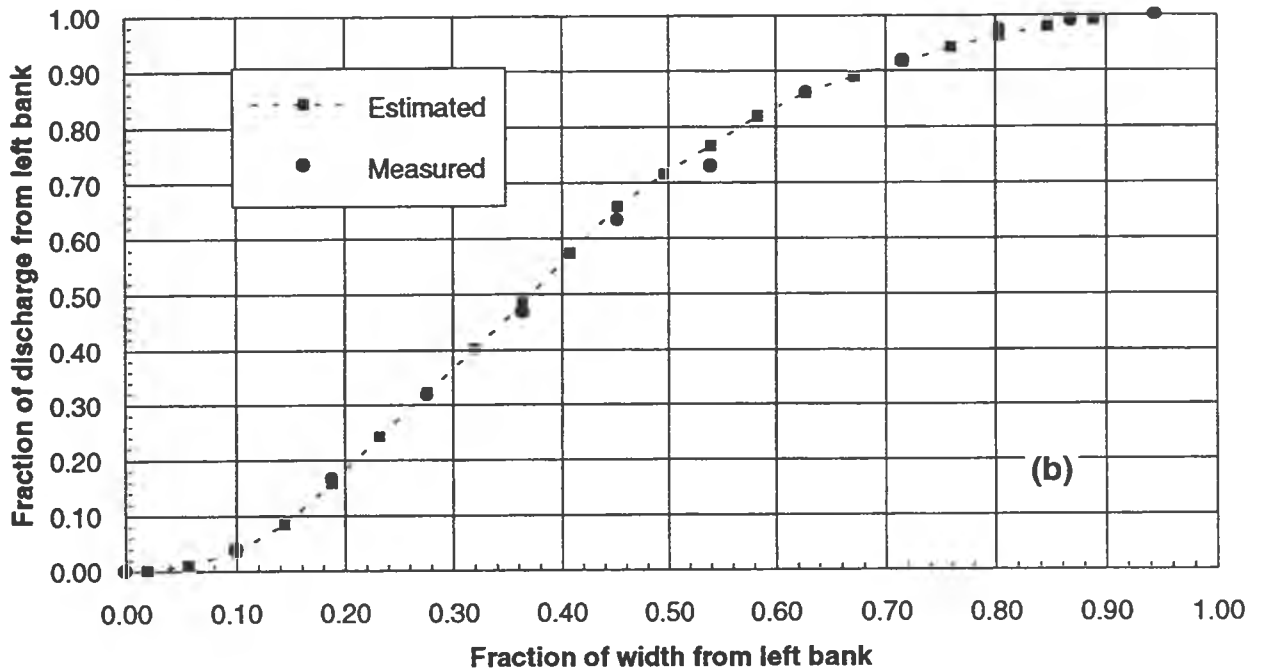


NORTHERN RIVER BASINS STUDY		
Peace River Time of Travel Study		
GROWTH OF TRAVEL TIMES WITH DISTANCE FROM INJECTION		
Scale as shown	93-06-15	FIGURE 3.7
northwest hydraulic consultants ltd. ALBERTA RESEARCH COUNCIL		

(a) SHAFTESBURY FERRY



(b) MACKENZIE CAIRN



NORTHERN RIVER BASINS STUDY

Peace River Time of Travel Study

**CUMULATIVE DISCHARGE DISTRIBUTIONS
ACROSS CHANNELS: SITES 0 & 1**

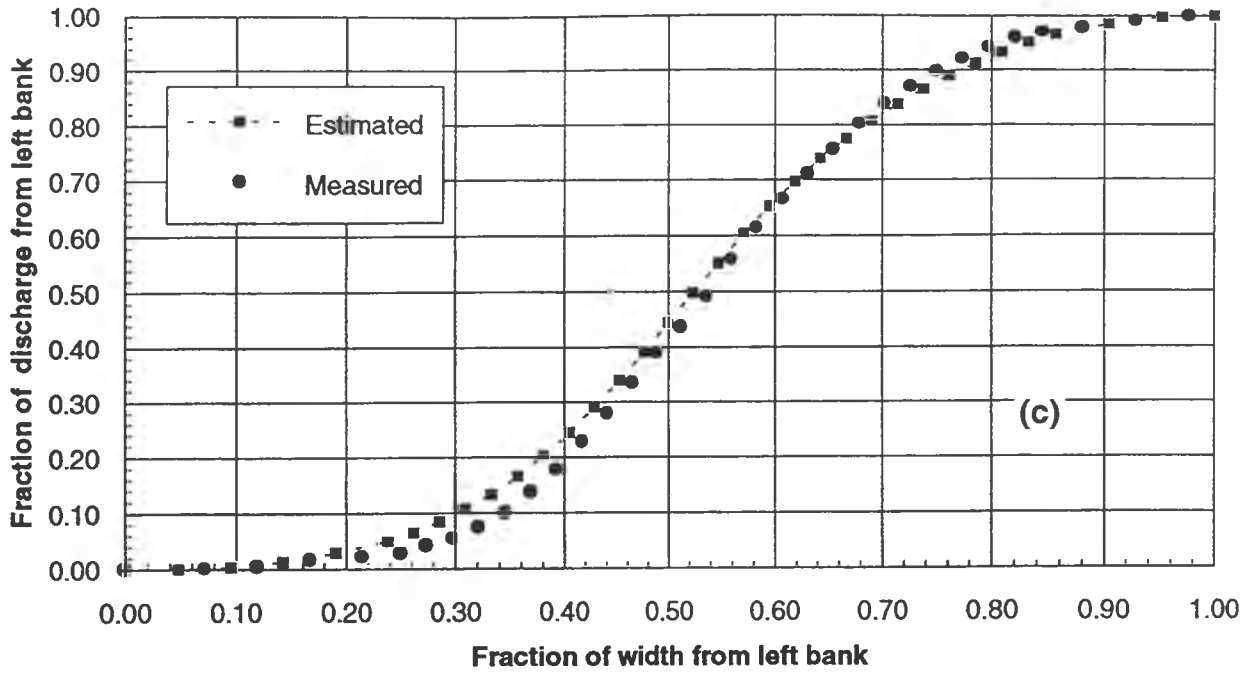
Scale as shown

93-06-15

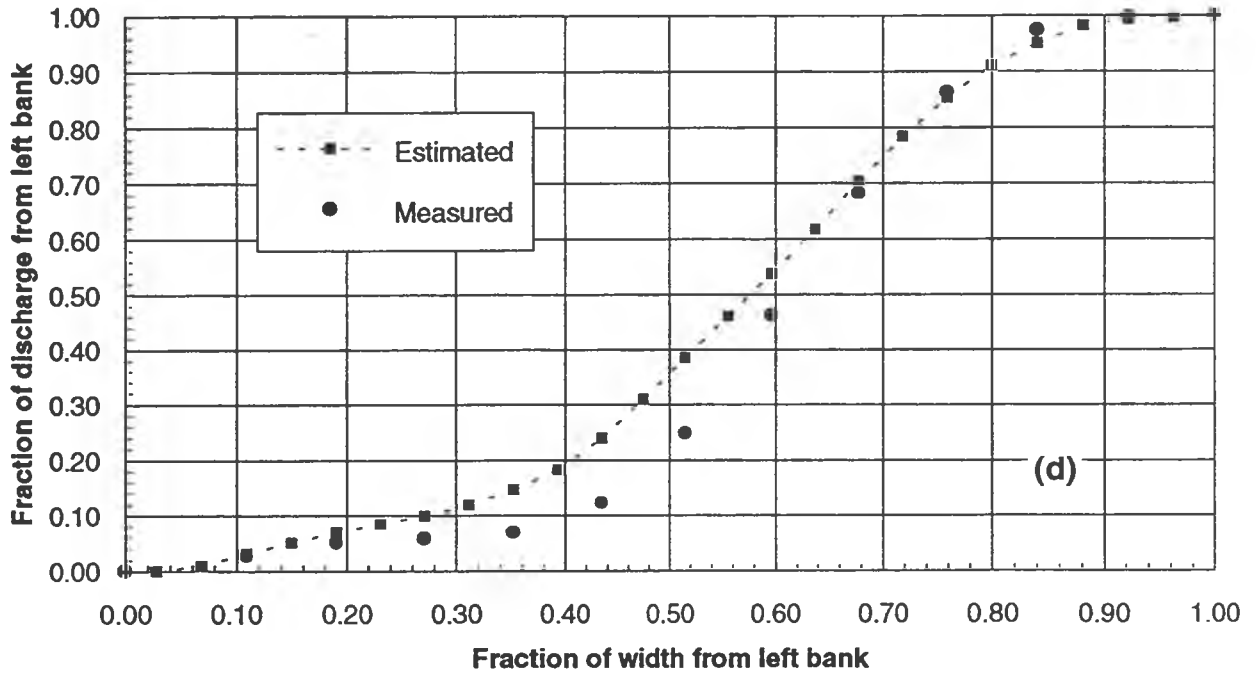
FIGURE 4.1a/b

northwest hydraulic consultants ltd.
ALBERTA RESEARCH COUNCIL

(c) PEACE RIVER



(d) DAISHOWA BRIDGE



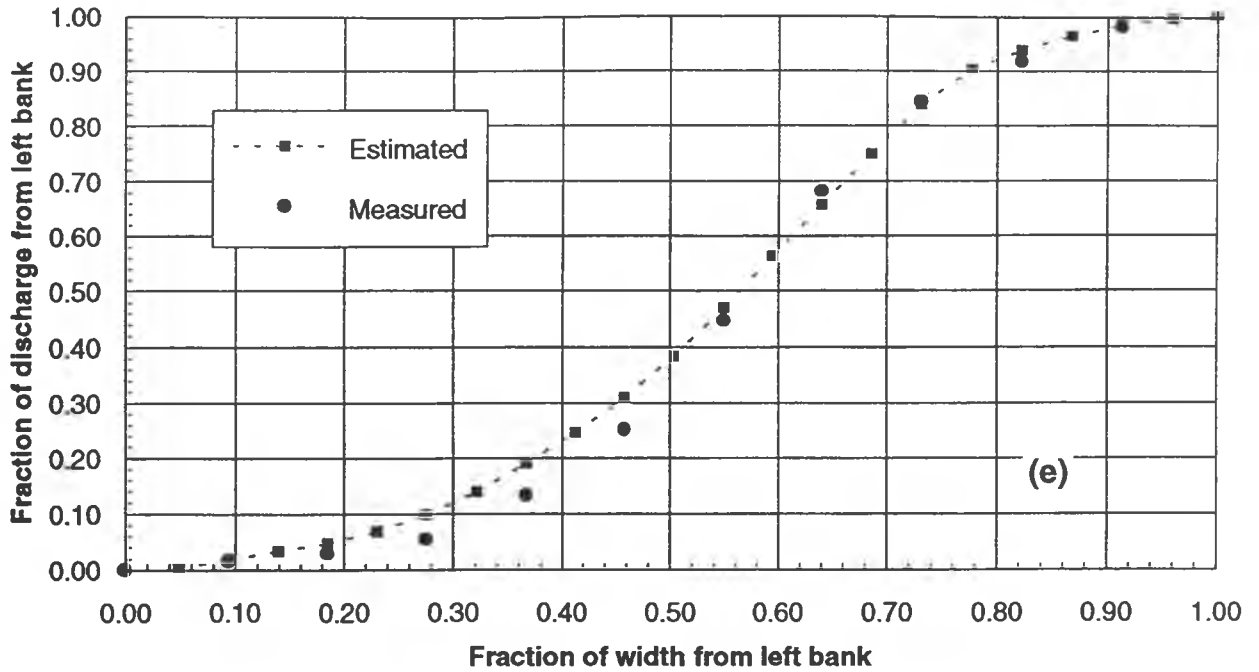
NORTHERN RIVER BASINS STUDY

Peace River Time of Travel Study
**CUMULATIVE DISCHARGE DISTRIBUTIONS
ACROSS CHANNELS: SITES 2 & 3**

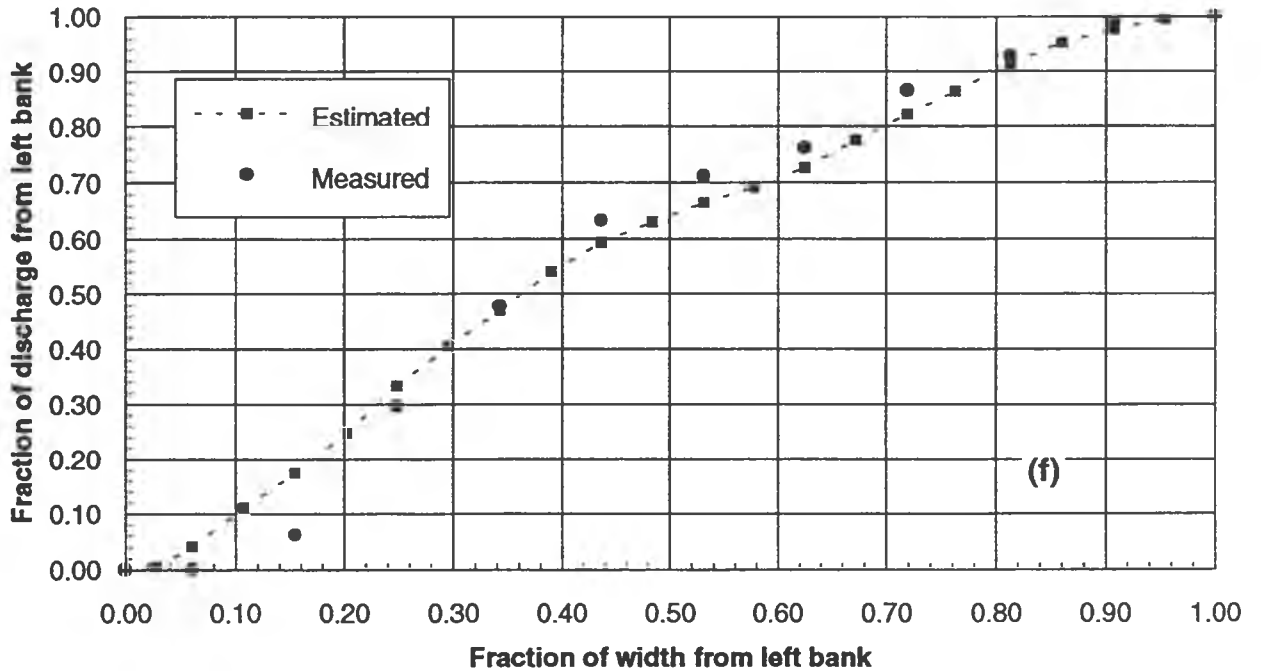
Scale as shown | 93-06-15 | FIGURE 4.1c/d

northwest hydraulic consultants ltd.
ALBERTA RESEARCH COUNCIL

(e) WHITEMUD RIVER



(f) NORTH STAR



NORTHERN RIVER BASINS STUDY

Peace River Time of Travel Study

**CUMULATIVE DISCHARGE DISTRIBUTIONS
ACROSS CHANNELS: SITES 4 & 5**

Scale as shown

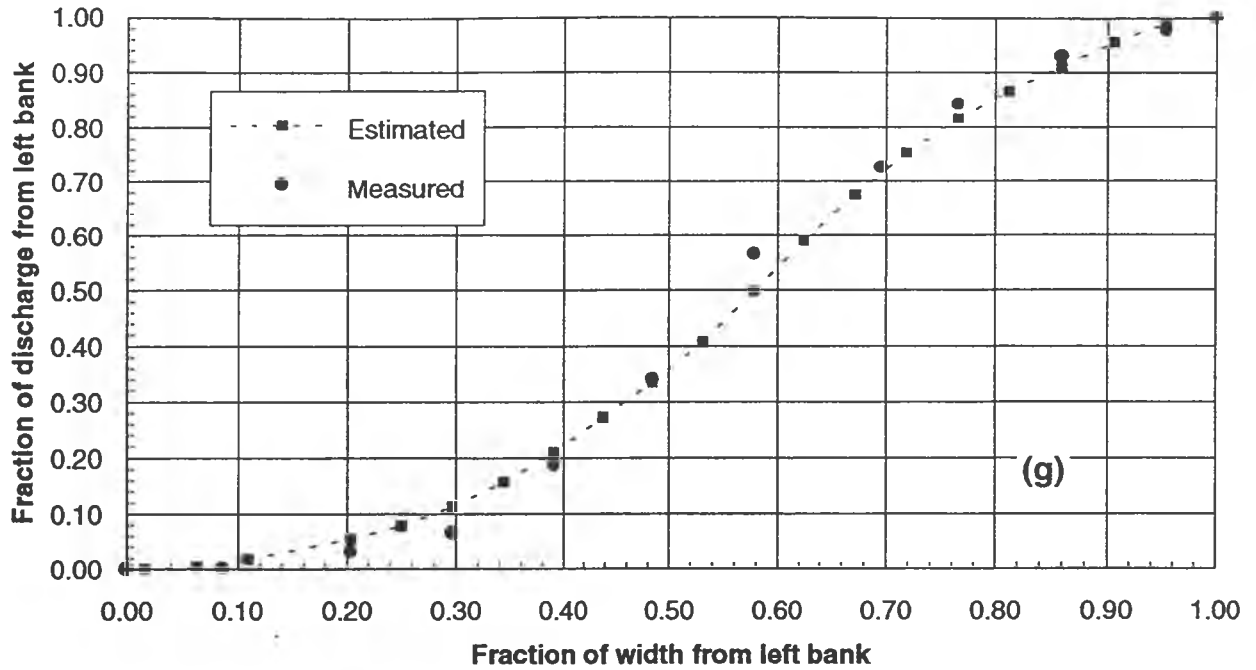
93-06-15

FIGURE 4.1e/f

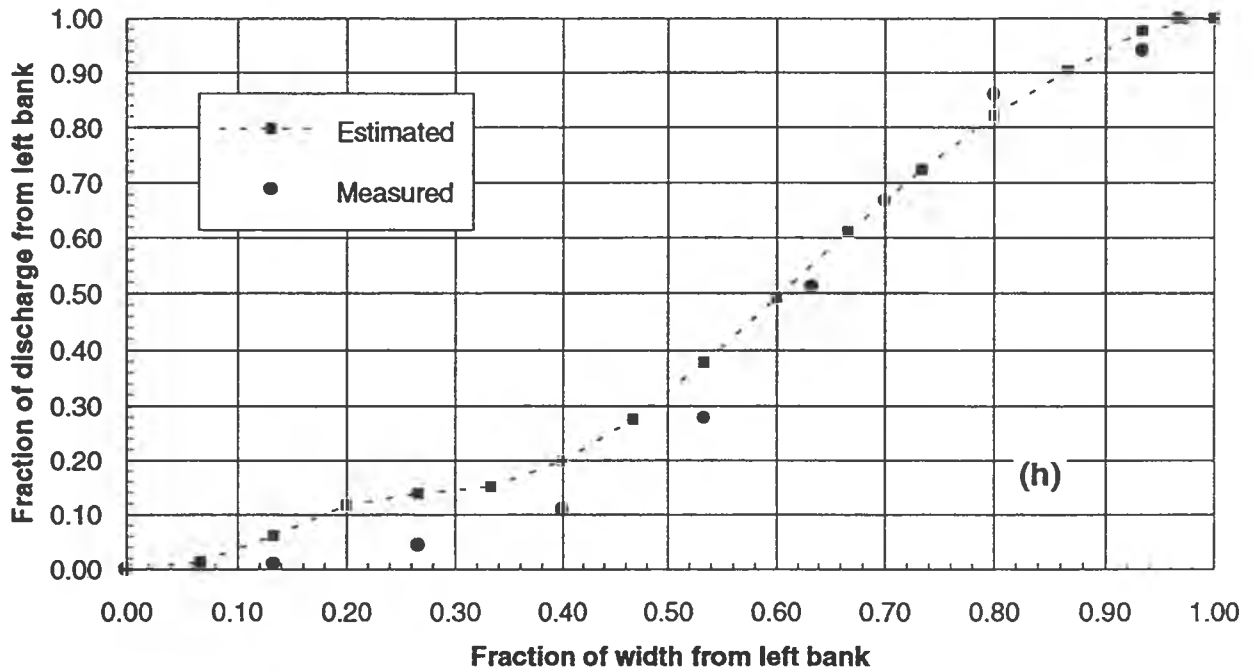
northwest hydraulic consultants ltd.

ALBERTA RESEARCH COUNCIL

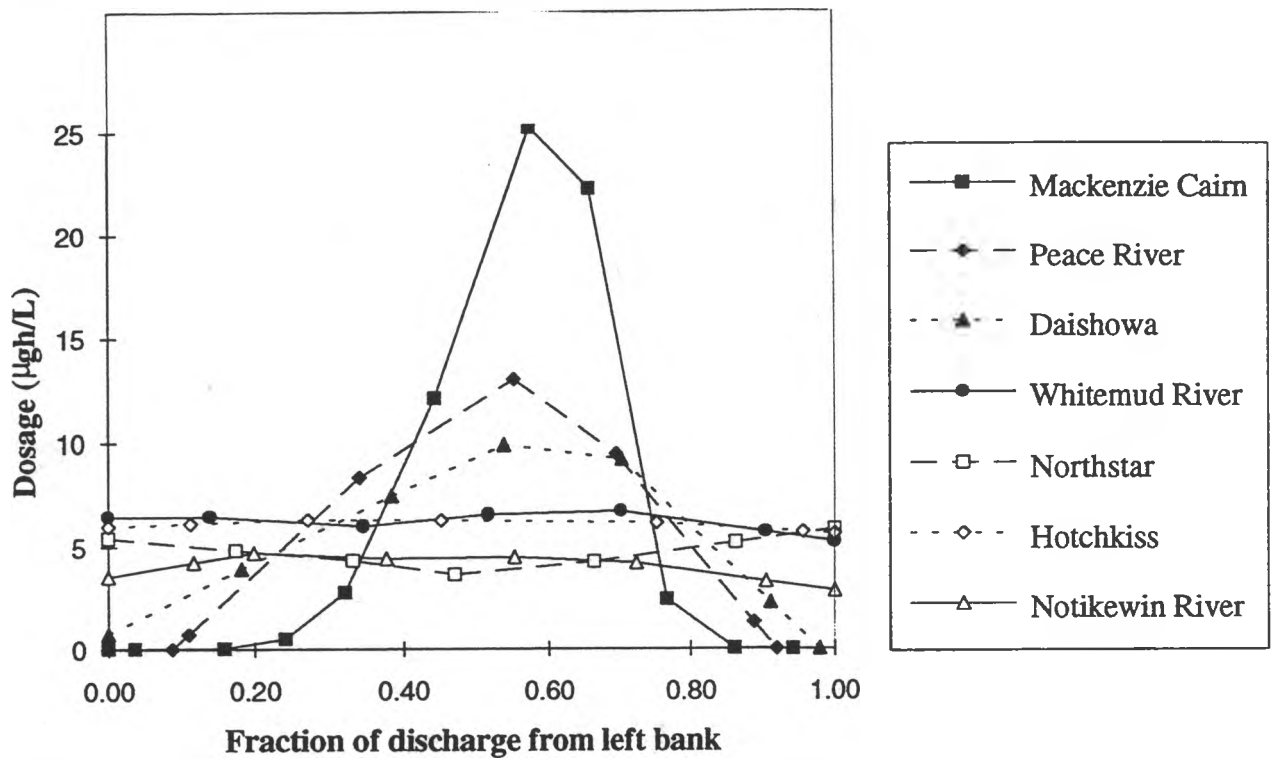
(g) HOTCHKISS



(h) NOTIKEWIN RIVER



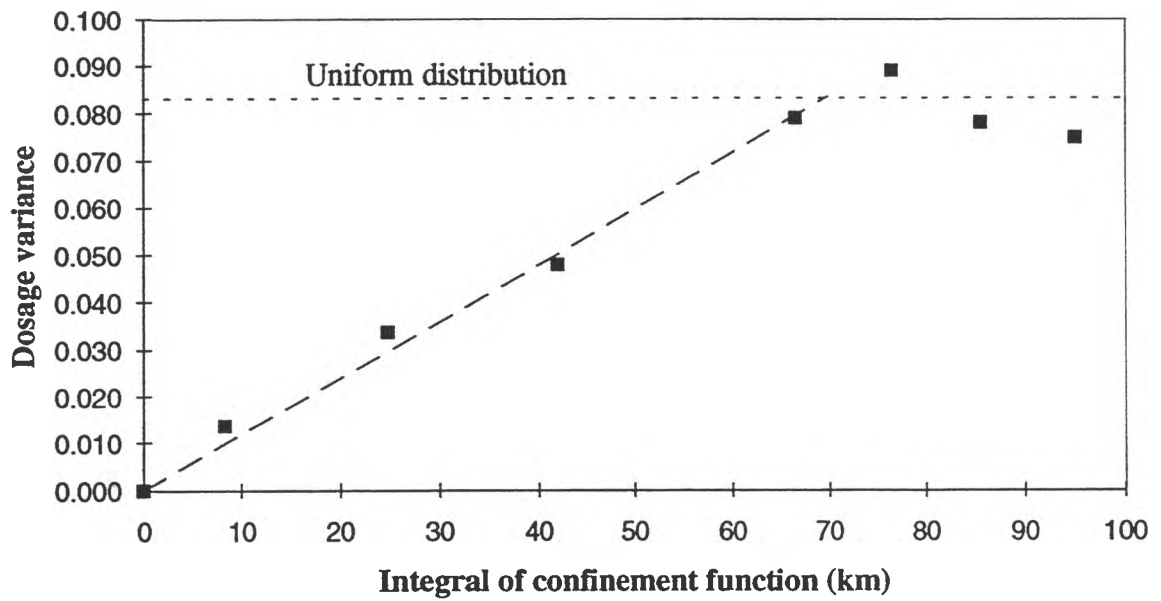
NORTHERN RIVER BASINS STUDY		
Peace River Time of Travel Study		
CUMULATIVE DISCHARGE DISTRIBUTIONS ACROSS CHANNELS: SITES 6 & 7		
Scale as shown	93-06-15	FIGURE 4.1q/h
northwest hydraulic consultants ltd.		
ALBERTA RESEARCH COUNCIL		



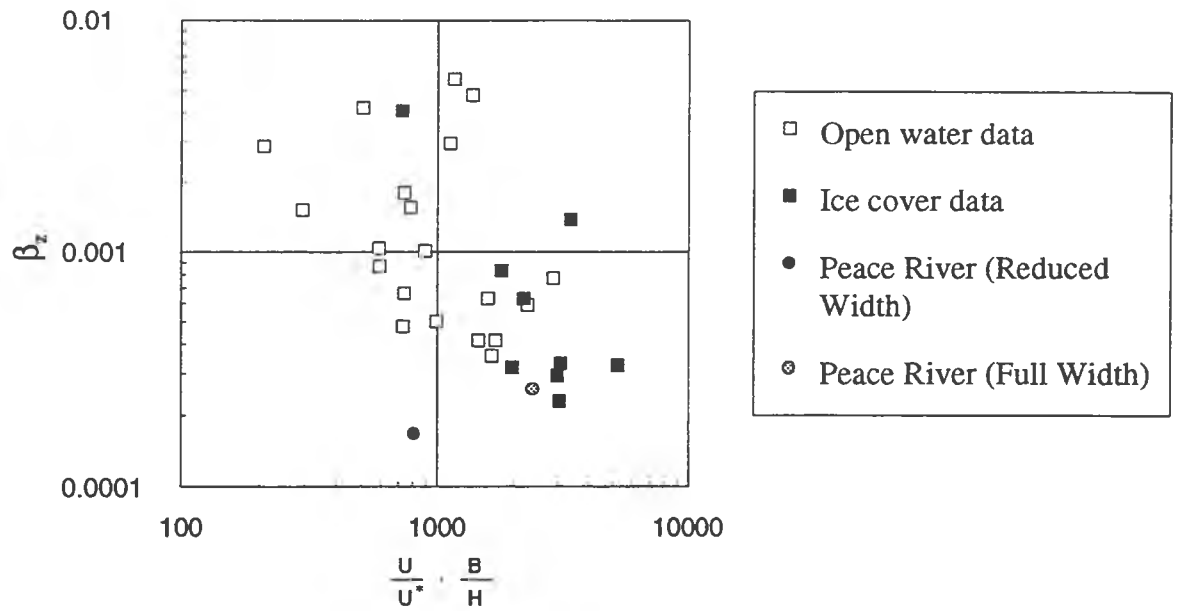
NORTHERN RIVER BASINS STUDY
 Peace River Time of Travel Study
**TRANSVERSE DOSAGE DISTRIBUTIONS
 FOR ALL SAMPLING SITES**

Scale as shown	93-06-15	FIGURE 4.2
----------------	----------	------------

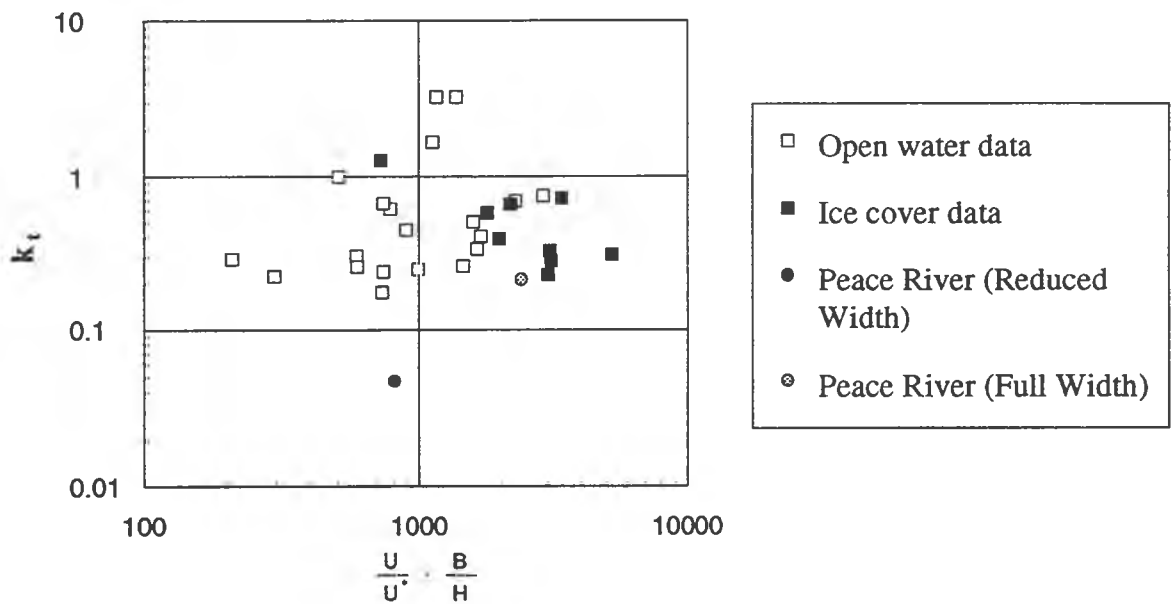
northwest hydraulic consultants ltd.
 ALBERTA RESEARCH COUNCIL



NORTHERN RIVER BASINS STUDY		
Peace River Time of Travel Study		
DOSAGE VARIANCE VERSUS INTEGRAL OF CONFINEMENT FUNCTION		
Scale as shown	93-06-15	FIGURE 4.3
northwest hydraulic consultants ltd. ALBERTA RESEARCH COUNCIL		



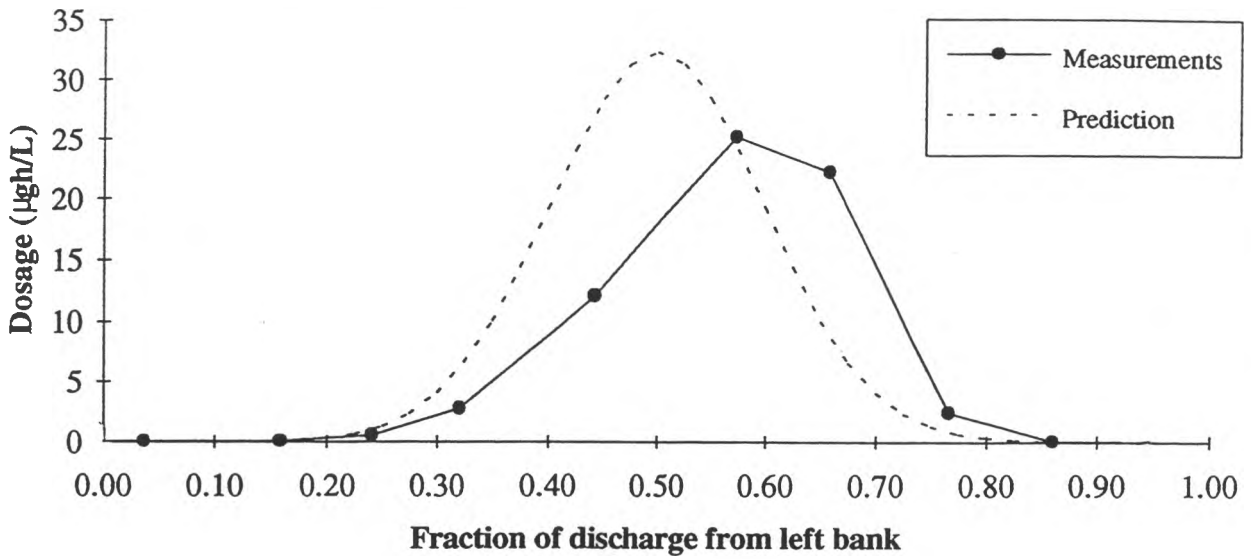
A. DIFFUSION FACTOR



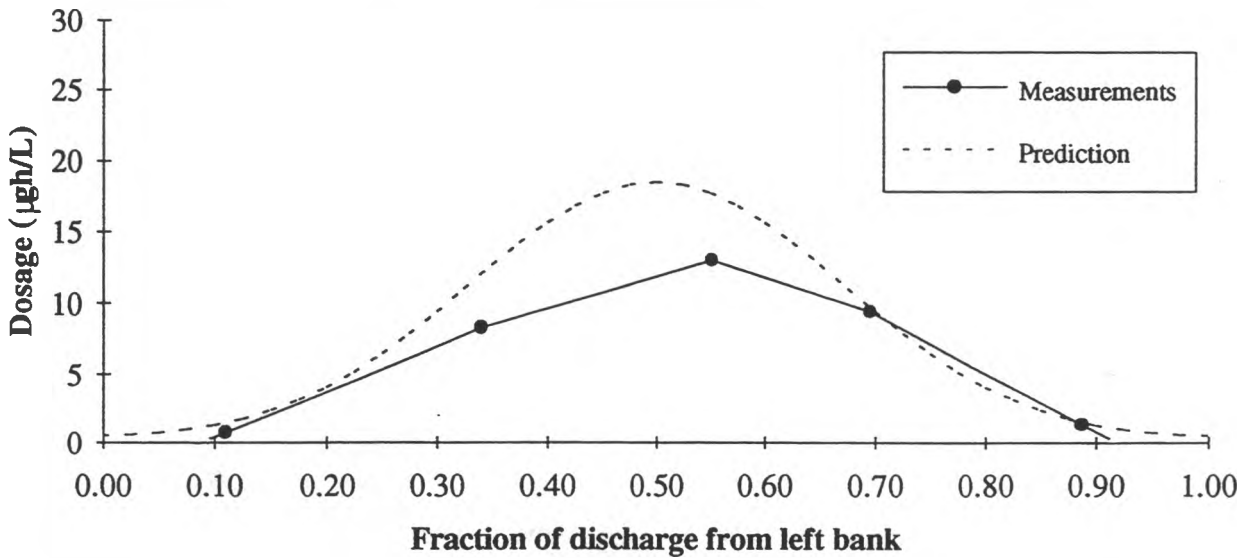
B. TRANSVERSE MIXING COEFFICIENT

NORTHERN RIVER BASINS STUDY		
Peace River Time of Travel Study		
DIMENSIONLESS COEFFICIENTS VERSUS HYDRAULIC PARAMETER		
Scale as shown	93-06-15	FIGURE 4.4
northwest hydraulic consultants ltd. ALBERTA RESEARCH COUNCIL		

Mackenzie Cairn



Peace River



NORTHERN RIVER BASINS STUDY

Peace River Time of Travel Study
**COMPARISONS OF MEASURED
 AND MODEL-PREDICTED DOSAGE
 DISTRIBUTIONS: SITES 1 & 2**

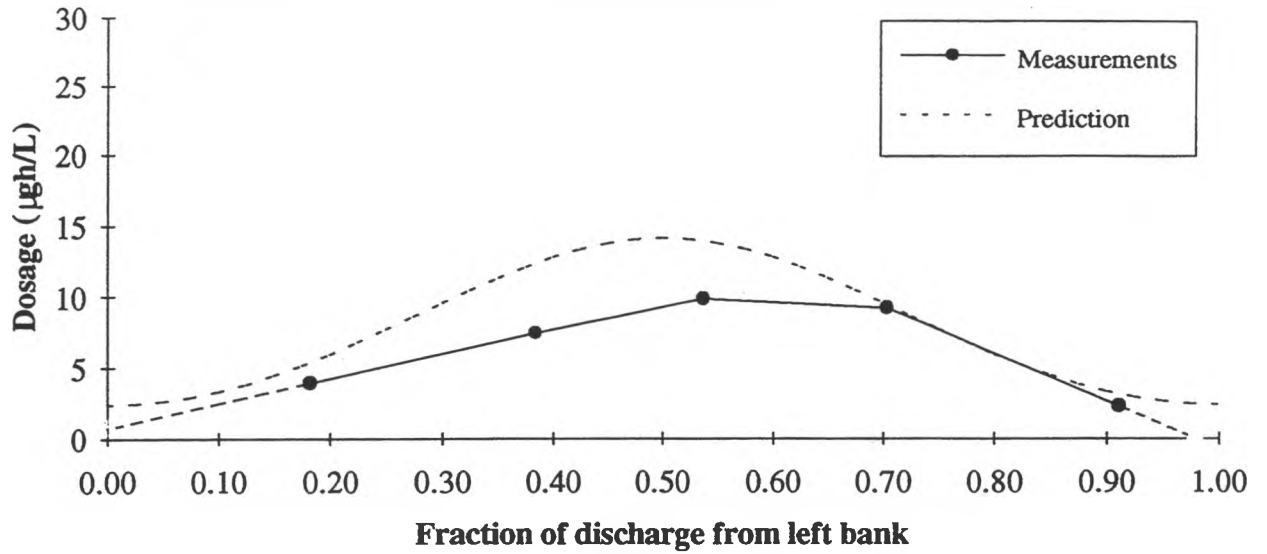
Scale as shown

93-06-15

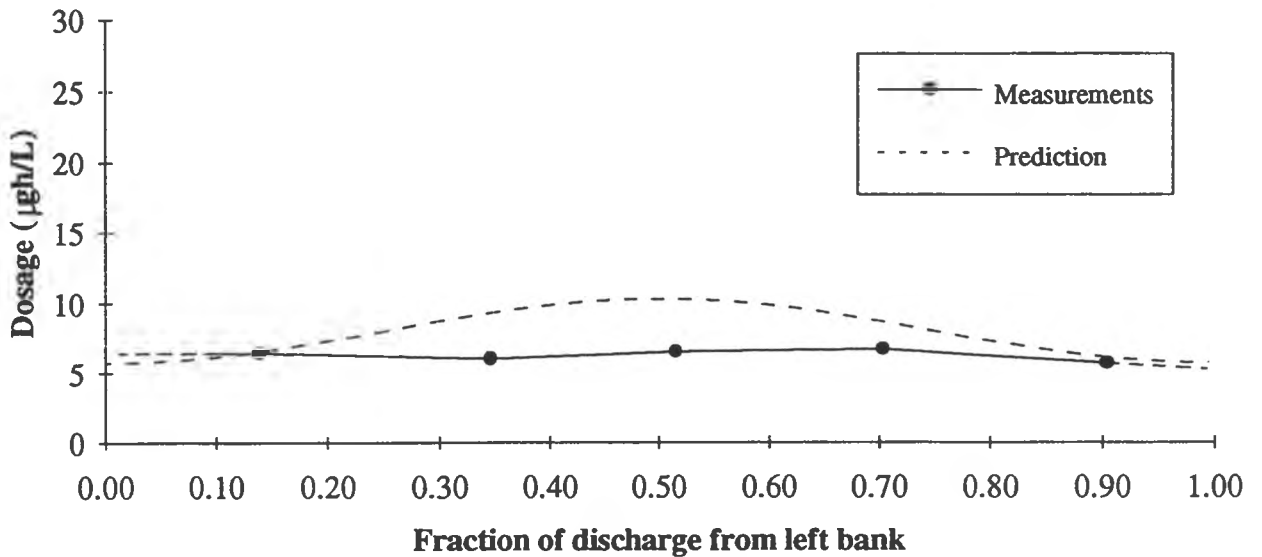
FIGURE 4.5a

northwest hydraulic consultants ltd.
 ALBERTA RESEARCH COUNCIL

Daishowa Bridge



Whitemud River



NORTHERN RIVER BASINS STUDY

Peace River Time of Travel Study
**COMPARISONS OF MEASURED
 AND MODEL-PREDICTED DOSAGE
 DISTRIBUTIONS: SITES 3 & 4**

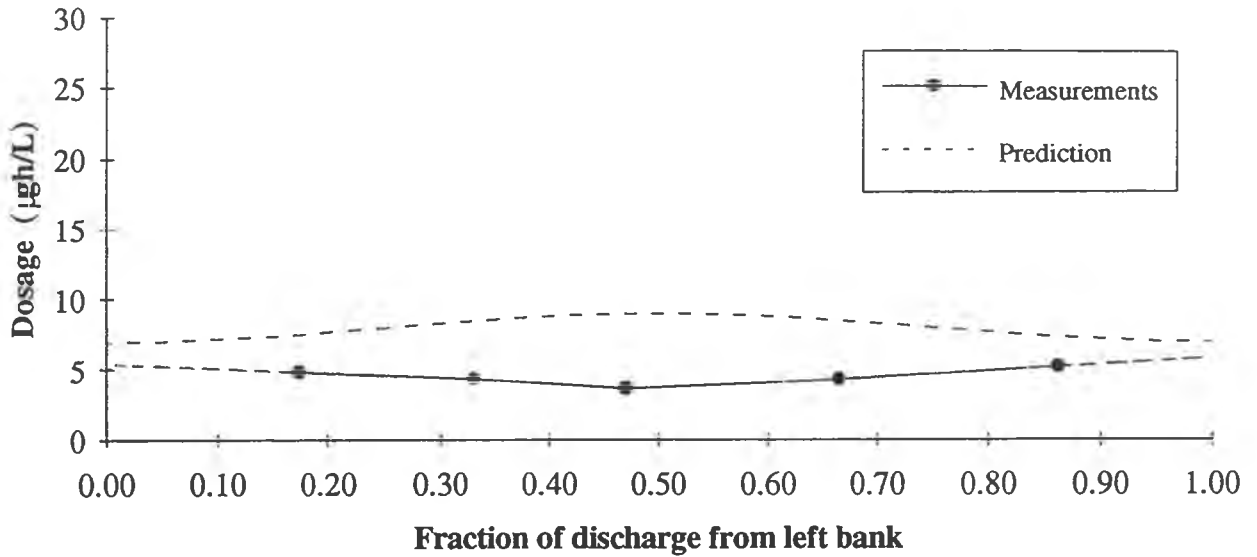
Scale as shown

93-06-15

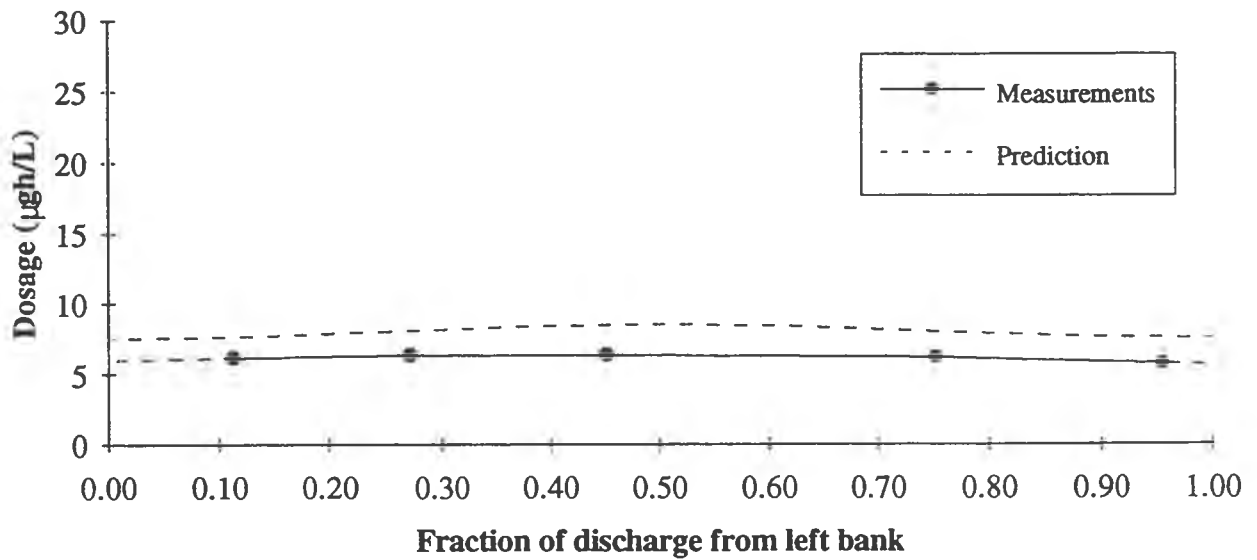
FIGURE 4.5b

northwest hydraulic consultants ltd.
 ALBERTA RESEARCH COUNCIL

Northstar Ice Bridge



Hotchkiss



NORTHERN RIVER BASINS STUDY

Peace River Time of Travel Study

**COMPARISONS OF MEASURED
AND MODEL-PREDICTED DOSAGE
DISTRIBUTIONS: SITES 5 & 6**

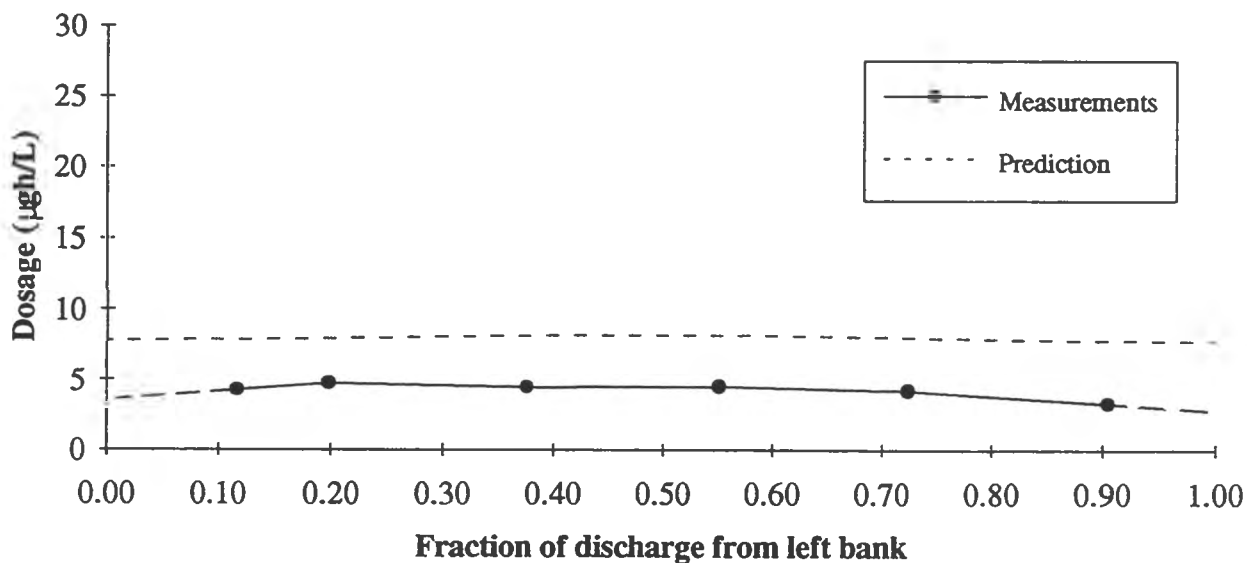
Scale as shown

93-06-15

FIGURE 4.5c

northwest hydraulic consultants ltd.
ALBERTA RESEARCH COUNCIL

Notikewin River



NORTHERN RIVER BASINS STUDY		
Peace River Time of Travel Study COMPARISONS OF MEASURED AND MODEL-PREDICTED DOSAGE DISTRIBUTIONS: SITE 7		
Scale as shown	93-06-15	FIGURE 4.5d
northwest hydraulic consultants ltd. ALBERTA RESEARCH COUNCIL		

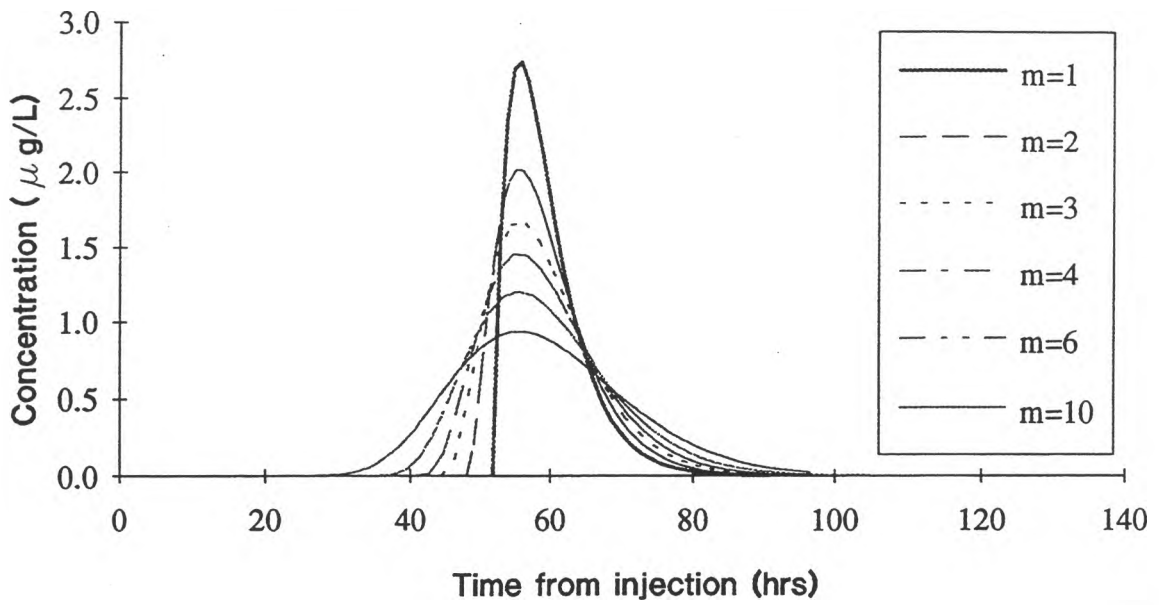


FIGURE 5.1 Sensitivity of storage model to storage zone number.

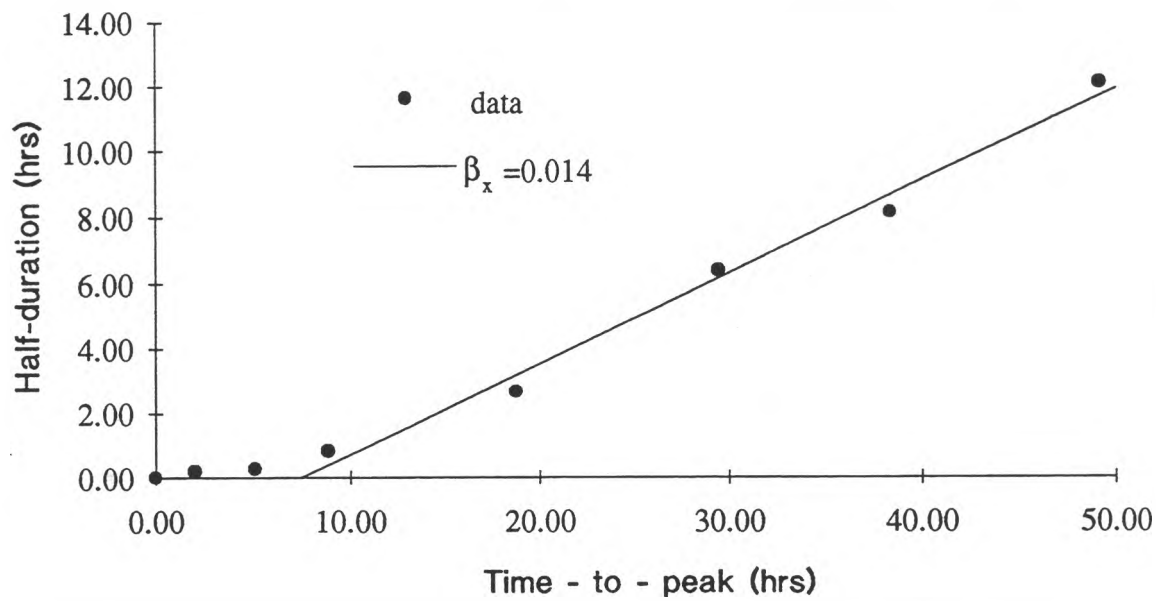


FIGURE 5.2 Variation of half-duration with time to peak (Peace River).

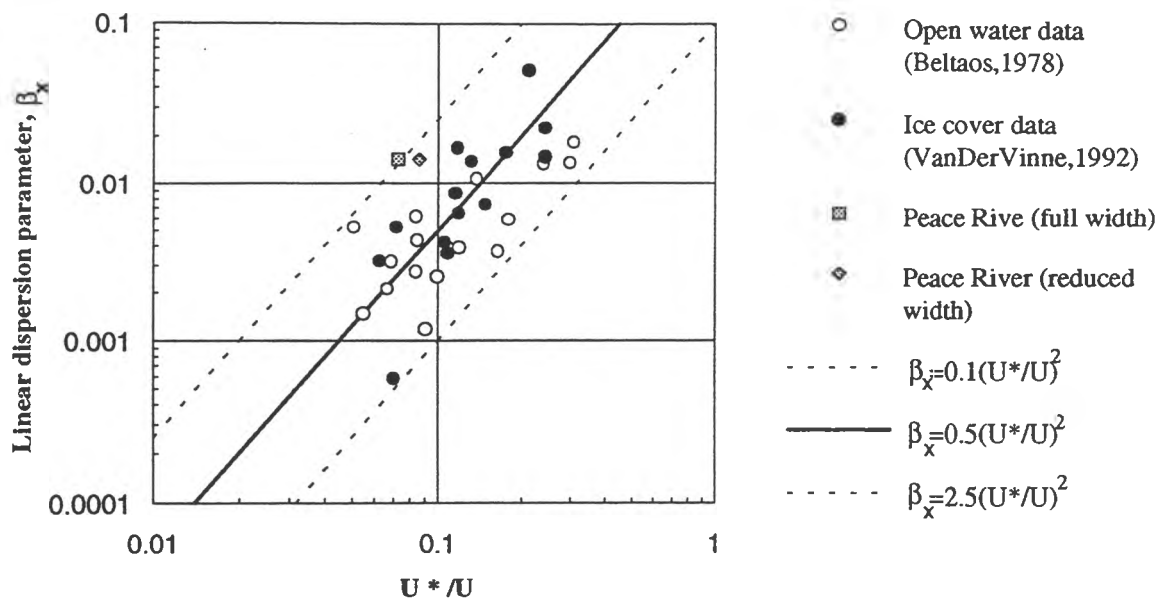


FIGURE 5.3 Linear dispersion parameter versus ratio of shear velocity to mean velocity.

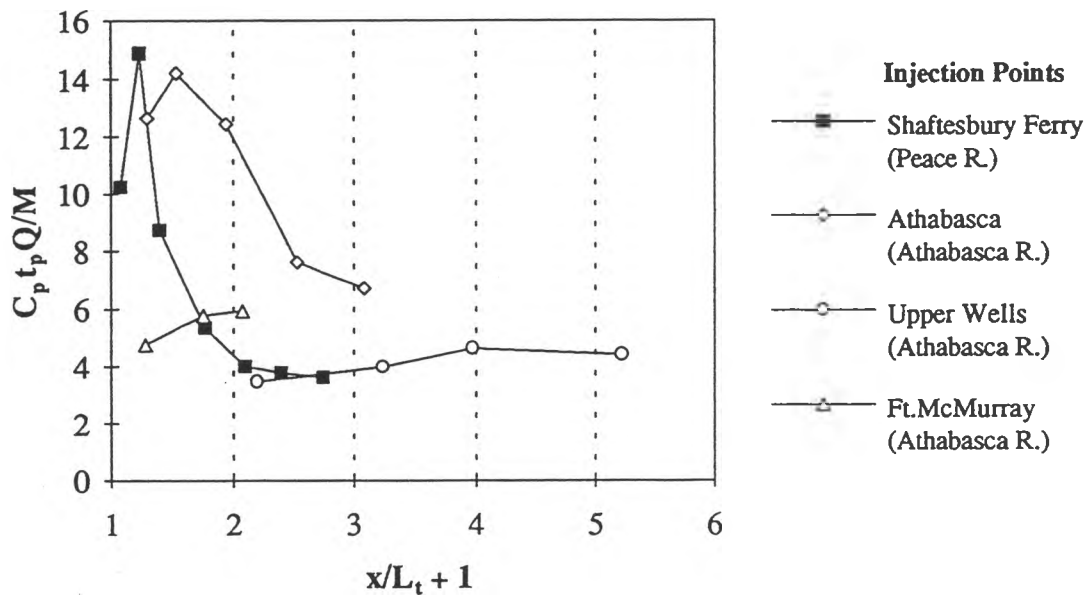
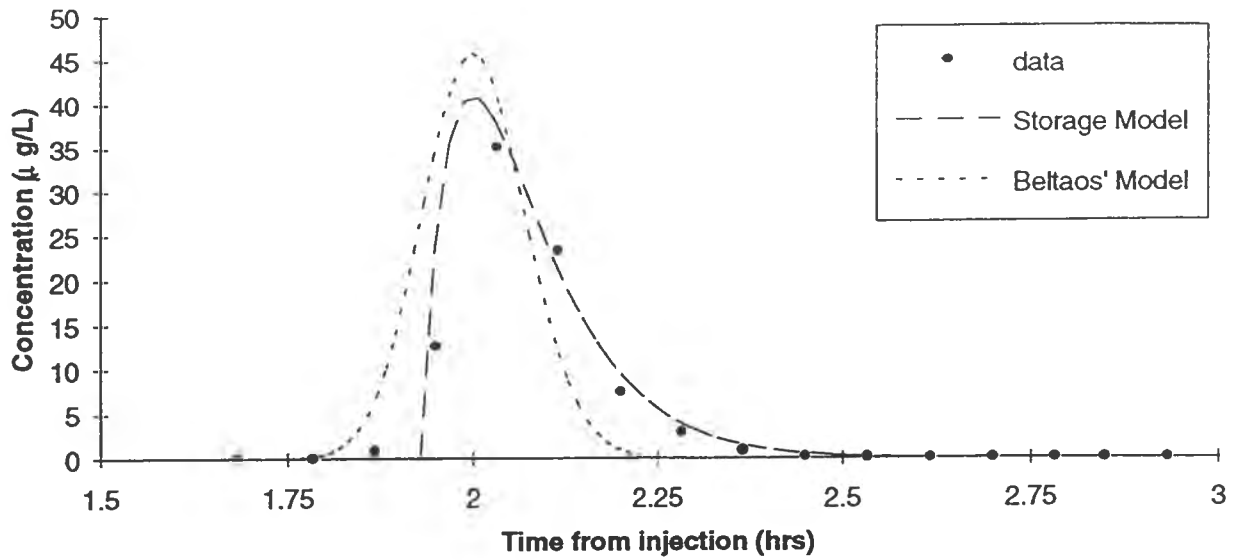
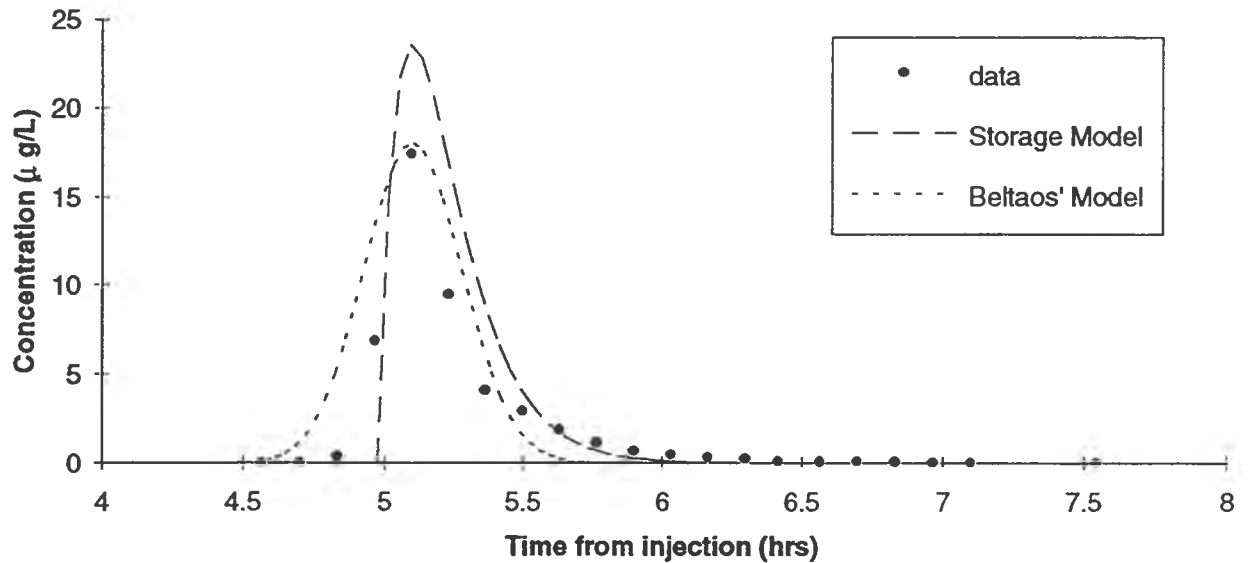


FIGURE 5.4 Dimensionless peak concentration versus dimensionless distance from injection: Peace and Athabasca Rivers.

Mackenzie Cairn



Peace River



NORTHERN RIVER BASINS STUDY

Peace River Time of Travel Study
COMPARISON OF MEASURED AND MODEL-PREDICTED DISTRIBUTIONS OF CONCENTRATION VERSUS TIME: SITES 1 & 2

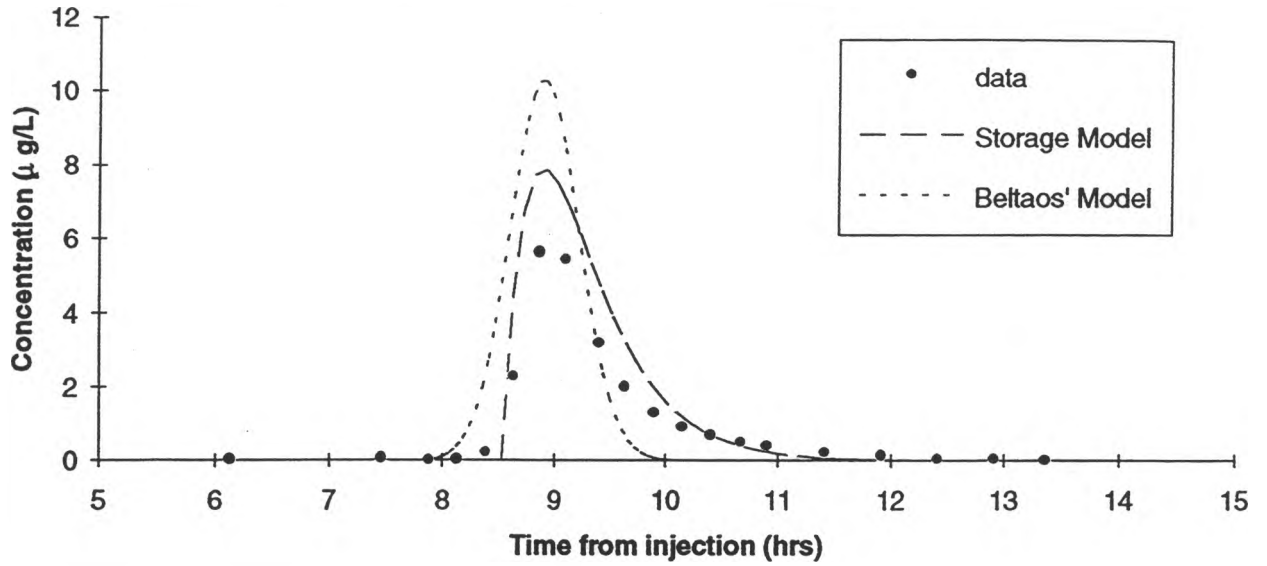
Scale as shown

93-06-16

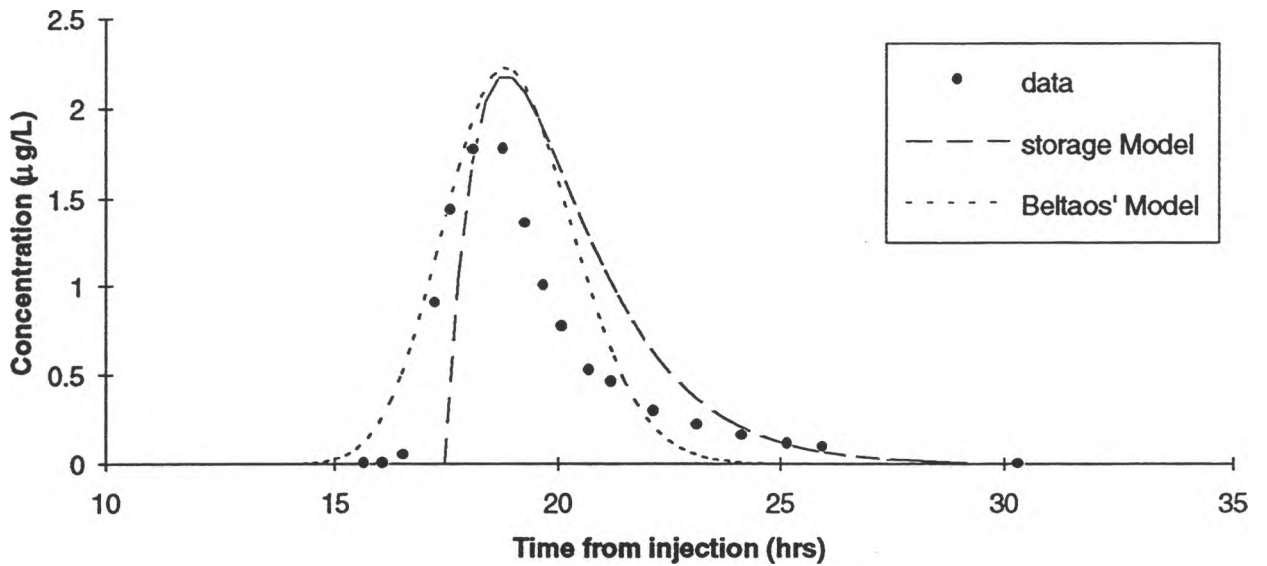
FIGURE 5.5a

northwest hydraulic consultants ltd.
 ALBERTA RESEARCH COUNCIL

Daishowa



Whitemud River



NORTHERN RIVER BASINS STUDY

Peace River Time of Travel Study

COMPARISON OF MEASURED AND MODEL-PREDICTED DISTRIBUTIONS OF CONCENTRATION VERSUS TIME: SITES 3 & 4

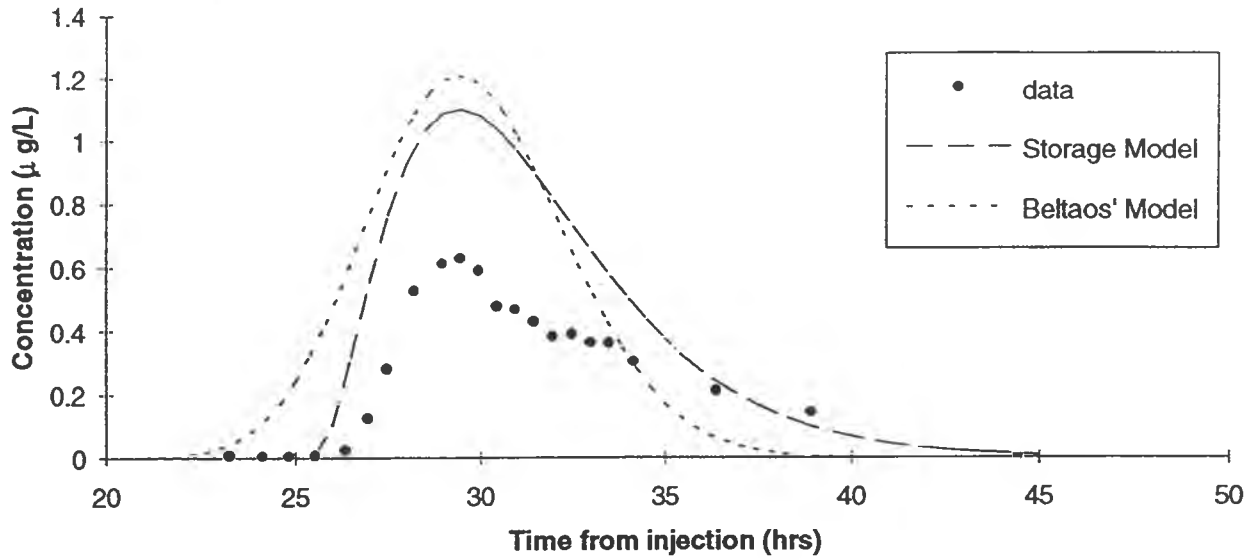
Scale as shown

93-06-16

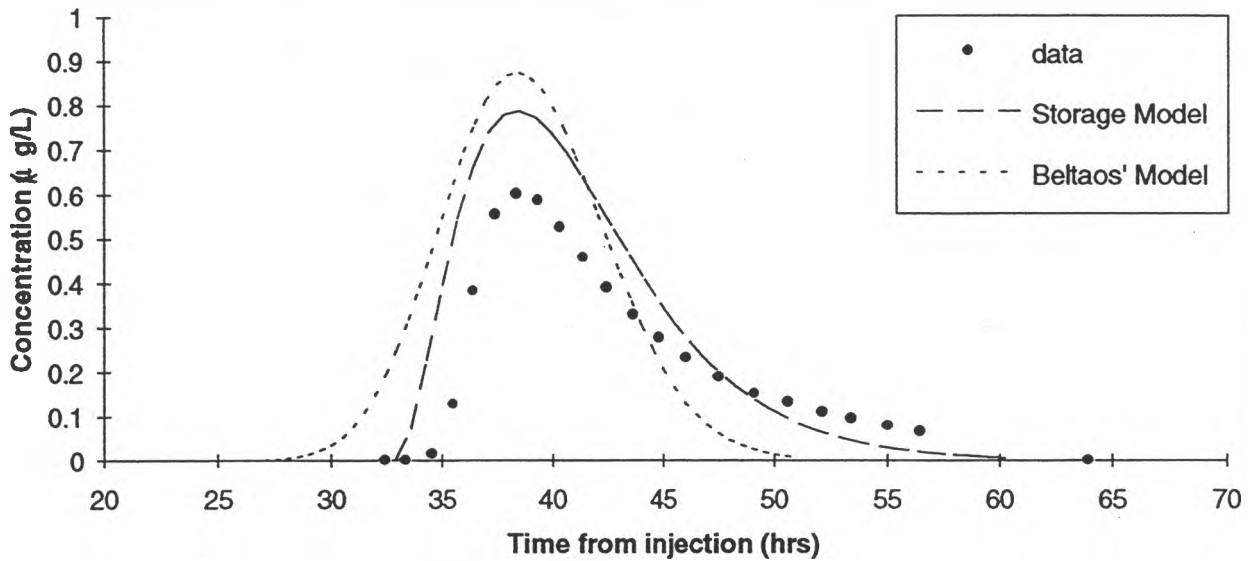
FIGURE 5.5b

northwest hydraulic consultants ltd.
ALBERTA RESEARCH COUNCIL

Northstar Ice Bridge

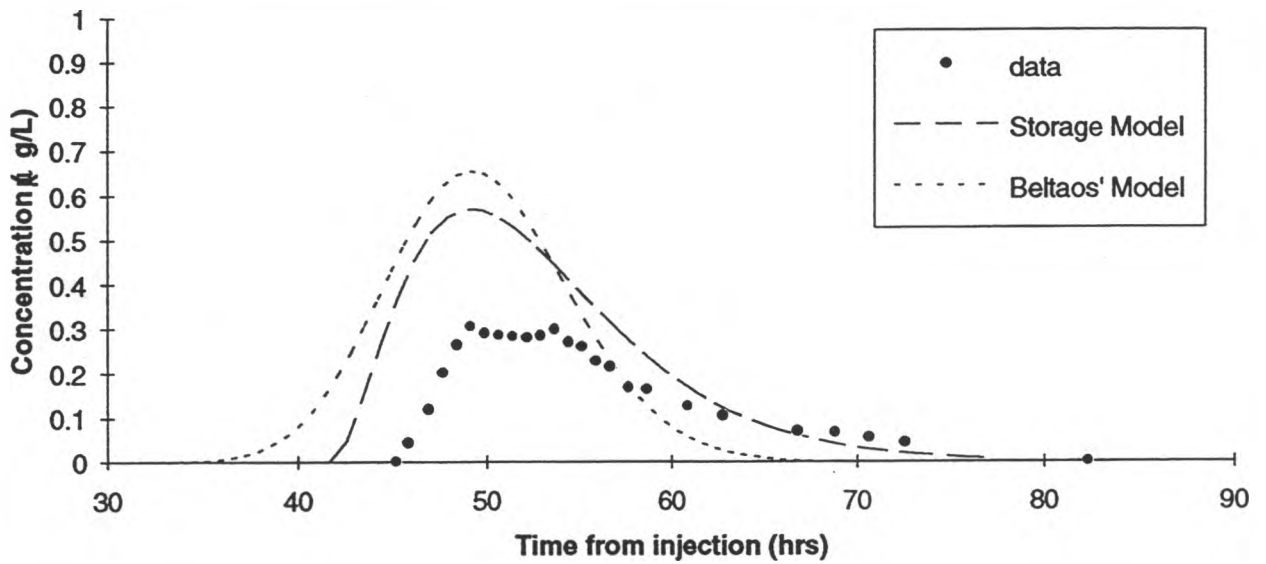


Hotchkiss



NORTHERN RIVER BASINS STUDY		
Peace River Time of Travel Study		
COMPARISON OF MEASURED AND MODEL-PREDICTED DISTRIBUTIONS OF CONCENTRATION VERSUS TIME: SITES 5 & 6		
Scale as shown	93-06-16	FIGURE 5.5c
northwest hydraulic consultants ltd. ALBERTA RESEARCH COUNCIL		

Notikewin River



NORTHERN RIVER BASINS STUDY

Peace River Time of Travel Study
COMPARISON OF MEASURED AND MODEL-PREDICTED DISTRIBUTIONS OF CONCENTRATION VERSUS TIME: SITE 7

Scale as shown | 93-06-16 | FIGURE 5.5d

northwest hydraulic consultants ltd.
 ALBERTA RESEARCH COUNCIL

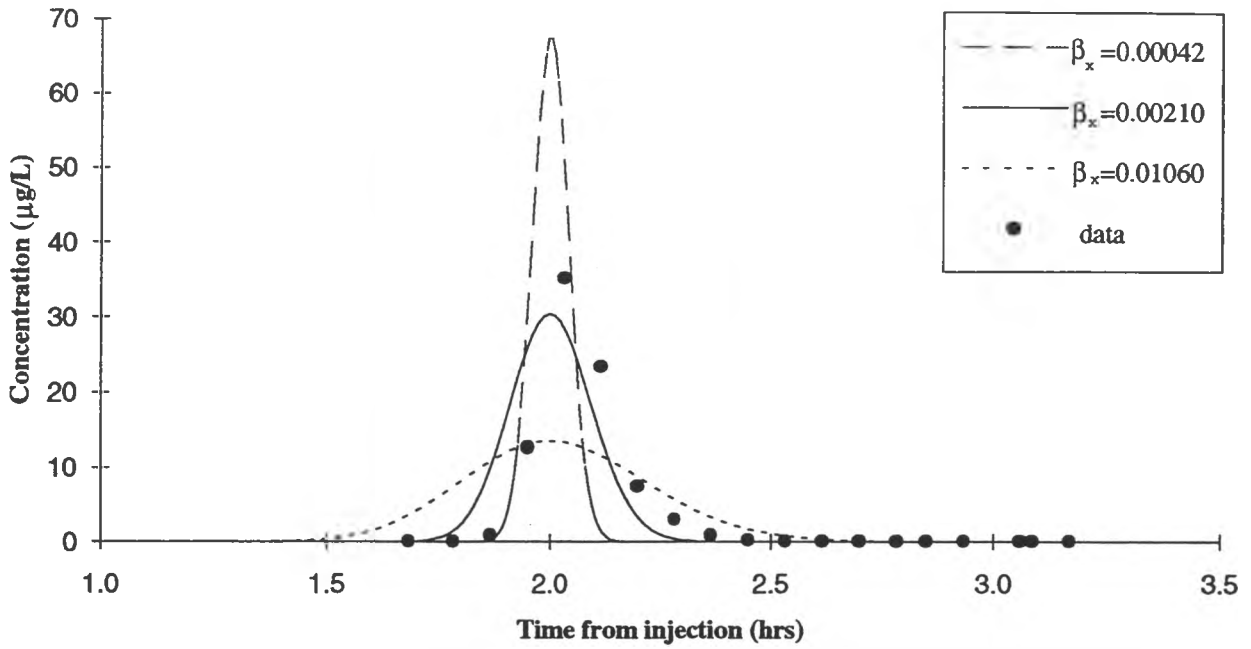


FIGURE 5.6 Sensitivity of Beltaos' model to possible range of linear dispersion parameter at Mackenzie Cairn site.

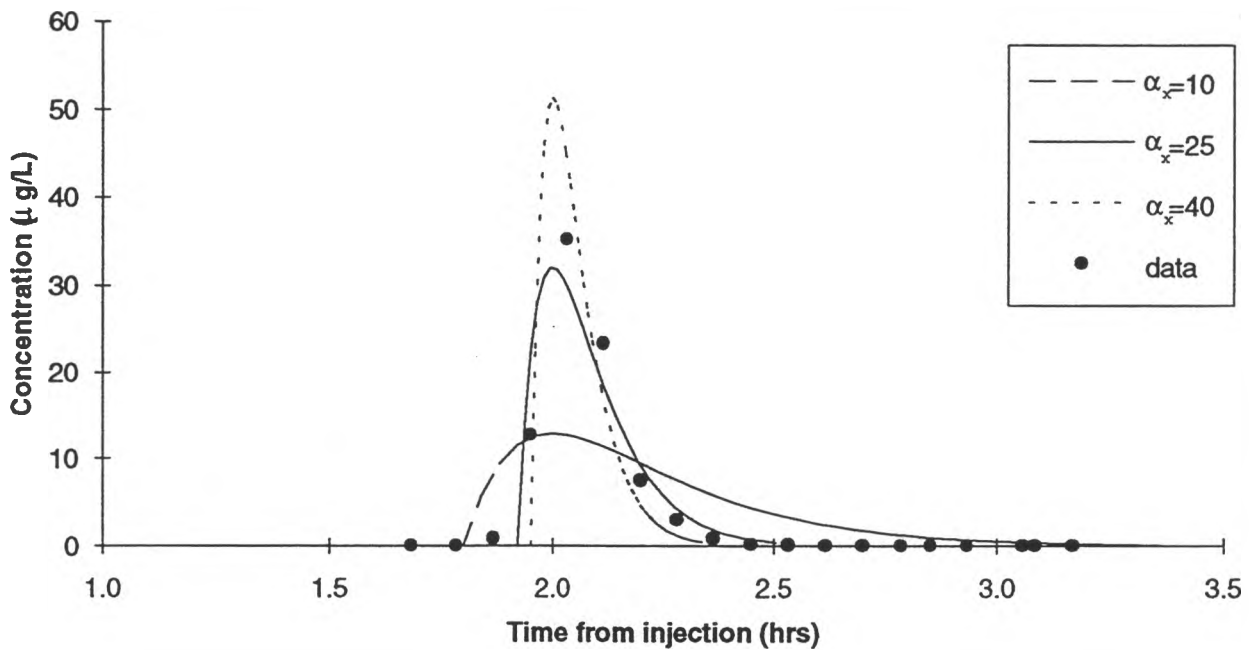


FIGURE 5.7 Sensitivity of storage model to possible range of storage coefficients at Mackenzie Cairn site.

SECTION 10
PHOTOGRAPHS

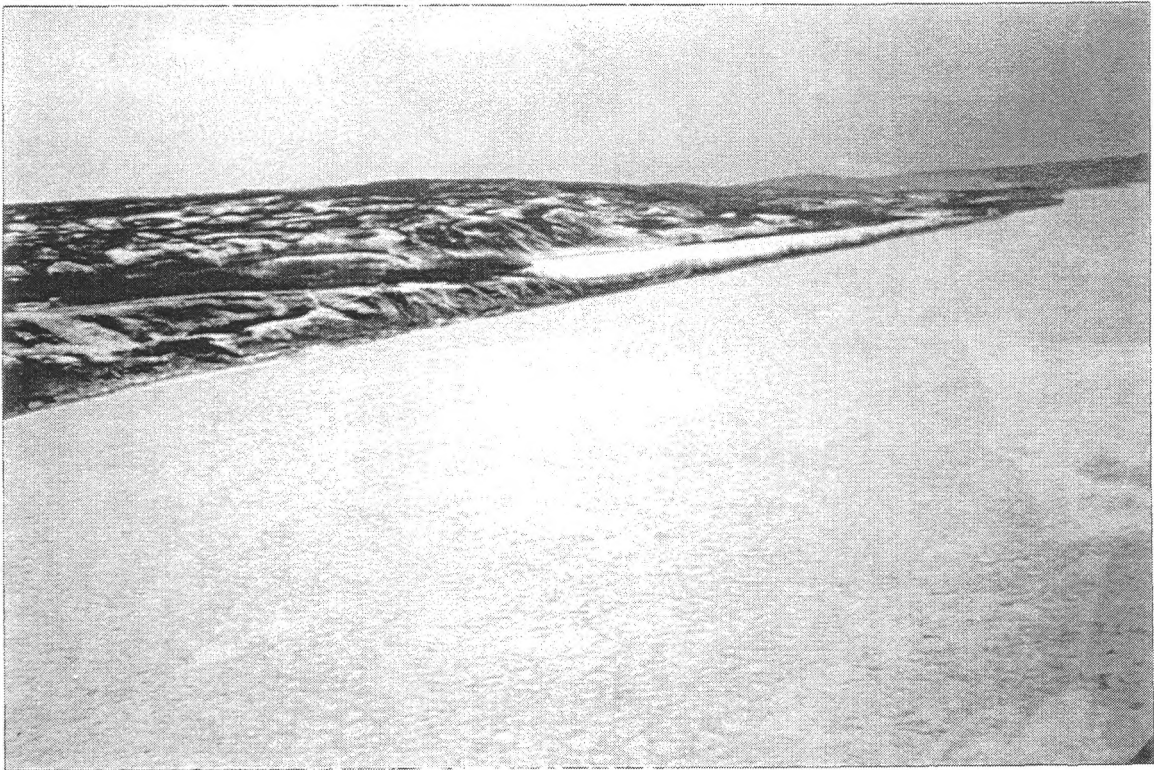


Photo 1. Juxtaposed ice cover in vicinity of Mackenzie Cairn: note well-defined circular ice floes.



Photo 2. Close-up of juxtaposed ice cover upstream of Peace River: note surface roughness due to crushing of floe edges.

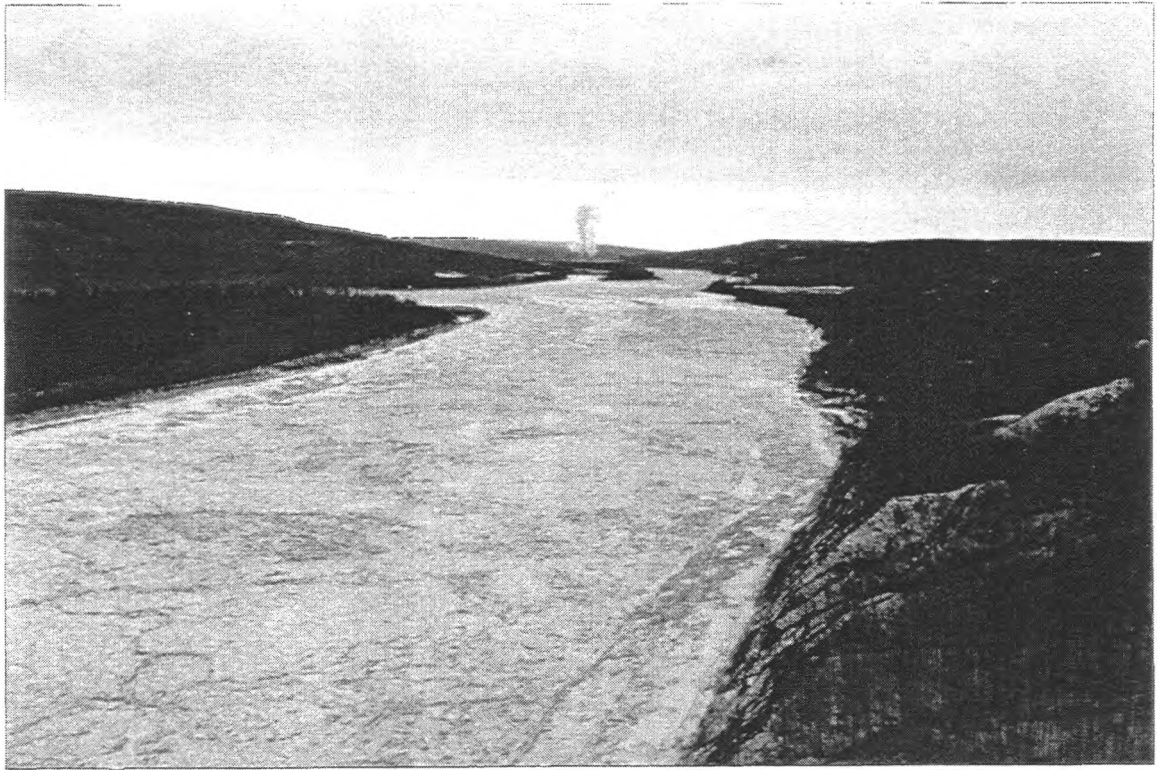


Photo 3. Juxtaposed ice cover downstream of Daishowa: note large ice rafts embedded in cover.

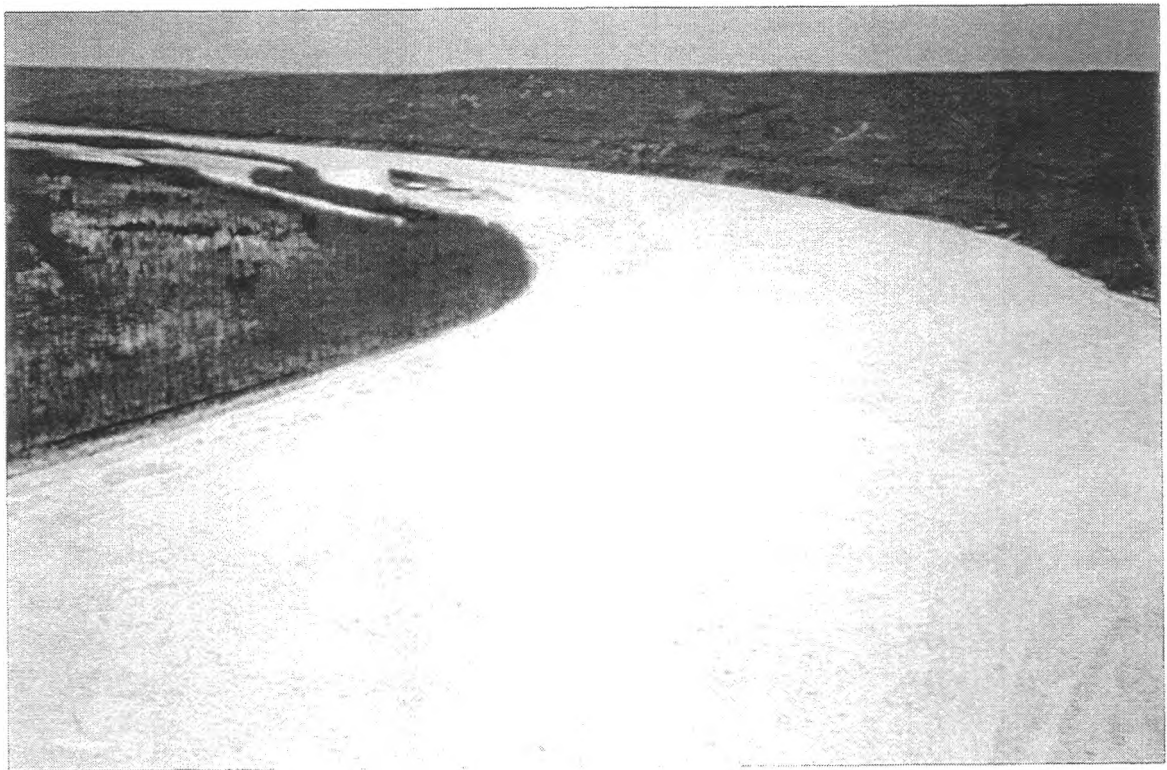


Photo 4. Juxtaposed ice cover with large embedded rafts just downstream of Cadotte River mouth.



Photo 5. Consolidated ice cover in vicinity of Notikewin River.



Photo 6. Close-up of consolidated cover at Notikewin River mouth: note large thick floes forming very rough surface.



Photo 7. Consolidated ice cover between high shear walls just downstream of North Star.



Photo 8. Ice "pebbles" formed by transport of frazil slush, as sampled at Hotchkiss site.

APPENDIX A
TERMS OF REFERENCE

NORTHERN RIVER BASINS STUDY

SCHEDULE A - TERMS OF REFERENCE

PROJECT 120-B1

TIME OF TRAVEL - PEACE RIVER

Description

A consultant will be retained to characterize the hydraulic and mixing characteristics for the Peace River under winter low flow conditions near the town of Peace River. The reach to be studied extends from upstream of the Smoky River confluence downstream to approximately the Notikewin River confluence. The purpose of this project is to assess the time of travel and the longitudinal and transverse dispersion for modelling pollutant transport along the river in this critical reach for use in a water quality model such as WASP.

In a normal winter the maximum extent of the ice front would be between Dunvegan and the B. C. border. During the winter releases from the dam will dominate the flow.

Objectives

1. Determine the mean river velocity between selected points along the Peace River during winter low flow under ice conditions by means of dye tests.
2. Determine the longitudinal and transverse dispersion co-efficients along the Peace River by means of dye tests.
3. Summarize the overall geomorphic, hydraulic and ice attributes at each injection and sample site.
4. Characterize the temporal and spacial representativeness of the information collected and calculated and provide a detailed evaluation of the potential to extrapolate the results to different stage, flow and ice conditions.

Study Location

The project area encompasses the Peace River main stem from just upstream of the Smoky River confluence to roughly the Notikewin River confluence.

Study Requirements

1. Determine the most suitable injection and sample sites for meeting the objectives.
2. Obtain permission from the Standards and Approvals Division of Alberta Environment for the application of dye or other materials to the river system within Alberta.

3. Conduct dye tests to determine the time of travel and longitudinal dispersion along the entire study reach. Transverse dispersion are also to be determined for three sub-reaches including:
 - (a) above the Smoky River confluence;
 - (b) below the Smoky river confluence; and
 - (c) the Daishowa outfall.

To ensure proper definition of transverse mixing, sampling locations should be closely spaced immediately downstream of the injection i.e., three locations approximately 8-10 km apart. At each location, 10 points should be sampled in the cross section, concentrated in the cross-sectional zone where the dye plume is forecast to concentrate. The number of samples per cross-section can be reduced to five at the downstream locations.

4. Determine the discharge at the site and time that samples are taken.
5. Summarize the overall hydraulic characteristics at the injection and each sample site. This would include:
 - (a) river slope;
 - (b) mean river velocity;
 - (c) river width;
 - (d) mean depth;
 - (e) ice characteristics;
 - (f) hydraulic radius
 - (g) cross section profiles surveyed to geodetic elevation; and
 - (h) other pertinent information.
6. The ice characteristics should include:
 - (a) thickness and local areal extent of basic ice types;
 - (b) extent of frazil ice deposits, including vertical distribution of approximate grain and void sizes; and
 - (c) historical representativeness of the ice (and flow) conditions under which the dye tests were conducted;
7. The falling limb of the dye concentration curve should be measured to at least the point of 20% of the maximum dye concentration and preferably to a lower concentration whenever logistically possible. For at least the last two cross sections, dye concentrations are to be measured to equipment detection levels (i.e., to quantify actual dye loss).
8. An ice core of the lower solid ice stratum and frazil ice deposits are to be taken from the approximate mid-point of each cross section and frozen for a subsequent analysis through the NRBS. Arrangements should be established with the NRBS office.

9. After the hydraulic surveys are complete a meeting will be held between the NRBS study personnel and the consultants to verify that the amount of dye to be injected will result in a peak concentration at the last sampling station of at least $1 \mu\text{g/l}$.
10. Write a report(s) which documents:
 - (a) flow velocity and discharge measurements;
 - (b) measured time of travel;
 - (c) longitudinal dispersion co-efficients;
 - (d) transverse dispersion co-efficients;
 - (e) details of the analytical approaches employed;
 - (f) the temporal and spacial representiveness of the measured time of travel and dispersion coefficients relative to historical ice and flow conditions and the potential to extrapolate the results to different stage, flow and ice conditions; and
 - (g) a summary.
11. Endeavour to utilize local contractors and services for the field studies and maintain a list of supplies and services utilized along with the money spent.
12. Progress reports, final manuscripts, figures, electronic data and photographic materials are to be delivered to the Study Office as per Schedule A. An electronic copy of the final report in Word Perfect compatible format is required.

APPENDIX B
LIST OF SYMBOLS

APPENDIX B

LIST OF SYMBOLS

B	- channel width (at underside of ice cover)
\bar{C}	- cross-section average concentration
C	- concentration
C_p	- peak concentration with respect to time
C_u	- velocity coefficient
C_∞	- final downstream concentration
D_x	- Fickian dispersion coefficient
D_z	- diffusion factor
e_x	- longitudinal mixing coefficient
e_z	- transverse mixing coefficient
f(x)	- confinement function
g	- gravitational acceleration constant
h	- local flow depth
H	- average flow depth in cross-section
k_p	- position parameter
k_t	- dimensionless transverse mixing coefficient
k_T	- temperature correction factor
L_L	- linear mixing length
L_t	- transverse mixing length
L_v	- vertical mixing length
m	- storage zone number
M	- total mass of pollutant
m_x	- longitudinal coefficient of curvature
m_z	- transverse coefficient of curvature
n	- integer
Q	- total discharge
q_c	- cumulative discharge at any point across channel (measured from left bank)
R	- hydraulic radius
S	- river slope
t	- time from injection
T	- sample temperature
T_e	- effective time constant of storage zone
T_o	- calibration temperature
t_p	- travel time of peak concentration
t_s	- local time for storage model
t_β	- time adjustment for Beltaos' model
u	- local longitudinal flow velocity
U	- average longitudinal flow velocity in cross-section

U	- shear velocity
w	- local transverse velocity
x	- longitudinal distance
z	- transverse distance
∞	- infinity
α_L	- linear mixing length factor
α_r	- dimensionless storage coefficient
β_x	- Beltaos' dispersion parameter
β_z	- dimensionless diffusion factor
ΔT	- half-duration of time-concentration distribution
η	- fraction of cumulative discharge across channel
η_i	- position of injection in cross-section
η_0	- centroid of dosage distribution
θ	- concentration dosage
θ_{LB}	- dosage at left bank
θ_{RB}	- dosage at right bank
ξ	- dimensionless distance
π	- circle constant
σ_η^2	- variance of dosage distribution across channel
σ_z^2	- variance of time-concentration distributions
χ	- dimensionless distance
ψ	- shape-velocity factor

APPENDIX C
FIELD DATA FROM DYE TEST

Mackenzie Caim

Background Concentration: 0.010 (ug/L)

Hole: 2

Sample Temperature (C)	Date (y:m:d)	Time (h:m)	Dye Concentration (ug/L)
11.0	93 Feb 27	11:00	0.078
4.4	93 Feb 27	11:10	0.050
4.0	93 Feb 27	11:15	0.050
3.6	93 Feb 27	11:20	0.049
2.0	93 Feb 27	11:25	0.034
4.4	93 Feb 27	11:30	0.037
4.0	93 Feb 27	11:35	0.036
4.0	93 Feb 27	11:40	0.030
4.2	93 Feb 27	11:45	0.037
3.4	93 Feb 27	11:50	0.036
3.0	93 Feb 27	11:55	0.035
2.6	93 Feb 27	12:00	0.035
20.0	93 Feb 27	12:05	0.000
20.0	93 Feb 27	12:10	0.000
20.0	93 Feb 27	12:15	0.000
20.0	93 Feb 27	12:20	0.000
20.0	93 Feb 27	12:25	0.000
20.0	93 Feb 27	12:30	0.000
20.0	93 Feb 27	12:35	0.000

Hole: 5

Sample Temperature (C)	Date (y:m:d)	Time (h:m)	Dye Concentration (ug/L)
8.4	93 Feb 27	11:20	0.027
9.4	93 Feb 27	11:25	0.028
9.0	93 Feb 27	11:30	0.020
9.4	93 Feb 27	11:35	0.028
3.4	93 Feb 27	11:40	0.875
10.0	93 Feb 27	11:45	2.209
9.2	93 Feb 27	11:50	2.163
11.2	93 Feb 27	11:55	0.496
2.6	93 Feb 27	12:00	0.125
9.6	93 Feb 27	12:05	0.028
12.4	93 Feb 27	12:10	0.031
4.2	93 Feb 27	12:30	0.037
	93 Feb 27	12:42	0.000

Hole: 4

Sample Temperature (C)	Date (y:m:d)	Time (h:m)	Dye Concentration (ug/L)
20.0	93 Feb 27	11:26	0.000
20.0	93 Feb 27	11:31	0.000
20.0	93 Feb 27	11:36	0.000
2.0	93 Feb 27	11:41	0.047
20.0	93 Feb 27	11:46	0.060
4.0	93 Feb 27	11:51	0.130
3.2	93 Feb 27	11:56	0.048
3.4	93 Feb 27	12:01	0.042
3.6	93 Feb 27	12:06	0.049
3.4	93 Feb 27	12:11	0.049
20.0	93 Feb 27	12:16	0.000
20.0	93 Feb 27	12:21	0.000
20.0	93 Feb 27	12:26	0.000

Hole: 6

Sample Temperature (C)	Date (y:m:d)	Time (h:m)	Dye Concentration (ug/L)
10.6	93 Feb 27	11:27	-0.002
11.4	93 Feb 27	11:32	0.030
13.0	93 Feb 27	11:37	1.177
13.4	93 Feb 27	11:42	12.189
10.2	93 Feb 27	11:47	14.343
10.4	93 Feb 27	11:52	4.722
12.6	93 Feb 27	11:57	0.681
11.2	93 Feb 27	12:02	0.110
11.6	93 Feb 27	12:07	0.030
13.0	93 Feb 27	12:12	0.032
	93 Feb 27	12:16	0.000

Mackenzie Cairn (continued)
Background Concentration: 0.010 (ug/L)

Hole: 7.5

Sample Temperature (C)	Date (y:m:d)	Time (h:m)	Dye Concentration (ug/L)
11.0	93 Feb 27	10:57	0.062
5.8	93 Feb 27	11:10	0.067
5.0	93 Feb 27	11:20	0.065
4.0	93 Feb 27	11:25	0.110
2.8	93 Feb 27	11:30	11.043
3.2	93 Feb 27	11:35	70.768
1.6	93 Feb 27	11:40	48.632
11.4	93 Feb 27	11:45	12.288
10.4	93 Feb 27	11:50	1.469
10.6	93 Feb 27	11:55	0.259
12.6	93 Feb 27	12:00	0.106
10.6	93 Feb 27	12:05	0.077
10.6	93 Feb 27	12:10	0.037
10.6	93 Feb 27	12:15	0.045
	93 Feb 27	12:29	0.000

Hole: 10

Sample Temperature (C)	Date (y:m:d)	Time (h:m)	Dye Concentration (ug/L)
19.4	93 Feb 27	11:00	0.019
20.4	93 Feb 27	11:15	0.000
20.2	93 Feb 27	11:20	0.000
20.2	93 Feb 27	11:25	10.604
19.6	93 Feb 27	11:30	154.794
19.6	93 Feb 27	11:35	91.899
20.2	93 Feb 27	11:40	7.923
20.6	93 Feb 27	11:45	0.995
20.0	93 Feb 27	11:50	0.434
20.0	93 Feb 27	11:55	0.293
20.0	93 Feb 27	12:00	0.192
20.0	93 Feb 27	12:05	0.141
20.6	93 Feb 27	12:10	0.102
20.0	93 Feb 27	12:15	0.091
20.0	93 Feb 27	12:20	0.081
20.4	93 Feb 27	12:25	0.061
20.0	93 Feb 27	12:30	0.081
20.0	93 Feb 27	12:35	0.040
	93 Feb 27	12:39	0.000

Hole: 9

Sample Temperature (C)	Date (y:m:d)	Time (h:m)	Dye Concentration (ug/L)
11.2	93 Feb 27	11:11	-0.002
11.6	93 Feb 27	11:16	-0.002
10.2	93 Feb 27	11:21	0.045
5.8	93 Feb 27	11:26	19.147
3.2	93 Feb 27	11:31	167.685
6.6	93 Feb 27	11:36	99.643
4.0	93 Feb 27	11:41	12.798
4.2	93 Feb 27	11:46	2.258
7.4	93 Feb 27	11:51	0.607
4.0	93 Feb 27	11:56	0.303
11.4	93 Feb 27	12:01	0.167
4.0	93 Feb 27	12:06	0.170
10.6	93 Feb 27	12:11	0.045
12.0	93 Feb 27	12:16	0.047
11.2	93 Feb 27	12:21	0.094
11.4	93 Feb 27	12:26	0.046
	93 Feb 27	12:33	0.000

Hole: 12

Sample Temperature (C)	Date (y:m:d)	Time (h:m)	Dye Concentration (ug/L)
20.0	93 Feb 27	11:17	0.000
20.0	93 Feb 27	11:22	0.000
20.0	93 Feb 27	11:27	2.292
20.0	93 Feb 27	11:32	16.266
20.0	93 Feb 27	11:37	8.427
20.0	93 Feb 27	11:42	1.110
20.0	93 Feb 27	11:47	0.394
20.0	93 Feb 27	11:52	0.182
20.0	93 Feb 27	11:57	0.141
20.0	93 Feb 27	12:02	0.081
20.0	93 Feb 27	12:07	0.050
20.0	93 Feb 27	12:12	0.040
20.0	93 Feb 27	12:17	0.040
	93 Feb 27	12:24	0.000

Mackenzie Cairn (continued)
Background Concentration: 0.010 (ug/L)

Hole: 14

Sample Temperature (C)	Date (y:m:d)	Time (h:m)	Dye Concentration (ug/L)
19.2	93 Feb 27	11:15	0.000
19.2	93 Feb 27	11:20	0.000
20.0	93 Feb 27	11:25	0.000
20.0	93 Feb 27	11:30	0.070
20.0	93 Feb 27	11:35	0.252
20.0	93 Feb 27	11:40	0.222
20.0	93 Feb 27	11:45	0.040
20.0	93 Feb 27	11:50	0.000
20.0	93 Feb 27	11:55	0.000

Hole: 17

Sample Temperature (C)	Date (y:m:d)	Time (h:m)	Dye Concentration (ug/L)
20.2	93 Feb 27	11:16	0.000
20.0	93 Feb 27	11:20	0.000
20.0	93 Feb 27	11:25	0.000
20.0	93 Feb 27	11:31	0.000
20.4	93 Feb 27	11:36	0.000
20.0	93 Feb 27	11:40	0.000
20.4	93 Feb 27	11:45	0.000
20.2	93 Feb 27	11:50	0.000
20.0	93 Feb 27	11:55	0.000
20.6	93 Feb 27	12:01	0.000
20.2	93 Feb 27	12:06	0.000
20.2	93 Feb 27	12:11	0.000
20.0	93 Feb 27	12:21	0.000
20.2	93 Feb 27	12:36	0.000

Peace River
Background Concentration: 0.015 (ug/L)

Hole: 8

Hole: 14

Sample Temperature (C)	Date (y:m:d)	Time (h:m)	Dye Concentration (ug/L)
4.4	93 Feb 27	14:04	0.004
5.2	93 Feb 27	14:12	0.003
5.2	93 Feb 27	14:20	0.000
7.6	93 Feb 27	14:28	0.002
6.8	93 Feb 27	14:36	0.033
6.6	93 Feb 27	14:44	0.278
9.2	93 Feb 27	14:52	0.588
9.4	93 Feb 27	15:00	0.661
8.4	93 Feb 27	15:08	0.860
8.8	93 Feb 27	15:16	0.835
10.6	93 Feb 27	15:24	0.761
8.6	93 Feb 27	15:32	0.497
5.8	93 Feb 27	15:40	0.368
4.8	93 Feb 27	15:48	0.153
6.6	93 Feb 27	15:55	0.079
7.8	93 Feb 27	16:04	0.054
6.8	93 Feb 27	16:12	0.211
5.2	93 Feb 27	16:20	0.041
6.8	93 Feb 27	16:28	0.013
5.6	93 Feb 27	16:36	0.010
	93 Feb 27	17:02	0.000

Sample Temperature (C)	Date (y:m:d)	Time (h:m)	Dye Concentration (ug/L)
4.2	93 Feb 27	14:04	-0.001
5.4	93 Feb 27	14:12	0.001
5.4	93 Feb 27	14:20	1.601
7.4	93 Feb 27	14:28	20.053
7.4	93 Feb 27	14:36	16.720
10.1	93 Feb 27	14:44	8.562
7.6	93 Feb 27	14:52	5.623
7.8	93 Feb 27	15:00	4.449
9.4	93 Feb 27	15:08	2.534
5.4	93 Feb 27	15:16	1.651
8.6	93 Feb 27	15:24	0.521
8.4	93 Feb 27	15:32	0.236
6.8	93 Feb 27	15:40	0.211
6.6	93 Feb 27	15:48	0.120
	93 Feb 27	15:58	0.000

Hole: 18

Sample Temperature (C)	Date (y:m:d)	Time (h:m)	Dye Concentration (ug/L)
5.4	93 Feb 27	14:04	0.002
5.6	93 Feb 27	14:12	0.000
6.0	93 Feb 27	14:20	0.007
7.4	93 Feb 27	14:28	2.054
5.4	93 Feb 27	14:36	45.424
5.0	93 Feb 27	14:44	28.383
5.6	93 Feb 27	14:52	9.453
4.6	93 Feb 27	15:00	6.126
5.2	93 Feb 27	15:08	3.172
3.2	93 Feb 27	15:16	1.121
8.8	93 Feb 27	15:24	0.575
7.6	93 Feb 27	15:32	0.524
7.2	93 Feb 27	15:40	0.298
6.8	93 Feb 27	15:50	0.171
	93 Feb 27	16:03	0.000

Peace River (continued)
Background Concentration: 0.015 (ug/L)

Hole: 21

Sample Temperature (C)	Date (y:m:d)	Time (h:m)	Dye Concentration (ug/L)
5.0	93 Feb 27	14:04	0.000
5.8	93 Feb 27	14:12	0.000
6.2	93 Feb 27	14:20	0.083
9.8	93 Feb 27	14:28	12.043
9.0	93 Feb 27	14:36	33.334
8.0	93 Feb 27	14:44	14.125
11.4	93 Feb 27	14:52	5.387
10.4	93 Feb 27	15:00	2.303
11.6	93 Feb 27	15:08	0.906
3.0	93 Feb 27	15:16	0.534
9.2	93 Feb 27	15:24	0.487
8.0	93 Feb 27	15:32	0.436
8.0	93 Feb 27	15:40	0.299
7.6	93 Feb 27	15:48	0.246
	93 Feb 27	16:24	0.000

Hole: 27

Sample Temperature (C)	Date (y:m:d)	Time (h:m)	Dye Concentration (ug/L)
5.8	93 Feb 27	14:04	0.002
7.2	93 Feb 27	14:12	0.004
7.6	93 Feb 27	14:20	0.002
8.8	93 Feb 27	14:28	0.029
6.8	93 Feb 27	14:36	0.157
11.2	93 Feb 27	14:44	0.476
6.8	93 Feb 27	14:52	0.993
5.0	93 Feb 27	15:00	1.727
7.6	93 Feb 27	15:08	1.888
7.2	93 Feb 27	15:16	1.436
5.6	93 Feb 27	15:24	0.836
4.8	93 Feb 27	15:32	0.529
6.0	93 Feb 27	15:40	0.351
5.8	93 Feb 27	15:48	0.368
4.8	93 Feb 27	15:56	0.237
5.0	93 Feb 27	16:04	0.214
4.8	93 Feb 27	16:12	0.174
5.2	93 Feb 27	16:20	0.138
	93 Feb 27	16:50	0.000

Daishowa
Background Concentration: 0.028 (ug/L)

Hole: 6

Sample Temperature (C)	Date (y:m:d)	Time (h:m)	Dye Concentration (ug/L)
4.0	93 Feb 27	17:38	0.034
3.6	93 Feb 27	17:53	0.048
3.8	93 Feb 27	18:08	0.237
2.2	93 Feb 27	18:22	1.821
2.4	93 Feb 27	18:36	2.669
3.0	93 Feb 27	18:54	2.521
2.8	93 Feb 27	19:08	1.875
2.2	93 Feb 27	19:24	1.324
1.8	93 Feb 27	19:39	0.956
2.8	93 Feb 27	19:54	0.772
6.8	93 Feb 27	20:10	0.680
3.8	93 Feb 27	20:24	0.559
2.6	93 Feb 27	20:55	0.315
2.8	93 Feb 27	21:25	0.184
2.8	93 Feb 27	21:55	0.038
1.4	93 Feb 27	22:25	0.067
	93 Feb 27	22:59	0.000

Hole: 9

Sample Temperature (C)	Date (y:m:d)	Time (h:m)	Dye Concentration (ug/L)
6.8	93 Feb 27	15:36	0.013
5.6	93 Feb 27	16:56	0.203
4.0	93 Feb 27	17:21	0.010
3.8	93 Feb 27	17:36	0.005
3.4	93 Feb 27	17:51	0.010
3.8	93 Feb 27	18:06	3.191
2.4	93 Feb 27	18:20	9.298
2.6	93 Feb 27	18:35	7.281
2.6	93 Feb 27	18:51	4.287
2.6	93 Feb 27	19:05	1.822
3.2	93 Feb 27	19:21	0.992
2.2	93 Feb 27	19:35	0.627
2.6	93 Feb 27	19:51	0.388
3.0	93 Feb 27	20:08	0.232
3.8	93 Feb 27	20:21	0.179
3.2	93 Feb 27	20:53	0.087
3.8	93 Feb 27	21:23	0.085
2.6	93 Feb 27	21:53	0.105
1.8	93 Feb 27	22:23	0.062
	93 Feb 27	23:06	0.000

Daishowa (continued)
Background Concentration: 0.028 (ug/L)

Hole: 11

Hole: 13

Sample Temperature (C)	Date (y:m:d)	Time (h:m)	Dye Concentration (ug/L)	Sample Temperature (C)	Date (y:m:d)	Time (h:m)	Dye Concentration (ug/L)
6.8	93 Feb 27	15:34	0.013	7.2	93 Feb 27	15:32	0.037
5.8	93 Feb 27	16:54	0.012	5.8	93 Feb 27	16:52	0.009
4.2	93 Feb 27	17:19	0.010	3.6	93 Feb 27	17:17	0.044
4.2	93 Feb 27	17:34	0.021	4.2	93 Feb 27	17:32	0.006
3.4	93 Feb 27	17:49	0.029	3.8	93 Feb 27	17:47	0.014
4.4	93 Feb 27	18:03	2.285	4.2	93 Feb 27	18:02	0.385
3.0	93 Feb 27	18:19	11.666	3.6	93 Feb 27	18:17	8.693
3.0	93 Feb 27	18:33	11.867	3.2	93 Feb 27	18:32	10.779
3.0	93 Feb 27	18:49	6.111	3.0	93 Feb 27	18:47	6.348
2.8	93 Feb 27	19:03	2.981	3.0	93 Feb 27	19:01	3.506
3.0	93 Feb 27	19:19	1.587	2.8	93 Feb 27	19:17	2.254
2.6	93 Feb 27	19:34	0.964	2.6	93 Feb 27	19:33	1.473
3.2	93 Feb 27	19:49	0.624	3.2	93 Feb 27	19:47	1.160
3.2	93 Feb 27	20:06	0.311	3.0	93 Feb 27	20:04	0.607
3.8	93 Feb 27	20:19	0.227	4.2	93 Feb 27	20:17	0.406
3.8	93 Feb 27	20:51	0.097	3.4	93 Feb 27	20:48	0.176
4.2	93 Feb 27	21:21	0.048	3.8	93 Feb 27	21:18	0.131
3.4	93 Feb 27	21:51	0.011	3.4	93 Feb 27	21:48	0.027
2.2	93 Feb 27	22:21	0.000	3.2	93 Feb 27	22:18	0.013
					93 Feb 27	22:45	0.000

Daishowa (continued)
Background Concentration: 0.028 (ug/L)

Hole: 16

Sample Temperature (C)	Date (y:m:d)	Time (h:m)	Dye Concentration (ug/L)
8.0	93 Feb 27	15:30	0.043
7.4	93 Feb 27	16:50	0.025
4.0	93 Feb 27	17:15	0.001
4.6	93 Feb 27	17:30	0.006
4.4	93 Feb 27	17:45	0.010
4.4	93 Feb 27	18:00	0.004
3.8	93 Feb 27	18:15	0.087
3.4	93 Feb 27	18:30	1.041
3.8	93 Feb 27	18:45	1.457
3.2	93 Feb 27	19:00	1.384
3.8	93 Feb 27	19:15	1.034
3.0	93 Feb 27	19:30	0.777
3.8	93 Feb 27	19:45	0.661
3.6	93 Feb 27	20:02	0.508
4.8	93 Feb 27	20:15	0.462
4.6	93 Feb 27	20:45	0.313
3.4	93 Feb 27	21:15	0.187
2.2	93 Feb 27	21:45	0.117
3.4	93 Feb 27	22:15	0.065
	93 Feb 27	22:51	0.000

Whitemud River
Background Concentration: 0.016 (ug/L)

Hole: 6

Sample Temperature (C)	Date (y:m:d)	Time (h:m)	Dye Concentration (ug/L)
3.8	93 Feb 28	02:49	0.023
4.2	93 Feb 28	03:23	0.647
5.2	93 Feb 28	04:00	1.810
5.6	93 Feb 28	04:30	1.923
3.8	93 Feb 28	04:57	1.654
4.8	93 Feb 28	05:23	1.101
5.2	93 Feb 28	05:56	0.851
4.6	93 Feb 28	06:26	0.709
2.8	93 Feb 28	07:27	0.445
2.8	93 Feb 28	08:26	0.339
4.9	93 Feb 28	09:26	0.264
3.4	93 Feb 28	10:27	0.188
3.0	93 Feb 28	11:16	0.168
	93 Feb 28	18:09	0.000

Hole: 11.5

Sample Temperature (C)	Date (y:m:d)	Time (h:m)	Dye Concentration (ug/L)
5.6	93 Feb 28	01:10	0.000
5.2	93 Feb 28	01:35	0.000
2.8	93 Feb 28	02:00	0.002
5.6	93 Feb 28	02:30	1.231
3.4	93 Feb 28	02:57	2.826
4.6	93 Feb 28	03:29	2.534
4.2	93 Feb 28	04:08	1.852
5.2	93 Feb 28	04:38	1.175
3.4	93 Feb 28	05:04	0.782
4.6	93 Feb 28	05:28	0.568
4.8	93 Feb 28	06:04	0.368
4.6	93 Feb 28	06:34	0.290
2.2	93 Feb 28	07:33	0.154
2.2	93 Feb 28	08:32	0.106
3.6	93 Feb 28	09:32	0.073
2.6	93 Feb 28	10:33	0.048
2.8	93 Feb 28	11:21	0.033
	93 Feb 28	13:05	0.000

Hole: 9.5

Sample Temperature (C)	Date (y:m:d)	Time (h:m)	Dye Concentration (ug/L)
3.8	93 Feb 28	01:54	-0.002
3.8	93 Feb 28	02:53	0.820
4.6	93 Feb 28	03:26	2.365
3.4	93 Feb 28	04:04	2.147
4.4	93 Feb 28	04:34	1.563
4.2	93 Feb 28	05:01	0.950
5.4	93 Feb 28	05:25	0.756
4.0	93 Feb 28	06:00	0.487
5.0	93 Feb 28	06:30	0.411
2.2	93 Feb 28	07:30	0.210
2.4	93 Feb 28	08:29	0.163
3.0	93 Feb 28	09:29	0.117
2.4	93 Feb 28	10:30	0.073
2.6	93 Feb 28	11:19	0.056
	93 Feb 28	13:58	0.000

Whitemud River (continued)
Background Concentration: 0.016 (ug/L)

Hole: 13.5

Hole: 16

Sample Temperature (C)	Date (y:m:d)	Time (h:m)	Dye Concentration (ug/L)	Sample Temperature (C)	Date (y:m:d)	Time (h:m)	Dye Concentration (ug/L)
3.0	93 Feb 28	02:02	0.000	7.2	93 Feb 28	00:40	0.022
3.4	93 Feb 28	03:00	2.880	7.2	93 Feb 28	02:43	0.022
4.8	93 Feb 28	03:32	2.353	3.6	93 Feb 28	03:05	0.619
4.2	93 Feb 28	04:12	1.883	5.4	93 Feb 28	03:35	1.469
5.6	93 Feb 28	04:42	1.124	4.8	93 Feb 28	04:15	1.606
3.2	93 Feb 28	05:07	0.719	5.4	93 Feb 28	04:45	1.312
4.8	93 Feb 28	05:32	0.571	4.8	93 Feb 28	05:10	1.058
4.4	93 Feb 28	06:08	0.414	4.8	93 Feb 28	05:35	0.891
4.6	93 Feb 28	06:38	0.290	4.6	93 Feb 28	06:12	0.486
2.4	93 Feb 28	07:37	0.174	5.4	93 Feb 28	06:42	0.574
2.6	93 Feb 28	08:35	0.111	3.0	93 Feb 28	07:40	0.403
3.8	93 Feb 28	09:38	0.081	3.4	93 Feb 28	08:38	0.299
2.6	93 Feb 28	10:36	0.053	3.6	93 Feb 28	09:38	0.208
2.8	93 Feb 28	11:24	0.039	3.2	93 Feb 28	10:39	0.149
	93 Feb 28	13:41	0.000	3.8	93 Feb 28	11:27	0.129
					93 Feb 28	16:31	0.000

Northstar Ice Bridge
Background Concentration: 0.015 (ug/L)

Hole: 3

Sample Temperature (C)	Date (y:m:d)	Time (h:m)	Dye Concentration (ug/L)
1.2	93 Feb 28	09:37	0.010
1.0	93 Feb 28	10:19	0.008
1.8	93 Feb 28	11:02	0.001
2.2	93 Feb 28	11:50	0.012
1.8	93 Feb 28	12:27	0.021
2.2	93 Feb 28	12:58	0.078
1.6	93 Feb 28	13:42	0.210
1.2	93 Feb 28	14:27	0.316
1.8	93 Feb 28	14:57	0.464
2.6	93 Feb 28	15:27	0.461
2.2	93 Feb 28	15:57	0.397
3.4	93 Feb 28	16:27	0.464
2.0	93 Feb 28	16:57	0.460
0.8	93 Feb 28	17:27	0.420
1.0	93 Feb 28	17:57	0.454
1.2	93 Feb 28	18:27	0.438
10.4	93 Feb 28	18:57	0.471
1.8	93 Feb 28	19:37	0.373
16.4	93 Feb 28	21:27	0.287
16.0	93 Mar 01	00:27	0.216
	93 Mar 01	09:36	0.000

Hole: 5

Sample Temperature (C)	Date (y:m:d)	Time (h:m)	Dye Concentration (ug/L)
4.8	93 Feb 28	08:36	0.010
0.4	93 Feb 28	09:31	0.000
1.0	93 Feb 28	10:16	-0.003
1.0	93 Feb 28	10:59	-0.003
2.2	93 Feb 28	11:47	0.004
1.6	93 Feb 28	12:24	0.125
1.8	93 Feb 28	12:55	0.295
1.6	93 Feb 28	13:36	0.507
2.2	93 Feb 28	14:24	0.633
2.6	93 Feb 28	14:54	0.620
3.8	93 Feb 28	15:24	0.743
2.6	93 Feb 28	15:54	0.534
2.4	93 Feb 28	16:24	0.396
1.8	93 Feb 28	16:54	0.367
1.6	93 Feb 28	17:24	0.352
1.4	93 Feb 28	17:54	0.337
1.4	93 Feb 28	18:24	0.331
2.6	93 Feb 28	18:54	0.342
2.0	93 Feb 28	19:34	0.271
17.0	93 Feb 28	21:34	0.186
16.0	93 Mar 01	00:20	0.124
	93 Mar 01	05:54	0.000

Northstar Ice Bridge (continued)

Background Concentration: 0.015 (ug/L)

Hole: 7

Hole: 11

Sample Temperature (C)	Date (y:m:d)	Time (h:m)	Dye Concentration (ug/L)	Sample Temperature (C)	Date (y:m:d)	Time (h:m)	Dye Concentration (ug/L)
5.2	93 Feb 28	08:45	0.008	1.6	93 Feb 28	09:23	0.001
0.6	93 Feb 28	09:29	0.000	0.8	93 Feb 28	10:09	0.000
0.6	93 Feb 28	10:13	0.000	1.6	93 Feb 28	10:53	-0.003
1.6	93 Feb 28	10:56	0.006	2.4	93 Feb 28	11:41	0.029
1.8	93 Feb 28	11:44	0.013	2.8	93 Feb 28	12:18	0.172
1.6	93 Feb 28	12:21	0.203	2.8	93 Feb 28	12:49	0.539
1.6	93 Feb 28	12:52	0.352	3.0	93 Feb 28	13:33	0.963
2.2	93 Feb 28	13:39	0.937	3.8	93 Feb 28	14:18	0.933
3.8	93 Feb 28	14:21	0.996	3.6	93 Feb 28	14:48	0.859
3.6	93 Feb 28	14:51	0.671	4.2	93 Feb 28	15:18	0.719
4.4	93 Feb 28	15:21	0.609	2.6	93 Feb 28	15:48	0.395
3.4	93 Feb 28	15:51	0.390	3.8	93 Feb 28	16:18	0.394
3.2	93 Feb 28	16:21	0.327	3.4	93 Feb 28	16:48	0.363
3.2	93 Feb 28	16:51	0.263	3.0	93 Feb 28	17:18	0.225
2.2	93 Feb 28	17:21	0.155	2.4	93 Feb 28	17:48	0.294
2.2	93 Feb 28	17:51	0.194	1.6	93 Feb 28	18:18	0.203
1.8	93 Feb 28	18:21	0.224	2.6	93 Feb 28	18:48	0.222
2.8	93 Feb 28	18:51	0.197	1.4	93 Feb 28	19:28	0.189
2.2	93 Feb 28	19:31	0.165	15.8	93 Feb 28	21:47	0.108
16.4	93 Feb 28	21:40	0.061	16.4	93 Mar 01	00:03	0.067
16.2	93 Mar 01	00:13	0.032		93 Mar 01	03:44	0.000
	93 Mar 01	03:01	0.000				

Northstar Ice Bridge (continued)
Background Concentration: 0.015 (ug/L)

Hole: 16

Sample Temperature (C)	Date (y:m:d)	Time (h:m)	Dye Concentration (ug/L)
4.4	93 Feb 28	09:16	0.006
2.4	93 Feb 28	10:05	0.000
2.4	93 Feb 28	10:50	0.021
4.6	93 Feb 28	11:38	0.001
4.4	93 Feb 28	12:15	0.010
2.6	93 Feb 28	12:46	0.083
2.6	93 Feb 28	13:30	0.342
4.6	93 Feb 28	14:15	0.577
3.2	93 Feb 28	14:45	0.700
5.6	93 Feb 28	15:15	0.747
3.6	93 Feb 28	15:45	0.695
3.8	93 Feb 28	16:15	0.640
1.8	93 Feb 28	16:45	0.581
3.0	93 Feb 28	17:15	0.546
2.8	93 Feb 28	17:45	0.517
2.0	93 Feb 28	18:15	0.460
3.2	93 Feb 28	18:45	0.415
2.6	93 Feb 28	19:25	0.368
17.2	93 Feb 28	21:54	0.277
16.2	93 Feb 28	23:57	0.189
	93 Mar 01	04:22	0.000

Hotchkiss

Background Concentration: 0.016 (ug/L)

Hole: 6

Hole: 9

Sample Temperature (C)	Date (y:m:d)	Time (h:m)	Dye Concentration (ug/L)	Sample Temperature (C)	Date (y:m:d)	Time (h:m)	Dye Concentration (ug/L)
3.2	93 Feb 28	17:44	-0.003	3.6	93 Feb 28	17:47	-0.001
4.6	93 Feb 28	18:40	0.000	4.0	93 Feb 28	18:43	0.000
4.2	93 Feb 28	19:50	-0.001	4.4	93 Feb 28	19:54	0.000
5.6	93 Feb 28	20:45	0.004	6.6	93 Feb 28	20:49	0.099
5.8	93 Feb 28	21:40	0.114	5.6	93 Feb 28	21:44	0.461
5.6	93 Feb 28	22:40	0.327	6.2	93 Feb 28	22:44	0.740
3.6	93 Feb 28	23:40	0.493	3.0	93 Feb 28	23:43	0.750
2.8	93 Mar 01	00:37	0.536	2.6	93 Mar 01	00:40	0.690
2.4	93 Mar 01	01:36	0.507	2.2	93 Mar 01	01:39	0.579
2.4	93 Mar 01	02:37	0.489	2.8	93 Mar 01	02:40	0.489
1.6	93 Mar 01	03:40	0.422	1.8	93 Mar 01	03:43	0.390
2.4	93 Mar 01	04:55	0.383	2.4	93 Mar 01	04:58	0.319
1.8	93 Mar 01	06:05	0.334	2.6	93 Mar 01	06:08	0.257
2.2	93 Mar 01	07:20	0.285	2.6	93 Mar 01	07:23	0.204
3.8	93 Mar 01	08:51	0.234	3.4	93 Mar 01	08:54	0.164
3.4	93 Mar 01	10:23	0.186	3.2	93 Mar 01	10:26	0.127
3.0	93 Mar 01	11:55	0.162	2.4	93 Mar 01	11:58	0.112
4.6	93 Mar 01	13:20	0.139	5.6	93 Mar 01	13:23	0.093
3.4	93 Mar 01	14:45	0.124	3.4	93 Mar 01	14:47	0.077
4.4	93 Mar 01	16:20	0.107	4.4	93 Mar 01	16:23	0.061
4.0	93 Mar 01	17:45	0.093	3.6	93 Mar 01	17:48	0.049
	93 Mar 02	02:57	0.000		93 Mar 01	23:48	0.000

Hole: 6

Frazil sampling

Sample Temperature (C)	Date (y:m:d)	Time (h:m)	Dye Concentration (ug/L)
8.2	93 Mar 01	14:55	0.071
7.2	93 Mar 01	16:20	0.010
3.6	93 Mar 01	17:57	0.027

Hotchkiss (continued)
Background Concentration: 0.016 (ug/L)

Hole: 11.5

Sample Temperature (C)	Date (y:m:d)	Time (h:m)	Dye Concentration (ug/L)
3.4	93 Feb 28	17:50	0.000
3.8	93 Feb 28	18:46	0.000
5.6	93 Feb 28	19:57	0.013
7.4	93 Feb 28	20:53	0.213
4.0	93 Feb 28	21:48	0.637
4.6	93 Feb 28	22:48	0.832
3.0	93 Feb 28	23:46	0.791
2.8	93 Mar 01	00:44	0.664
2.6	93 Mar 01	01:43	0.544
2.6	93 Mar 01	02:44	0.434
2.2	93 Mar 01	03:47	0.355
2.0	93 Mar 01	05:02	0.272
2.8	93 Mar 01	06:12	0.221
3.0	93 Mar 01	07:27	0.177
3.4	93 Mar 01	08:57	0.137
3.4	93 Mar 01	10:29	0.109
3.2	93 Mar 01	12:01	0.091
4.6	93 Mar 01	13:30	0.076
4.0	93 Mar 01	14:50	0.063
4.4	93 Mar 01	16:26	0.048
3.8	93 Mar 01	17:51	0.041
	93 Mar 02	01:52	0.000

Hole: 14

Sample Temperature (C)	Date (y:m:d)	Time (h:m)	Dye Concentration (ug/L)
4.6	93 Feb 28	17:53	0.000
4.0	93 Feb 28	18:49	0.000
5.2	93 Feb 28	20:00	0.003
6.8	93 Feb 28	20:57	0.104
6.4	93 Feb 28	21:52	0.427
5.0	93 Feb 28	22:52	0.655
2.6	93 Feb 28	23:49	0.713
2.4	93 Mar 01	00:47	0.703
2.6	93 Mar 01	01:46	0.602
2.6	93 Mar 01	02:47	0.480
2.6	93 Mar 01	03:50	0.398
2.0	93 Mar 01	05:03	0.316
4.6	93 Mar 01	06:15	0.258
3.4	93 Mar 01	07:30	0.209
4.2	93 Mar 01	09:00	0.165
3.8	93 Mar 01	10:33	0.129
3.4	93 Mar 01	12:04	0.111
5.6	93 Mar 01	13:36	0.086
4.6	93 Mar 01	14:53	0.075
5.8	93 Mar 01	16:29	0.059
4.2	93 Mar 01	17:45	0.047
	93 Mar 01	23:04	0.000

Hole: 11.5

Frazil sampling

Sample Temperature (C)	Date (y:m:d)	Time (h:m)	Dye Concentration (ug/L)
35.2	93 Mar 01	14:55	0.025
14.0	93 Mar 01	14:55	0.018
3.2	93 Mar 01	16:26	0.004
8.4	93 Mar 01	17:57	0.009

Hotchkiss (continued)

Background Concentration: 0.016 (ug/L)

Hole: 18

Sample Temperature (C)	Date (y:m:d)	Time (h:m)	Dye Concentration (ug/L)
4.6	93 Feb 28	17:56	-0.001
5.0	93 Feb 28	18:51	0.000
5.4	93 Feb 28	20:04	0.000
5.8	93 Feb 28	21:00	0.000
6.2	93 Feb 28	21:56	0.009
5.0	93 Feb 28	22:56	0.064
3.0	93 Feb 28	23:53	0.175
3.6	93 Mar 01	00:50	0.319
3.8	93 Mar 01	01:49	0.400
3.4	93 Mar 01	02:50	0.443
2.6	93 Mar 01	03:53	0.416
2.8	93 Mar 01	05:06	0.396
2.2	93 Mar 01	06:18	0.363
3.8	93 Mar 01	07:33	0.327
4.2	93 Mar 01	09:03	0.282
2.6	93 Mar 01	10:37	0.231
4.4	93 Mar 01	12:08	0.215
5.8	93 Mar 01	13:40	0.180
5.2	93 Mar 01	14:55	0.158
5.8	93 Mar 01	16:32	0.142
4.6	93 Mar 01	17:57	0.122
	93 Mar 02	02:49	0.000

Notikewin River

Background Concentration: 0.016 (ug/L)

Hole: 7

Sample Temperature (C)	Date (y:m:d)	Time (h:m)	Dye Concentration (ug/L)
3.0	93 Mar 01	07:13	0.002
0.8	93 Mar 01	08:26	0.001
1.0	93 Mar 01	09:10	0.007
1.2	93 Mar 01	09:56	0.015
3.2	93 Mar 01	10:40	0.048
3.0	93 Mar 01	11:25	0.090
2.2	93 Mar 01	12:10	0.133
3.2	93 Mar 01	12:55	0.195
3.8	93 Mar 01	13:43	0.263
3.2	93 Mar 01	14:25	0.299
3.2	93 Mar 01	15:10	0.306
2.8	93 Mar 01	15:55	0.296
2.6	93 Mar 01	16:40	0.274
2.2	93 Mar 01	17:25	0.284
1.8	93 Mar 01	18:10	0.249
1.8	93 Mar 01	19:10	0.223
2.6	93 Mar 01	20:10	0.215
2.2	93 Mar 01	22:23	0.180
2.2	93 Mar 02	00:20	0.154
1.6	93 Mar 02	04:20	0.096
2.2	93 Mar 02	06:20	0.102
1.4	93 Mar 02	08:10	0.079
2.4	93 Mar 02	10:05	0.064
	93 Mar 02	18:14	0.000

Hole: 10

Sample Temperature (C)	Date (y:m:d)	Time (h:m)	Dye Concentration (ug/L)
1.6	93 Mar 01	07:17	0.022
0.2	93 Mar 01	08:24	0.089
0.6	93 Mar 01	09:08	0.190
1.0	93 Mar 01	09:54	0.269
1.2	93 Mar 01	10:38	0.328
2.2	93 Mar 01	11:23	0.360
1.6	93 Mar 01	12:08	0.364
1.8	93 Mar 01	12:53	0.356
2.6	93 Mar 01	13:41	0.367
2.4	93 Mar 01	14:23	0.339
1.2	93 Mar 01	15:08	0.302
2.0	93 Mar 01	15:53	0.302
2.0	93 Mar 01	16:38	0.296
1.4	93 Mar 01	17:23	0.240
0.8	93 Mar 01	18:08	0.223
1.8	93 Mar 01	19:08	0.178
1.6	93 Mar 01	20:08	0.175
1.8	93 Mar 01	22:16	0.119
2.0	93 Mar 02	00:16	0.111
1.6	93 Mar 02	04:16	0.069
1.4	93 Mar 02	06:16	0.058
1.8	93 Mar 02	08:08	0.049
3.2	93 Mar 02	10:03	0.039
	93 Mar 02	17:44	0.000

Hole: 10

Frazil sampling

Sample Temperature (C)	Date (y:m:d)	Time (h:m)	Dye Concentration (ug/L)
4.8	93 Mar 01	22:16	-0.006
11.4	93 Mar 02	00:16	-0.007
8.5	93 Mar 02	04:16	0.007
4.2	93 Mar 02	06:16	0.001

Notikewin River (continued)
Background Concentration: 0.016 (ug/L)

Hole: 12

Hole: 13.5

Sample Temperature (C)	Date (y:m:d)	Time (h:m)	Dye Concentration (ug/L)	Sample Temperature (C)	Date (y:m:d)	Time (h:m)	Dye Concentration (ug/L)
3.0	93 Mar 01	06:50	0.000	3.0	93 Mar 01	05:31	0.000
3.0	93 Mar 01	07:23	0.069	3.0	93 Mar 01	07:32	0.150
1.0	93 Mar 01	08:22	0.192	1.8	93 Mar 01	08:20	0.210
2.0	93 Mar 01	09:06	0.309	2.2	93 Mar 01	09:04	0.363
1.6	93 Mar 01	09:52	0.377	2.6	93 Mar 01	09:50	0.447
3.2	93 Mar 01	10:36	0.474	4.0	93 Mar 01	10:34	0.491
3.8	93 Mar 01	11:21	0.420	4.2	93 Mar 01	11:19	0.380
3.4	93 Mar 01	12:06	0.443	3.8	93 Mar 01	12:04	0.362
3.4	93 Mar 01	12:51	0.355	3.2	93 Mar 01	12:49	0.340
4.0	93 Mar 01	13:39	0.333	5.0	93 Mar 01	13:37	0.311
3.8	93 Mar 01	14:21	0.297	4.2	93 Mar 01	14:19	0.273
2.2	93 Mar 01	15:06	0.278	4.2	93 Mar 01	15:04	0.321
2.4	93 Mar 01	15:51	0.253	2.6	93 Mar 01	15:49	0.235
2.6	93 Mar 01	16:36	0.241	3.8	93 Mar 01	16:34	0.243
2.8	93 Mar 01	17:21	0.209	2.8	93 Mar 01	17:19	0.176
2.4	93 Mar 01	18:06	0.193	2.8	93 Mar 01	18:04	0.181
3.0	93 Mar 01	19:06	0.137	2.8	93 Mar 01	19:04	0.116
2.6	93 Mar 01	20:06	0.131	3.6	93 Mar 01	20:04	0.135
2.8	93 Mar 01	22:13	0.096	2.6	93 Mar 01	22:10	0.089
3.0	93 Mar 02	00:13	0.072	2.8	93 Mar 02	00:10	0.068
2.0	93 Mar 02	04:12	0.044	1.8	93 Mar 02	04:08	0.043
2.0	93 Mar 02	06:12	0.042	1.6	93 Mar 02	06:08	0.031
2.6	93 Mar 02	08:06	0.033	2.6	93 Mar 02	08:04	0.030
2.4	93 Mar 02	10:01	0.022	3.6	93 Mar 02	09:59	0.023
	93 Mar 02	13:54	0.000		93 Mar 02	15:56	0.000

Notikewin River (continued)
Background Concentration: 0.016 (ug/L)

Hole: 15

Sample Temperature (C)	Date (y:m:d)	Time (h:m)	Dye Concentration (ug/L)
3.4	93 Mar 01	06:57	0.000
3.4	93 Mar 01	07:38	0.062
1.4	93 Mar 01	08:18	0.124
2.8	93 Mar 01	09:02	0.229
3.2	93 Mar 01	09:48	0.326
5.0	93 Mar 01	10:32	0.342
5.6	93 Mar 01	11:17	0.341
4.6	93 Mar 01	12:02	0.311
3.4	93 Mar 01	12:47	0.328
5.4	93 Mar 01	13:35	0.318
4.4	93 Mar 01	14:17	0.288
4.2	93 Mar 01	15:02	0.335
3.6	93 Mar 01	15:47	0.282
3.4	93 Mar 01	16:32	0.274
3.8	93 Mar 01	17:17	0.215
3.4	93 Mar 01	18:02	0.213
3.6	93 Mar 01	19:02	0.132
3.4	93 Mar 01	20:02	0.145
3.0	93 Mar 01	22:07	0.125
3.2	93 Mar 02	00:07	0.083
2.6	93 Mar 02	04:04	0.057
1.2	93 Mar 02	06:04	0.042
3.2	93 Mar 02	08:02	0.043
3.6	93 Mar 02	09:57	0.030
	93 Mar 02	14:16	0.000

Hole: 17

Sample Temperature (C)	Date (y:m:d)	Time (h:m)	Dye Concentration (ug/L)
2.2	93 Mar 01	07:18	0.000
2.2	93 Mar 01	07:45	0.053
1.4	93 Mar 01	08:15	0.025
2.2	93 Mar 01	09:00	0.067
1.0	93 Mar 01	09:46	0.132
4.0	93 Mar 01	10:30	0.179
3.8	93 Mar 01	11:15	0.215
1.8	93 Mar 01	12:00	0.159
3.2	93 Mar 01	12:45	0.232
2.6	93 Mar 01	13:33	0.175
2.4	93 Mar 01	14:15	0.227
2.8	93 Mar 01	15:00	0.276
1.6	93 Mar 01	15:45	0.260
3.2	93 Mar 01	16:30	0.279
1.0	93 Mar 01	17:15	0.218
1.2	93 Mar 01	18:00	0.238
1.8	93 Mar 01	19:00	0.197
1.2	93 Mar 01	20:00	0.173
2.6	93 Mar 01	22:04	0.131
3.2	93 Mar 02	00:04	0.115
2.4	93 Mar 02	04:00	0.088
1.6	93 Mar 02	06:00	0.093
1.8	93 Mar 02	08:00	0.078
3.8	93 Mar 02	09:55	0.067
	93 Mar 02	21:36	0.000

Hole: 17

Frazil sampling

Sample Temperature (C)	Date (y:m:d)	Time (h:m)	Dye Concentration (ug/L)
19.2	93 Mar 01	22:04	0.039
4.8	93 Mar 02	00:04	0.014
11.6	93 Mar 02	04:00	0.014
3.8	93 Mar 02	06:00	0.004

3 1510 00149 8162
